



Development of a CFRTP Manufacturing Method to Improve Low Velocity Impact Resistance of Aerospace Structures

A Thesis submitted for the Degree of Doctorate of
Cranfield University

by

Yoan Delporte

August 2020

© Cranfield University 2020. All rights reserved. No part of this thesis may be reproduced without the written permission of the copyright holder.

Principal Supervisor: Dr. Hessam Ghasemnejad

Associate Supervisor: Prof. Dr. Phil Webb

Abstract

A continuous carbon fiber reinforced Polymer was manufactured using a Fused Deposition Modelling method. Current Fused Deposition Modelling machine are not able to manufacture Carbon Fiber Reinforced Thermoplastic Polymer composite therefore modification and novel designs needed to be made and integrated to the Fused Deposition Modelling machine to achieve a final product. To investigate the benefits of our composite a comparison with available composites on the market composed of similar materials needed to be performed. We investigated the different aspect of the requirements needed to manufacture test samples. We focused on manufacturing method able to integrate continuous Carbon Fiber simultaneously to a thermoplastic. In the slicing software a custom g code sequence has been developed to forward the continuous Carbon Fiber through the Bowden tube to the hotend. This procedure allowed the hotend to move freely between the layup of the printed part. Also C code library has been developed to analyse the geometry of the part to recognise the amount of Carbon Fiber, which needs to be pushed through the Bowden tube connected to the hotend. We investigated the mechanical properties as well as the process parameters of the individual materials used to manufacture our Carbon Fiber Reinforced Thermoplastic Polymer samples. In addition Carbon Fiber Reinforced Thermoplastic low velocity impact samples have been produced to investigate the potential of our composite in comparison to available products on the market like Short Carbon Fiber Polyamide filaments. The low velocity performances of the Continuous Carbon Fiber Thermoplastic Polymer samples have been promising compared to conventional Short Carbon Fiber Polyamide samples. The advantages of using an Fused Deposition Modelling machine to manufacture composites is the ease to choose between numerous fiber orientations, which a significantly important feature for impact applications. In addition a potential case study for aerospace structure applications of our Carbon Fiber Reinforced Thermoplastic Polymer will be investigated and discussed. The novelty behind this research is in the coding sequence allowing the fiber cutting system to trigger at a specific moment in order to integrate the necessary amount of fiber according to the distance of the hotend travelled on the heat bed. Another novelty is in the unique servo actuated fiber cutting system using a specific cutting mechanism. The contribution to the knowledge is the study of the behaviour of a thermoplastic composite under low velocity impact. To

investigate the effect of process parameters on a thermoplastic composite. To develop a novel cutting system and code control. Vibration cancellation method for even and continuous integration of continuous carbon fiber cutting method for precise carbon fiber cutting and integration to thermoplastic via Bowden extrusion system. Coding for the motherboard firmware as well as G code for the slicer have been optimised in order to produce quality samples. The effect of hardware on process parameters have been investigated though tensile tests. Low velocity impact performance of continuous carbon fiber polyamide has been also investigated and tested.

Acknowledgements

This PhD project would have been possible without the help and support of many people who I would like to show my gratitude.

First of all, I would like to express my deepest gratitude to my supervisor, Dr. Hessam Ghasemnejad, for his guidance and constant support during my PhD at Cranfield University. His support has always been present as well as his encouragement to pursue a variety of research topics. I also would like to thank my second supervisor, Prof. Phil Webb, from Cranfield University for being part of his department. Shout out to the secretary of our department Rachael Wiseman for having to deal with my constant material and equipment purchase quotation requests. I am extremely grateful to the technician Jim Hurley from the composite lab, who gave me priceless guidance to understand numerous carbon fiber reinforced composite applications and characteristics.

I also greatly acknowledge the lab technician Mr. Jarryd Braithwaite for his great assistance during the experiments. Last but not least, I would like to thank my beloved wife, Anaïs Jacob, who always pushes me to go beyond the limits and who had to listen to my daily complains about the issues encountered in my research. I am extremely grateful to my family and in-laws for their love and endless support. Without the support and funding from the Luxembourgish government and Ministry of Defence this research wouldn't have been possible.

Declaration

I hereby declare that the work presented in this dissertation is original and has not been submitted for a degree or diploma at any other university or institution. Information derived from the published and unpublished work of others has been acknowledged in the text and references are given in the list of sources.

Content

Chapter 1	16
1.1. Introduction.....	17
1.2. Research objectives.....	18
1.3. Thesis structure	19
Chapter 2	20
2.1 Fused Deposition Modelling background.....	21
2.2 Composite material.....	22
2.2.1 Polymer composite.....	23
2.2.2 Thermosetting resins	23
2.2.3 Thermoplastic resins.....	24
2.2.4 Polyamide resin	25
2.3 Fiber reinforcement.....	26
2.3.1 Glass Fiber.....	26
2.3.2 Carbon Fiber.....	27
2.3.3 Fiber orientation.....	27
2.3.4 Lamination theory.....	29
2.3.5 Prepregs.....	30
2.3.6 Carbon fiber reinforced thermoplastic polymer	31
2.4 Additive manufacturing	31
2.5 Rapid prototyping	32
2.6 FDM design	33
2.6.1 Cartesian coordinates	35
2.7 Delta printers.....	36
2.8 Cartesian printers.....	38
2.9 Polar printers	39
2.10. Carbon Fiber Reinforced Thermoplastic Polymer Printer.....	40
2.11. Filaments	42

2.12.	Design requirements for aerospace structures	44
2.13.	Energy absorption.....	45
2.14.	Low velocity impact setup.....	46
2.14.1.	Impactor	48
2.15.	Mechanical properties and process parameters.....	48
2.16.	Test samples	49
2.17.	G code	50
2.18.	Problem definition and objectives.....	51
Chapter 3		52
3.1.	Introduction.....	53
3.2.	Actual design	53
3.2.1.	Frame.....	53
3.2.2.	Vibrations.....	55
3.2.3.	Electrical components	56
3.2.4.	Extrusion system.....	57
3.2.5.	Heated bed.....	59
3.3.	Fiber cutter	60
3.3.1.	Design 1	60
3.3.2.	Design 2	61
3.4.	G code for slicer and programming.....	62
3.5.	Containment chamber	63
Chapter 4.....		65
4.1.	Introduction.....	66
4.2.	Material consideration	66
4.2.1.	Filament quality control	66
4.3.	Filament storage.....	67
4.4.	Process parameters	69
4.4.1.	Surface treatment	69
4.4.2.	Material flow	70

4.4.3.	Spacing paths	72
4.5.	Extrusion	73
4.6.	Nozzle diameter	75
4.7.	Skirt	76
4.8.	Influence of temperature and speed	76
4.9.	Toolpath control	77
4.10.	Tensile test samples	78
4.11.	Low velocity impact sample	79
Chapter 5	81
5.1.	Introduction.....	82
5.2.	Material characterisation.....	82
5.2.1.	Tensile testing.....	82
5.2.2.	Nozzle diameter and layer height correlation.....	84
5.2.3.	Effect of temperature on layer adhesion	88
5.3.	Experiment Setup.....	90
5.4.	Low velocity impact test results	92
5.4.1.	Nylon 910	93
5.4.2.	Short Carbon Fiber Nylon (SCFRN).....	93
5.4.3.	Continuous Carbon Fiber Nylon (CCFRN).....	94
5.5.	Test values	95
5.6.	Experimental errors	99
Chapter 6	100
6.1.	Conclusions	101
6.2.	Contribution to the science.....	102
6.3.	Future Work.....	102
Chapter 7	103
Chapter 8	108
Appendix A	109

Appendix B	113
Appendix C	114

List of Tables

Table 2.2-1: Thermosets vs Thermoplastics [8]	24
Table 4.4-2: Heated bed surface treatment.....	70
Table 4.11-1: Impact test results.....	80

List of Figures

Figure 2.2-1: Composite structure	22
Figure 2.3-1: Fiber orientations	28
Figure 2.3-2: Symmetrical lamina layup	29
Figure 2.3-3: Laminate geometry [19].....	29
Figure 2.6-1: Cyclopes extrusion system [29]	34
Figure 2.6-2: Dual extrusion printer configuration [30]	35
Figure 2.6-3: 2 dimensional cartesian coordinate system.....	35
Figure 2.6-4: 3 dimensional cartesian coordinate system.....	36
Figure 2.7-1: Anycubic Kassel Delta FDM machine [41]	37
Figure 2.7-2: Extruder stepper motor with 92t hobbed gear	37
Figure 2.8-1: Prusa MK2 cartesian FDM machine	39
Figure 2.9-1: Polar3d polar FDM machine	40
Figure 2.10-1: Maker forged Mark 2 CFRTP FDM machine	41
Figure 2.10-2: Mark 2 printed samples	41
Figure 2.13-1: Impact behaviour of an object air to ground	46
Figure 2.14-1: Drop tower	47
Figure 2.14-2: Low velocity impact test sample clamping system	48
Figure 2.16-1: Tensile sample geometry	49
Figure 2.16-2: Low velocity impact sample dimensions.....	50
Figure 3.2-1: Original rail guides for x axis gantry	54
Figure 3.2-2: Linear bearing rails for x, y and z axis	54
Figure 3.2-3: Single Z axis lead screw a, Z axis spring loaded backlash system b. .	55
Figure 3.2-4: Final FDM design and test print	56
Figure 3.2-5: Duet WIFI 2 32 bit board [42]	57
Figure 3.2-6: a) Extrusion systems Cyclops vs b) Dual extrusion hot end	58
Figure 3.2-7: Final design dual extrusion system with radial fans	59
Figure 3.2-8: e3D 240V AC heated bed [29]	59
Figure 3.2-9: e3D silicon thermistor pad [29].....	60
Figure 3.3-1: Cutter 1 clamping design.....	61
Figure 3.3-2: Cutter 2 Bowden design	62
Figure 3.5-1: Containment chamber with extraction fans and temperature regulator	63
Figure 3.5-2: Filtration system.....	64

Figure 4.2-1: Uneven filament diameter (a) vs even filament diameter (b)	67
Figure 4.3-1: Filament storage container with dehumidifying system.....	68
Figure 4.4-1: Material deposition on heated bed.....	70
Figure 4.4-2: Effect of nozzle height on material deposition	71
Figure 4.4-3: Voids between material paths along the plane.....	72
Figure 4.5-1: Hobbed gear cross-section and nylon filament	74
Figure 4.7-1: Skirt deposition around the printed sample	76
Figure 4.10-1: Tensile test sample.....	78
Figure 4.11-1: Low velocity impact sample	79
Figure 5.2-1: DIC tensile test	83
Figure 5.2-2: Tensile test samples.....	83
Figure 5.2-3: Effect of layer height on UTS Nylon samples with 0.6mm nozzle	84
Figure 5.2-4: Effect of layer height on UTS SCFRN samples with 0.6 mm nozzle ...	85
Figure 5.2-5: Effect of layer height on UTS Nylon samples with 0.8 mm nozzle	86
Figure 5.2-6: Effect of layer height on UTS SCFRN samples with 0.6 mm (yellow) vs 0.8 mm (red) nozzle	87
Figure 5.2-7: Effect of layer height on UTS CCFRN samples with 0.8 mm nozzle ...	88
Figure 5.2-8: Effect of temperature on UTS with samples printed on XY plane (red) and Z plane (yellow).....	89
Figure 5.3-1: CCFRN low velocity impact sample	90
Figure 5.3-2: Impactor dimensions	91
Figure 5.3-3: Drop tower sample gantry	91
Figure 5.3-4: Drop tower setup	92
Figure 5.3-1: Nylon 910 samples after impact.....	93
Figure 5.4-2: SCFRN low velocity impact samples	94
Figure 5.5-1: CCFRN low velocity impact samples	95
Figure 5.5-2: Energy absorption of the samples	96
Figure 5.5-3: Force generation of the samples	97
a Figure 5.4-10	98
Figure 5.5-5: Force- time graphs	98

Nomenclature

2D	Two-Dimensional
3D	Three-Dimensional
ABS	Acrylonitrile Butadiene Styrene
AM	Additive Manufacturing
CAD	Computer Aided Design
CAE	Computer Aided Engineering
CAM	Computer Aided Manufacturing
CCFRP	Continuous Carbon Fiber Reinforced Polymer
CCFRN	Continuous Carbon Fiber Reinforced Nylon
CFRP	Carbon Fiber Reinforced Polyamide
CFRTP	Carbon Fiber Reinforced Thermoplastic Polyamide
CNC	Computer Numerical Control
CMB	Controlled Metal Build-Up
DFMA	Design for Manufacture and Assembly
DLP	Digital light processing
DMD	Direct Metal Deposition
DOE	Design of Experiments
DP	Degree of Polymerisation
DSPC	Direct Shell Production Casting
EBM	Electron Beam Melting
EOS	Electro Optical Systems
FDM	Fused Deposition Modelling
FDMC	Fused Deposition of Multiple Ceramic
FFF	Fused Filament Fabrication
HIPS	High Impact Polystyrene
IGES	Initial Graphics Exchange Specification
IJD	Ink-Jet Deposition
FGM	Functionally Graded Material

G code	G programming language
GF	Glass Fiber
GFRP	Glass Fiber Reinforced Polymer
LAM	Laser Additive Manufacturing
LEM	Laminated Engineering Materials
LENS	Laser Engineered Net Shaping
LOM	Laminated Object Manufacturing
M2-3DP	Multi-Material 3D Printer
MEM	Melted Extrusion Modelling
MJM	Multi Jet Modelling system
MJS	Multiphase Jet Solidification
M-RPM	Multi-Functional Rapid Prototyping and Manufacturing
NURBS	Non-Uniform Rational B-Spline
PA	Polyamide
PC	Polycarbonate
PEEK	Polyether-etherketone
PE	Polyethylene
PEI	Polyetherimide
PLT	Paper Lamination Technology
POM	Precision Optical Manufacturing
PP	Polypropylene
PS	Polyphenylene Sulfide
PTFE	Polytetrafluorethylene
RFP	Rapid Freeze Prototyping
RP	Rapid Prototyping
RTM	Rapid Tool Maker
SAHP	Selective Adhesive and Hot Press
SCFRTP	Short Carbon Fiber Reinforced Thermoplastic Polymer
SCFRN	Short Carbon Fiber Reinforced Nylon
SCS	Solid Creation System

SGC	Solid Ground Curing
SLA	Stereo Lithography Apparatus
SLM	Selective Laser Melting
SLS	Selective Laser Sintering
SSM	Slicing Solid Manufacturing
SSR	Solid State Relay
STL	Stereolithography File
UAV	Unmanned Aerial Vehicle
UC	Ultrasonic consolidation

Chapter 1

Introduction

1.1. Introduction

Additive manufacturing is a growing manufacturing method to produce prototypes for industrial applications in different domains like Aerospace, Automotive industry, Space, Civil engineering or medical. The most common manufacturing methods in additive manufacturing are injected moulding and fused deposition modelling or also called fused filament fabrication. However, none of these existing methods can provide a fully integrated continuous carbon fibre bundle integration to a thermoplastic matrix. Carbon fibre reinforced thermoplastic polyamide are a future solution for producing less waste using recyclable materials such as Nylon. Unlike common materials used in rapid prototyping known as Polylactic acid, Acrylonitrile butadiene, Polyethylene terephthalate glycol, etc, Nylon as well as Polycarbonate and Polyether Ether Ketone have the advantage of being long molecular materials. Such materials can be recycled numerous times without losing any mechanical properties after the recycling process. As a composite matrix materials it makes them more suitable than others especially if recycling is part of our project requirements. In this study we will investigate the different requirements to achieve a quality carbon fiber reinforced thermoplastic polyamide composite. In addition we will develop a manufacturing method to produce quality tensile testing samples in order to investigate the mechanical properties and process parameters to produce samples. In addition carbon fiber reinforced thermoplastic polyamide low velocity impact samples will be produced to investigate the potential of our composite in comparison to available products on the market like short fiber reinforced thermoplastic polymer filaments.

From the process parameters a wide range of vital properties will be gathered in order to set our fused deposition modelling machine accordingly to the materials used to manufacture our samples. We investigated the process parameters and impact behaviour of pure Nylon 910, short carbon fiber reinforced polymer and continuous carbon fiber reinforced polymer samples. The advantages of using an fused deposition modelling machine to manufacture composites is the ease to choose between numerous fiber orientations, which is a significantly important feature for impact applications and the manufacturing process doesn't require any supervision.

Furthermore, a potential case study for aerospace structure applications of our carbon fiber reinforced thermoplastic polymer will be investigated and discussed.

1.2. Research objectives

The main objective of this research is to develop an advanced manufacturing method to create a composite materials using carbon fiber and nylon thermoplastic polyamide materials known as carbon fiber reinforced thermoplastic polyamide composites. Low velocity impact behaviour of these new developed materials will be the second objective of this research will be discussed in details through the drop tower impact testing methods. Vibration cancellation method for even and continuous integration of continuous carbon fiber cutting method for precise carbon fiber cutting and integration to thermoplastic via Bowden extrusion system. Coding for the motherboard firmware as well as G code for the slicer have been optimised in order to produce quality samples. The effect of hardware on process parameters have been investigated through tensile tests. Low velocity impact performance of continuous carbon fiber polyamide has been also investigated and tested.

The main goals of this work can be summarised as follows,

1. Development of advanced additive manufacturing machine known as Fused Deposit Modelling (FDM). The novelty behind the FDM machine is that continuous carbon fiber can be integrated into a thermoplastic matrix. Moreover the novel cutting mechanism of the cutting system sizes the required amount of carbon fiber length to the amount of thermoplastic extruded along the toolpath of the extrusion system.
2. Development of advanced CFRTP composite materials samples including laminate design effect. A unique lamination is achieved due to a specific g code sequence developed and offers an unrestricted lamination orientation along the lamina.
3. Energy absorption of CFRTP composite materials against short carbon fiber reinforced thermoplastics nylon and pure nylon. The comparison of these three materials allows us to have a unique representation of the energy absorption capacity of our CFRTP composite to existing composites and materials available in the market.

1.3. Thesis structure

This section presents a concise overview of the different chapters appearing in this thesis.

Chapter 2: Theoretical background

The additive manufacturing of reinforced thermoplastic composites are discussed in detail. The influence of various parameters such as material selection, laminate design, low velocity impact, structural geometry are discussed in details.

Chapter 3: Design

Several FDM machine design and application are investigated. Existing CFRTP machines are discussed in this chapter. The development of an additive manufacturing machine is discussed in terms of design, development, assembly, setup and coding in detail.

Chapter 4: Manufacturing

In this chapter several manufacturing challenges are highlighted as well as the influence of process parameters on the manufacturing process of the test samples. Furthermore nylon-, SCFRTP- and CFRTP samples are manufactured according to British Standard testing methods. Also mechanical properties will be determined for each material composition.

Chapter 5: Experimental Studies

All manufactured samples in Chapter 4 will be tested and analysed under quasi-static and low-velocity impact loading conditions. The outcomes will be compared with the mechanical properties and impact resistance of pure thermoplastic nylon and short carbon fiber reinforced nylon composite.

Chapter 2

Theoretical background

2.1 Fused Deposition Modelling background

Standard FDM machines are not able to integrate continuous carbon fiber into a thermoplastic matrix without undergoing significant modifications and major upgrades to the rapid prototyping manufacturing method. Besides the existing layup process the fiber integration to a heated matrix is not an easy procedure. Untreated Carbon fiber tow will curl inside the extrusion system resulting in a clogging of the hotend. Standard extrusion systems are built to extrude one material at a time on a heated build platform. Stacking layers of carbon fiber coated with a thermoplastic cannot be considered as a carbon fiber integration to a matrix. The continuous carbon fiber is not integrated into the thermoplastic matrix material. As a result mechanical properties and impact resistance are influenced negatively. Moreover, a controlled extrusion system needs to extrude two materials at the same time without causing any clogging of the hotend. Experimental extrusion systems have been tested but only with similar materials, which have the same mechanical and thermal properties to be extruded simultaneously.

For this research we focus on the impact resistance capabilities of a new composite using a rapid prototyping approach. Compared to CFRP manufacturing methods, which are expensive, time consuming and require heavy machinery. CFRTTP composites are a promising yet new alternative to CFRP. The rapid prototyping approach offers multiple cost effective advantages like reduced cycle time, low cost manufacturing, recycling, upgradable and environmental friendly material use [1].

Composites are used for lightweight structures, which are operating in harsh environments and require a specific weight to strength and weight to stiffness ratio. Recently a lot of interest has emerged for low velocity impact applications of thermoplastics in automotive, aerospace and space industry.

Usually a structure is designed sustain a consequent amount of damage without failing in several situations like service load condition and the poorest allowable material quality in the most severe operating environment. An experimental structural approach has been followed in this research using the principals of structural mechanics with structural analysis tools.

2.2. Composite material

A composite is a matrix material reinforced with fiber material contained in a matrix body (Figure 2.2-1). The two materials have different mechanical and chemical properties, which are distinct from each other gathered together to form a composite material. Concrete is for example a composite. The matrix is made of cement, sand and gravel. The reinforcement is in this case not fiber but steel rods [2].

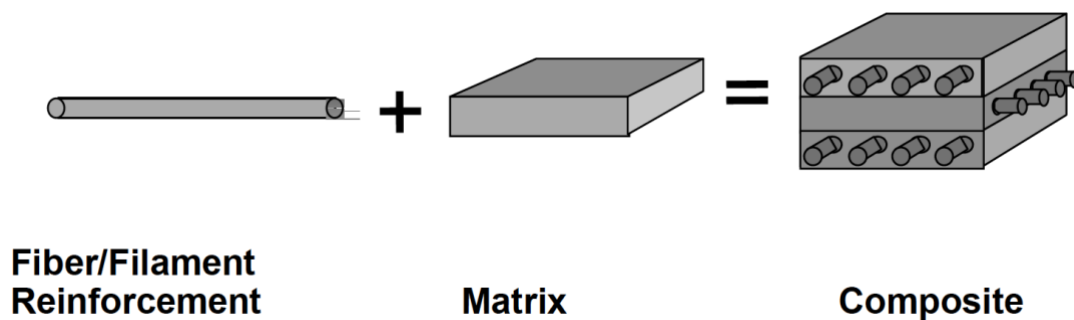


Figure 2.2-1: Composite structure

The objective with composites is to achieve a finished product, which has outstanding mechanical properties and is lightweight. The matrix acts as a binder for the fiber, to increase the bond between the fibers/ matrix coupling agents and coatings are applied to the surface of the fiber. The surface treatment will improve the bonding between the fibers and the matrix. The better the bonding the higher is the interfacial strength between the fibers and the matrix. Thus, once the fibers are properly bonded with the matrix loads applied to the matrix are immediately transferred the fiber, which has an impact flexural strength and impact resistance of the matrix [1]. The CFRP is manufactured by stacking laminas of carbon fiber/ epoxy on top of each other.

Fiber reinforced composites are particularly interesting for several applications like aerospace, snow- and aquatic sports, automotive, wind energy, defence, and infrastructures. They contribute to the overall weight reduction due to their high stiffness to weight ratio resulting in parts reduction for a airframes and structures. Widely used on the market are the well-known glass-, carbon- and aramid fibers. However, in cost- sensitive and high volume industrial applications, carbon fiber is not recommended due to its high cost. However, carbon fiber is lighter and has a stiffness to weight ratio five times higher than steel [3].

In terms of advanced lightweight structures CFRP are well known. The CFRP matrix is a polymer resin, some resins have their own curing process. In order for the CFRP to reach its maximal mechanical properties most resins need to be cured. Common resins used for CFRP are gathered in two major groups of polymers, thermosetting and thermoplastics.

2.2.1 Polymer composite

As mentioned earlier a composite is a material manufactured by the combination two or more materials as separate phase. Through the combination of a polymer and another material for example fibers (glass, carbon, aramid, Kevlar, etc) have unique mechanical properties are achieved. Synthetic polymeric composites are commonly used on the market; these are polymer reinforced ether glass- carbon thermoplastic or thermosetting resin reinforced composites. More exotic combinations like carbon reinforced rubber, mica- or silica reinforced resins and impregnated or bonded polymer wood or concrete. Not only CFRPs are composites, coating material known as crystalline polymers are considered as composites too. Bones for example are perfectly engineered natural composites, a bone is minerals bonded with collagen [2].

2.2.2. Thermosetting resins

They are pre-polymers, which are monomers in pre-curing process and in an intermediate molecular mass state. They are ready to be polymerized into an irreversible high molecular weight state by a curing process. The curing process is different for each resin type. The curing can be brought up by heat, chemical reaction or irradiation with ultraviolet light, electron beam or infrared. Some thermosetting do not require heat or pressure to harden. They are inexpensive, resist to high temperatures and strong. However, they are more brittle than thermoplastics and less environmental friendly in regards of the recycling process. Moreover, some curing processes are long, costly, require technical attention and dangerous for the environment. The recycling process of carbon fiber polymers is expensive and the amount of material gathered after the process is very poor. This is due to the heterogeneous nature of the matrix [4]. A three dimensional network between the fiber and the thermosetting resin is achieved due to the chemical reaction that undergoes the resin and crosslinks the polymer chains and connects the laminas to each other.

carbon fiber reinforced polymers with thermosetting resin have a high temperature resistance, high dimensional stability and a good resistance to chemicals due to their three dimensional cross-linked structure. In bulk form thermosetting have a low toughness.

2.2.3. Thermoplastic resins

Some polyamide resins like nylon are made of long molecules with strong monomer bonds, which are processed once they reach their melting temperature. The fact that thermoplastics resins have long molecules makes them reliable to be reused after undergoing a recycling process. Moreover, recycled thermoplastics can be rapidly reprocessed [5]. When a thermoplastic is processed through thermal exposure, its chemical composition is not affected by the heat process. The heating process is very simple, once the thermoplastic is heated at its melt temperature, the discrete molecules will melt to a viscous liquid. Depending on the thermoplastic, the processing temperature is between 260°C (polyamide or Nylon) and 310°C [6]. Unlike thermosets where the recycling process is irreversible, thermoplastics are reversible in a way that the matrix material can be separated from the fiber reinforcement and both can be reused separately. By simply reheating the thermoplastic to its melting temperature, the resin can form another shape if desired without any major effect on the mechanical properties of the resin. Some thermoplastics like PEEK or high impact polystyrene have a high energy absorption capacity, although others like Polylactic acid are sensitive to heat and corrosion. However, PEEK is a semi-crystalline microstructure, which exhibits improved temperature and chemical resistance. The downside is the manufacturing process of PEEK. It requires a temperature of approximately 343°C [7], which can be a problem for standard Additive Manufacturing methods like Fused Deposition Modelling. A brief comparison between thermosets and thermoplastic can be seen in table (2.2-1).

Table 2.2-1: Thermosets vs Thermoplastics [8]

Resin Type	Process temperature	Process time	Chemical resistance	Toughness
Thermosets	Low	High	High	Low
Thermoplastics	High	Low	Low	High

To manufacture a composite using thermoplastics several methods can be applied, for example injected moulding, extrusion, rotational moulding, vacuum forming and compression moulding [9]. Thermoplastics can also be bonded with other thermoplastics such as ABS, Nylon, PC, PEEK, PEI, PE, PS and PP through heating process.

High impact polystyrene is another thermoplastic, which meets the requirements of this research. HIPS as mentioned in the name is a suitable material for impact testing, its melting temperature is around 180°C and 3D printing temperature is between 230-260°C. It has a good impact resistance, excellent for machining and it is low cost. Unfortunately, it has a poor chemical and heat resistance [10]. Despite the advantages of thermoplastics towards thermoset the development of continuous fiber reinforced thermoplastics matrix composites is small compared to CFRP with thermosets. The reason is because of the difficulty to integrate the continuous fiber to the matrix during the manufacturing process.

2.2.4. Polyamide resin

Nylon or polyamide resins are very durable, they are commonly used in automotive, prosthetics and textile [11]. Nylon 66, which is an engineered hexamethylenediamine and adipic acid polyamide shows remarkable properties suitable for gears and bearings. It is a semi crystalline polyamide with a high abrasion resistance, rigidity and thermal stability [12][13]. This polyamide has a high tensile strength and melting point making it suitable for piston guides, impact plates and friction strips [14]. The combination of Nylon 66 and short carbon fiber has been evaluated by [15]. The research shows higher tensile and compression values than pure nylon 66 resin. The increase of fiber volume fraction significantly improved the mechanical properties of the composites up to a pound. By increasing the fiber volume fraction internal voids inside the composite are formed caused by the overflow of short fibers in the matrix. Reinforced nylon 66 with short carbon fiber has enhanced mechanical properties compared to pure nylon 66. The fiber content added to the resin is represented in % of the resins total mass.

Nylon 910 from Taulman is commonly used for medical prosthesis, robotic assembly parts, food products. Small shrinkage after extrusion (0.084 mm/mm), modulus (502.85 MPa), tensile stress (55.85 MPa) and it has a tensile elongation of 32%. If

structural adjustments of the printed part have to be conducted a carbide drill or rotary head-tool will be required. Nylon Alloy 910 can be processed at a temperature range of 250-255°C, which is a temperature within the range of FDM manufacturing [16].

2.3. Fiber reinforcement

Fibers are the most important constituent in CFRP materials. They share the major amount of load applied to the laminate and have the largest volume fraction in the CFRP laminate. Several parameters are unique to each fiber type like the density, the electrical conductivity, compressive strength and modulus, the tensile strength and modulus, fatigue- failure and strength. To make a CFRP lamina the following fiber properties need to be studied and adapted to the primary function of the desired CFRP: Fiber volume fraction, fiber length and the fiber orientation. For this research the carbon fiber will be continuous, chopped carbon fibers have a much lower strength to weight ratio than continuous carbon fiber [17][18].

2.3.1. Glass Fiber

Glass fiber reinforced polymer composites are widely used in the industry. The fiber itself can be found on the market under the form of mat, cloth, roving or fiber. Glass fibers have a relatively low stiffness compared to carbon fiber, however glass fibers has a higher static failure strength and better fatigue strength. The downside of glass fiber is its higher weight compared to carbon fiber. Glass fiber are widely used in both automotive and aerospace industry. In the industry the main reason why glass fiber is widely used in comparison to carbon fiber is because of its price. Depending on the applications glass fiber is less rigid then carbon fiber. Therefore when added to a nylon matrix the rigidity will increase combining the tensile strength of nylon and the stiffness of carbon fiber together offering suitable composite for our impact testing. Moreover, glass fiber is difficult to separate from a matrix resin therefore most of the products manufactured with glass fiber reinforced polymer like boats end up in landfills. It is important to consider the environmental impact when manufacturing composite materials with an decrease in resources recyclable materials have to be considered.

2.3.2. Carbon Fiber

In advance composite material applications, carbon fiber is one of the most interesting materials on the market. Due to its high failure- and fatigue strength, stiffness, heat resistance but most importantly its low weight. Compared with other fiber reinforcement materials on the market carbon fiber is very attractive for aerospace applications. Fiber reinforced polymer composites are ideal for domains where weight saving and reliability is a priority. Moreover, carbon fiber has a high strength to weight- and stiffness to weight ratio. Carbon fiber is used with several matrix materials like polymers, ceramic or carbon. Commonly carbon fiber is combined with a polymer matrix like thermoplastics or thermosets. Thermosets are more difficult to recycle mostly the carbon fiber is damaged due to the high heat required to melt down the thermoset resin. The outcome of such a procedure is a weakened recycled carbon fiber, which is also known as chopped or short fiber. Once recycled the thermoset resin is of no use. In our case the short fiber reinforced nylon filament used as a comparison with the continuous carbon fiber nylon samples is made of recycled carbon fiber combine with a nylon thermoplastic matrix.

2.3.3. Fiber orientation

The incorporation of a large number of fibers parallel to each other in the longitudinal direction of the fiber (unidirectional) is called a lamina or ply. Composites with unidirectional fiber orientations have the highest mechanical properties compared to triaxial or quadriaxial fabrics figure (2.3-1.2/a). There are many different fiber orientations possible like for example the bi- or multidirectional fiber orientation figure (2.3-2.2b/ c). However, bi- and multidirectional fibers have higher transverse strength and modulus than unidirectional fibers. Moreover, there are methods to increase the strength and modulus of bi- and multidirectional fibers, by increasing for example the number of fibers in the respective fiber directions. The downside of this reinforcement is the weight increase of the lamina, which is not dramatic for one ply but usually a composite has more than 20 plies.

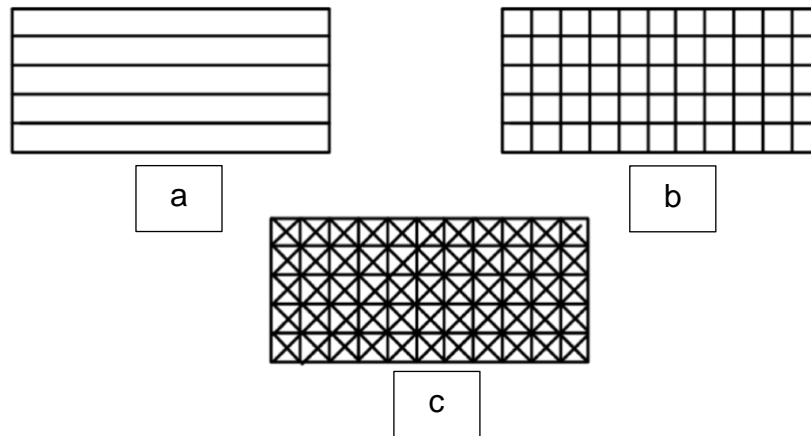


Figure 2.3-1: Fiber orientations

For this research we are looking for a fiber configuration, which offers the highest strength and modulus in the longitudinal fiber direction. The typical fiber orientations are 0° , 45° , 90° , -45° . When each ply has a different fiber orientation and they are sewn together, specific mechanical properties emerge from the CFRP. This configuration allows loads to be shared more efficiently between the fibers, which leads to higher tensile and flexural modulus.

The thickness of each lamina is in a range of 0.1 to 1 mm. The thicker the composite the more given load it will be able to support and maintain its initial deflection. There are a few types of laminates and lamination codes. For a unidirectional laminate all laminas are oriented in the 0° . In an angle ply laminate the laminas are oriented in alternative angles: $[\theta/-\theta/\theta/-\theta]^\circ$ for angles, which are different then 0° and 90° . Whereas, in a cross ply laminate the fibers are oriented in alternate layers: $[0/90/0/90]^\circ$. Finally, symmetric laminate is more common in the domain of research. Their laminas orientation are symmetrical about the centreline of the laminate figure (2.3-2). Each ply above the midplane is identical from the material to the thickness of the lamina and fiber orientation angle. The lamination code is the following: $[45/0/-45/90]^\circ s$. The 'S' indicates a symmetry about the midplane.

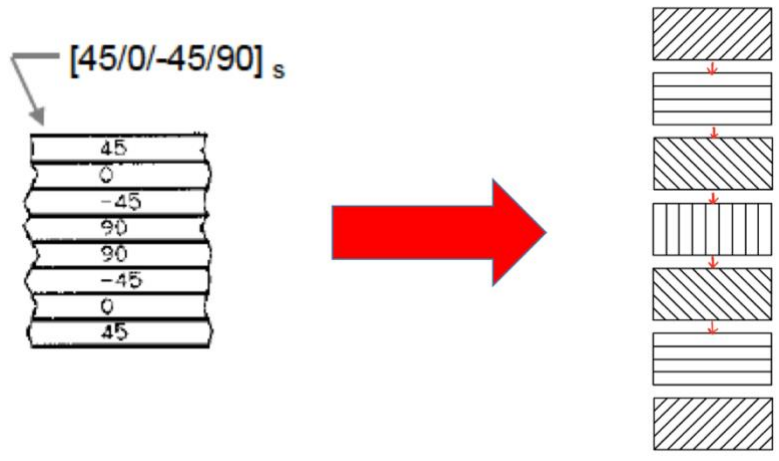


Figure 2.3-2: Symmetrical lamina layup

2.3.4. Lamination theory

We use the lamination theory in order to calculate the strains and stresses in each lamina of the laminate. First the stiffness of the matrix for the laminate has to be determined, then the midplane strains and curvature from the applied moments and forces to the laminate. Thus, calculate the midplane strains and stresses for each lamina. In figure (2.3-3) we can see the lamination theory with the dimensions and between the layers.

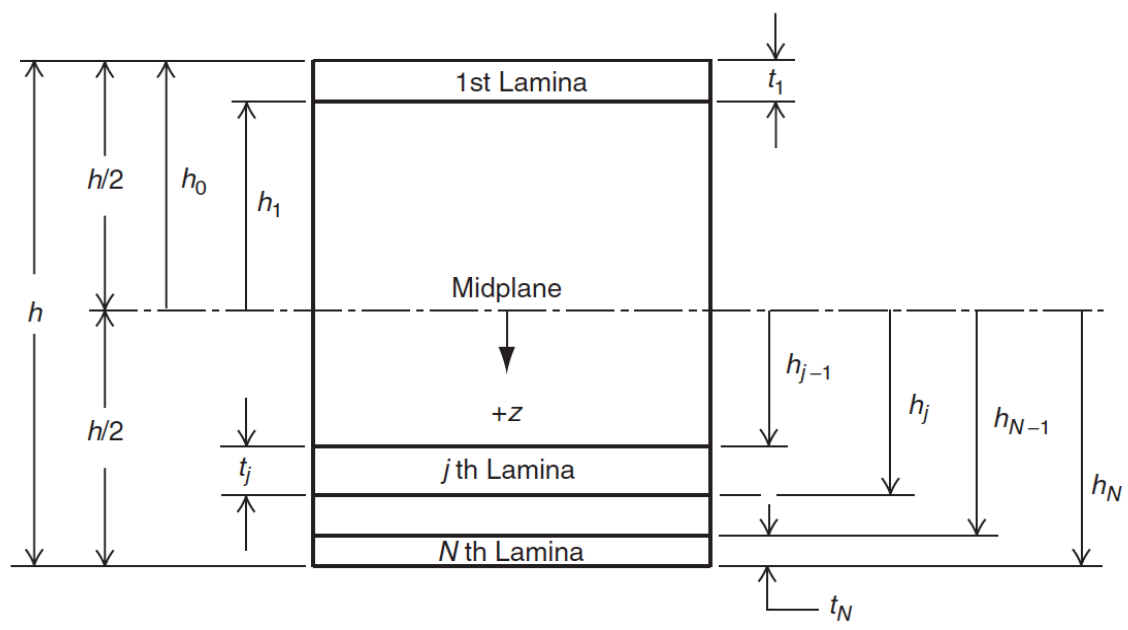


Figure 2.3-3: Laminate geometry [19]

$$\begin{aligned}\varepsilon_{xx} &= \varepsilon_{xx}^0 + zk_{xx} \\ \varepsilon_{yy} &= \varepsilon_{yy}^0 + zk_{yy} \\ \varepsilon_{xy} &= \gamma_{xy}^0 + zk_{xy}\end{aligned}$$

Equation (2.3-1)

In equation (2.3-1) ε_{0xx} and ε_{0yy} are the midplane normal strains (laminate). γ_{0xy} is the midplane shear strain (laminate), k_{xx} , k_{yy} are the bending curvatures (laminate), k_{xy} is the twisting curvature (laminate) and z is the distance from the midplane and the thickness of the lamina. Force and momentum are applied to the laminate and related to the midplane strains and curvatures equation (2.3-1). In crashworthiness the lamination layup is critical for the capacity of the composite as it changes the mechanical properties of the sample. The effect of the lamination design on the energy absorption of the composite during impact is crucial for its crashworthiness capacity. A stable collapse $[\pm 45^\circ/\pm 45^\circ]_n$ layup of the laminas results into obtaining a lower energy absorption value than a $[0^\circ/90^\circ]_n$ lamination showed by Thornton and Edwards [20]. A variation in the specific energy absorption of carbon fiber-, glass fiber epoxy $[02/\pm\theta]$ samples all increase with increasing θ showed by Schmueser and Wickliffe [21].

2.3.5. Prepregs

A Prepreg composite is made of continuous carbon fibers parallel to each other (Roving) impregnated in a corresponding resin volume to fiber volume content rolled around a cylindrical forming package. In order to be processed, the prepreg is cut into samples, which are stacked together with the required lamina orientation. Once the laminate is layered up, it will be cured into the final shape through compression moulding called batch moulding [22]. In order to compare the efficiency and mechanical properties of the nylon Alloy 910 CFRP, prepreg samples will be manufactured and tested. The reason why prepreg is chosen for this research is because prepreg has already the corresponding volume fraction of epoxy to the corresponding fiber content.

2.3.6. Carbon fiber reinforced thermoplastic polymer

Manufacturing a CFRTP composite isn't as straight forward as manufacturing CFRP. To manufacture a CFRP composite a lot of processing and handling is required whereas the key to manufacture CFRTP lays almost entirely in the process parameters and toolpath control of the FDM printer. Before jumping to the manufacturing of the CFRTP samples a few variables need to be considered. As mentioned earlier on the chapter after running some tests on the material and nozzle the ideal conditions and parameters have been determined to manufacture in the most efficient way our CFRTP sample for tensile and impact testing.

2.4. Additive manufacturing

Additive manufacturing is a manufacturing method different than conventional methods such as CNC machining, casting or moulding. Rapid Prototyping is an additive manufacturing method able to create complex geometries using as building material known as amorphous plastic also called thermoplastics. Thermoplastics become mouldable when they are subjected to a specific temperature. They have an impressive dimensional stability and impact resistance. Moreover, parts made of thermoplastics can be recycled. The recycled raw material is processed to small pellets, blended and extruded into a new filament. They can be recycled indefinitely because their molecular chain does degrade but very slowly when it undergoes several melting processes. By combining the mechanical properties of carbon fiber and thermoplastic a cheap, strong, durable and light composite can be manufactured where high strength, stiffness and impact resistance are required. The carbon fiber used for this project is a continuous carbon fiber filament. A rapid prototyping approach using Fused Deposit Modelling to manufacture the new composite. FDM is a leading technology in the domain of Rapid Prototyping, parts are built layer by layer by depositing the melted thermoplastic on the heat bed/ building platform [23][24][25]. The matrix made of a thermoplastic called Nylon 910, which has a higher tensile strength than any existing co-polyester and a high durability discussed in the material subsection. Advanced composites are used in many domains especially in aerospace, medical and military. Pure carbon fiber reinforced composite constituted of carbon fiber mixed with a resin/ hardener matrix are very expensive. Especially the

manufacturing process is very time consuming and expensive. Rapid prototyping is a perfect cost effective solution to manufacture composites, which are low cost, light, recyclable, highly automated and have a high stiffness and strength along the direction of the reinforcement. The application of this composite are limitless from aircrafts, navy, automotive and other moving structures. Due to this manufacturing method not only entire structures can be manufactured but also spare parts like panels or gears because they can be recycled and reproduced.

2.5. Rapid prototyping

Rapid prototyping draws the interest of many industrial applications. It is used since the 80s to produce models and prototypes before a company launch the mass production of a product. In a not so distant future rapid prototyping can be used to produce anything from aerospace applications to common everyday usage tools like house hold products. Rapid prototyping gathers a group of techniques used to produce anything form the geometrical data extracted from a Computer Aided Design (CAD) [23][24][26]. The CNC subtractive method is a very common rapid prototyping method. This method is significantly time consuming and a lot of waste is produced during the manufacturing process unlike the Fused Deposit Modelling (FDM), Stereo lithography Apparatus (SLA), Laminated Object Modelling (LOM), Selective Laser Sintering (SLS) [27]. FDM parts are manufactured on a printing platform called the heat bed or build platform by depositing the manufacturing material via a hot end on the building platform. It is a very promising manufacturing technology, it belongs to the additive manufacturing methods like building a brick wall, which is also an additive manufacturing product. FDM achieves a controlled forming quality and has a high degree of automation and minimal maintenance. There are many advantages related to this technology, it is ecological by using eco-friendly material (non-petroleum based material), low cost (low energy consumption), high automation (once calibrated it runs no need of supervision), can realise complex geometries, parts can be easily recycled and reused. Because recycling is important for the future generations and the preservation of our planet, most of the thermoplastics used for FDM can be recycled. It is crucial to find environmental friend thermoplastics moreover thermoplastics with promising mechanical properties, which can be used for composite applications.

Unfortunately, parts made of pure thermoplastics have poor mechanical properties, this is when the combination between carbon fiber and thermoplastics gets interesting. The new composite leads to astonishing mechanical improvement. Not only mechanical properties can be improved but also chemical-, heat resistance and weight reduction can be achieved, expanding the application areas of this novel composite to different domains where high structural expectations are required.

2.6. FDM design

In 1984 Charles W. Hull developed the first working 3d printer, which was then commercialised in 1989 by the company 3D Systems. His machine was a Stereolithography apparatus (SLA) or also known as laser printer converting liquid plastic into solid objects. In the meantime, S. Scott and Lisa Crump patented the first Fused Deposition Modelling (FDM) machine in late 1989 and founded Stratasys Ltd. In 2005 their patents expired, which led the build plans and technology of the FDM machine to become part of an open source community founded by Dr. Adrian Bowyer who was a senior lecturer in mechanical engineering at the University of Bath in the United Kingdom. He created the open source community called RepRap [28]. Due to the open source community a countless amount of improvements and discoveries and have been made over the past ten years regarding FDM printers. A large variety of FDM machines can be found on the market. For this research focused on a form of desktop or also called consumers FDM machine. The open source community is driven by engineers, architects, movie makers, artists and hobbyists. With desktop printers companies can produce a preliminary prototype model of a Computational Aided Design (CAD) and reduce their initial project costs and time. A typical FDM desktop printer has to be able to self-replicate itself.

Desktop FDM printers are divided into three main categories. Delta, Polar and Cartesian. Besides the Polar FDM machine both Cartesian and Delta FDM printers use Cartesian coordinates to determine the X, Y and Z position of the hotend on the print surface.

To manufacture CFRTP composites a modified extrusion system has to be used in order to efficiently extrude the combination of the modified carbon fiber filament to the melting thermoplastic. The thermoplastic is fed to the extrusion system via a stepping

motor grabbing through a gear mounted on it rotating axis the thermoplastic filament, which is guided through a pipe to the extrusion system. The same principle can be used in order to feed the extrusion system with the carbon fiber filament. There are ideal extrusion systems for this purpose called Cyclopes figure (2.6-1). It is constituted of a core fitted with heatsinks followed by a heater. The heatsinks keep the material in solid form allowing the material to slide drag less through the pipe. The heater, which follows the heatsinks is the component where the material is melted and led to a slightly bigger chamber then the intake part of the extrusion system.

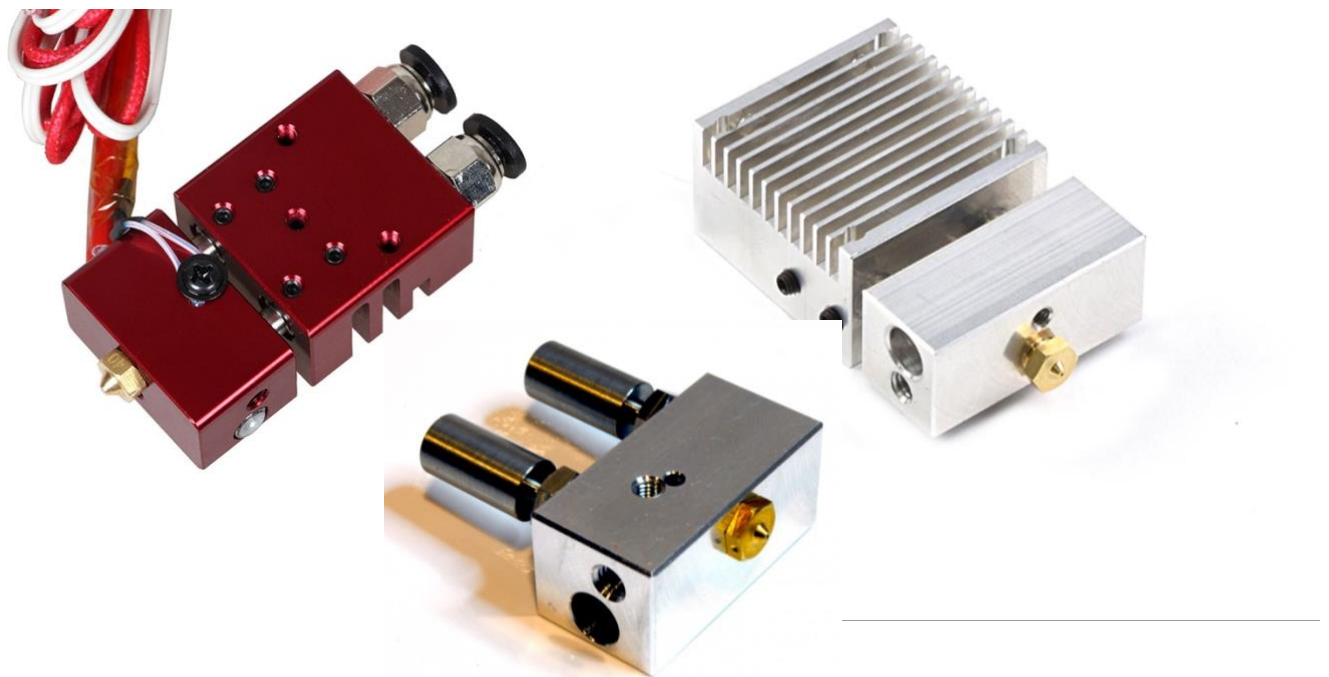


Figure 2.6-1: Cyclopes extrusion system [29]

In this case the extrusion system needs to be heated between 245-250 °C which is the required heat for nylon 910. Moreover, it is a full metal core extrusion system, which is crucial when a high temperature is required otherwise it would get damaged through the high heat. The filament has a diameter of 1.75 mm, several nozzles with different diameters (0.2 - 0.4) mm will be tested in order to find the optimal nozzle to manufacture the composite. A typical cartesian FDM machine can be seen in figure (2.6-2).

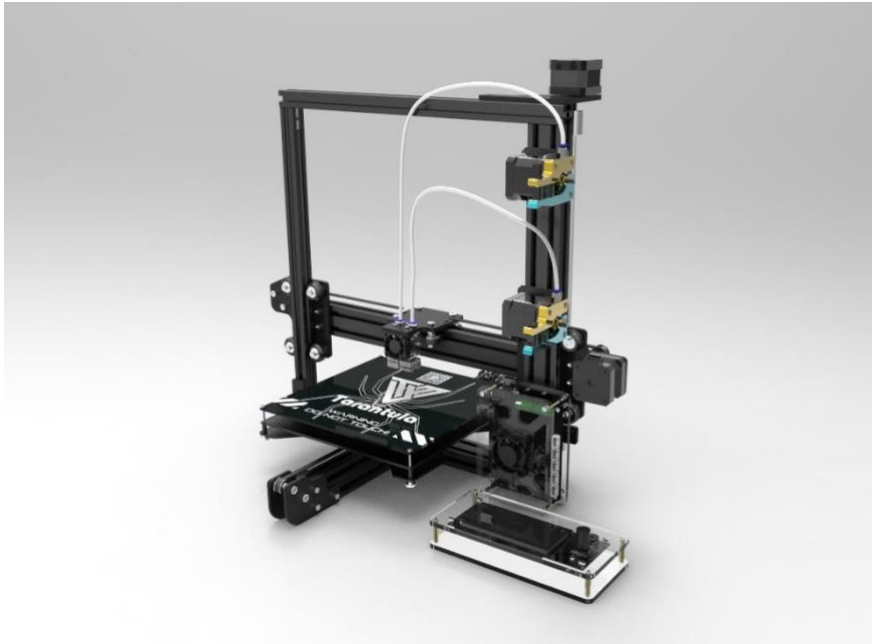


Figure 2.6-2: Dual extrusion printer configuration [30]

2.6.1 Cartesian coordinates

Cartesian coordinates refer to a 2- or 3 dimensional orientation of an object in a space. In a two dimensional space a specific X and Y position of this object or point is taken on a X and Y plane. The two dimensional cartesian coordinate system can be seen in figure (2.6-3).

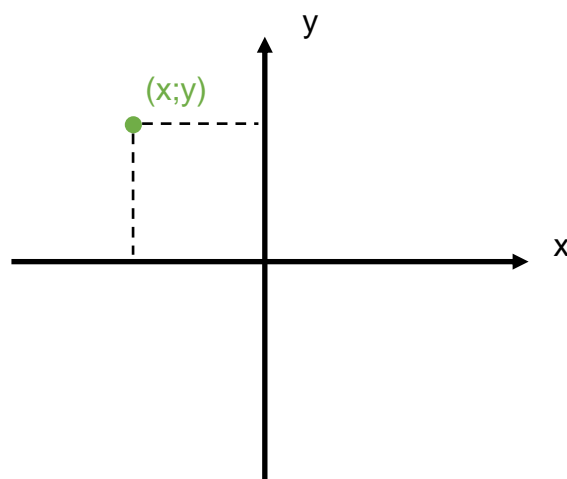


Figure 2.6-3: 2 dimensional cartesian coordinate system

In the case of a three dimensional orientation the Cartesian system has three perpendicular axes to each other. The motion of the tool head for a CNC machine as well as the hotend on an FDM machine is defined by cartesian coordinates in a three dimensional space. The Cartesian FDM machines are named after the Cartesian coordinate system used to position the hotend on the build platform. Every single motion of the hotend for each layers has (x;y;z) coordinates, which allows it to deposit material at each given point. The Cartesian configuration is the most common on the market for both desktop as well as professional machines, due to the simplicity of the mathematical calculations involved in the positioning of the hot end. The three dimensional cartesian coordinate system can be seen in figure (3.2-2).

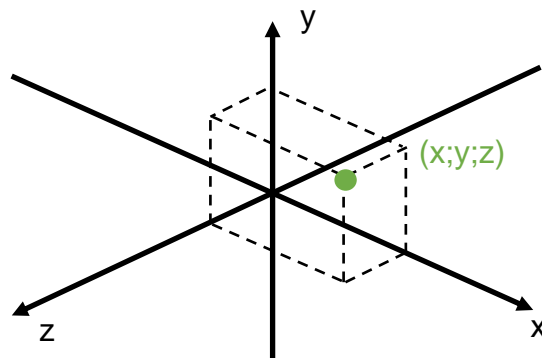


Figure 2.6-4: 3 dimensional cartesian coordinate system

2.7. Delta printers

Delta printers are using the same Cartesian coordinate system than Cartesian printers. The difference between a Cartesian and a Delta printer is the motion of the axes and the build platform or heat bed. On a Delta printer the hotend is attached to three separate arms, which are actuated by three independent stepper motors. The stepper motors move the three arms holding the hotend in a parallelogram form to the desired X, Y and Z coordinates on the heat bed. The heat bed is fixed to the bottom of the frame of the printer. A typical delta printer can be seen in figure (2.7-3).

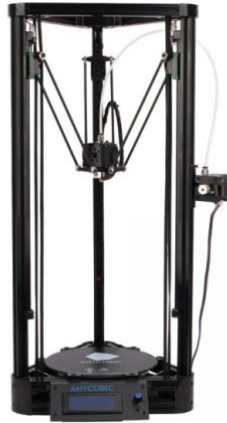


Figure 2.7-1: Anycubic Kassel Delta FDM machine [41]

The advantage of a Delta printer is the low inertia of the hotend motion. In order to keep the inertia as low as possible the filament material feeding mechanism has to be a Bowden system compared to the direct drive system commonly used on Cartesian printers. Due to its lightweight the hotend can move faster than a Cartesian printer where the hotend is attached to one or two solid axes for the X axis only. The Bowden extrusion considerably decreases the weight of the hotend and print time but it is limited with the materials it can feed into the hotend. For instants the hotend is connected to the extrusion stepping motor through a Polytetrafluorethylene (PTFE) tube to reduce the friction between the material and the tube during travel from the motor to the hotend figure (2.7-4). This allows the stepping motor hobbed gear to push the material to the hotend without digging into the material.



Figure 2.7-2: Extruder stepper motor with 92t hobbed gear

A Bowden system is unpractical to feed flexible or brittle materials to the hotend. The distance and lack of retraction power between the actual point where the material is fed from the hobbed gear of the extrusion motor and the melting zone of the hotend. This could cause the material to elongate or break inside the PTFE tube or more likely between the entrance of the PTFE tube and the hobbed gear of the stepping motor. It is also challenging to build a containment chamber for the printer in order to print some materials that require a stable environmental temperature to prevent warping off the heat bed. Therefore Delta printers are usually used to build tall or circular objects with standard Thermoplastics like PLA, which don't require any specific temperature controlled environment.

2.8. Cartesian printers

Cartesian printers owe their name from the Cartesian system used for the hotend orientation along the X, Y and Z axes. There are numerous variants of Cartesian printers on the market. The cost is usually the main factor that influences industries or hobbyist to purchase a certain type of printer. The most popular low cost printers on are based on the Prusa i3 model. The name Prusa came from its creator Josef Prusa who launched in 2010 the Prusa Mendel. Josef simplified the original open source community Mendel printer, which was a complex design with many parts. In 2012 Josef launched the first i3 model called the original Prusa i3. Commonly the Y axis is the heat bed actuated by a stepping motor, which is connected to the heated via a rubber timing belt. The hotend is mounted to one or two axes actuated by its own stepping motor also connected via a timing belt. Regarding the Z axis some printers have on axis but this configuration leads to vibration and stability issues, which are reflected in the objects manufactured. Commonly the Z axis is actuated by two stepper motors mounted on their continuous leadscrew located on each side of the gantry. A typical cartesian printer can be seen in figure (2.8-1).

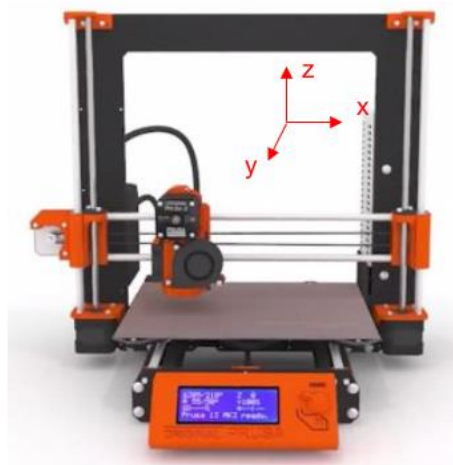


Figure 2.8-1: Prusa MK2 cartesian FDM machine

With the exponential increase in companies manufacturing 3D printers all over the world, the technology keeps improving although the concept has its improvement limits. Most of the improvements lay in the sensor, motherboard, stepper motors, stepper drivers, heat bed and most importantly the hotend. The design of the Cartesian 3D printer hasn't changed since the original Prusa in 2012. The hotend is the crucial part of a 3D printer. If the hotend can't reach the desired temperatures the melt the thermoplastic material the deposition of the material on the heated bed will result in design errors. The design errors can be uneven layers and weak bindings between the layers of material or clogging inside the heat chamber of the hotend. In our case the hotend needs to have a sufficient volume in the melting chamber to properly imbed the filament into the thermoplastic.

2.9. Polar printers

Polar 3D printers use polar coordinates instead of Cartesian coordinates to create an object. The build platform tilts and moves along the X and Y axis whereas the hotend moves along the Z axis figure (2.9-1). Polar printers are mechanically and structurally lighter to build than other printers. Only two stepper motors are required in order to execute the motions of the build platform and the hot end whereas Cartesian and Delta printers need at least three motors. Polar 3D printers are still in their early stage of development and are not yet as reliable as the Cartesian and delta 3D printers. They

are new on the market and suffer from design issues like a missing heated bed for materials that need heat in order to stick to the heated bed.

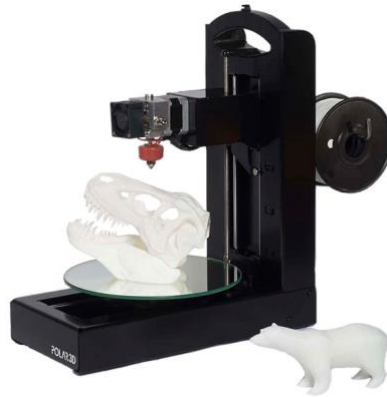


Figure 2.9-1: Polar3d polar FDM machine

2.10. Carbon Fiber Reinforced Thermoplastic Polymer Printer

The very first commercialised Composite 3D printer was launched by Markforged [40] in 2016 called the Mark two figure (2.10-1). Markforged developed the Mark two in order to combine a specific Thermoplastic with either Glass, Kevlar or Carbon fiber. The Mark two is a Cartesian 3D printer, which can be only controlled by a slicing software developed by Markforged. The internal temperature inside the machine must not reach more than 40°C otherwise the hotend will have an excess of heat and the thermoplastic will deform before it reaches the hotend as the hotend already emits heat.



Figure 2.10-1: Maker forged Mark 2 CFRTP FDM machine

This machine can only combine a specific thermoplastic developed by the company in order ease the adhesion of the fiber to the thermoplastic. Unfortunately, the composite manufactured by the Mark two can't be identified as an actual composite laminated structure because the carbon fiber is stack up on the surface of the previous layer of thermoplastic. The carbon only covers certain layers of the composite like a sandwich layup. The Carbon fiber is only deposited on the surface of the previously printed thermoplastic layer and due to the nylon based surface coated Carbon fiber the fiber is placed on the surface of the thermoplastic by the hotend and bonded with the previous layer of thermoplastic figure (2.10-2). The downside of this method is the lack of embedding of the matrix with the carbon fiber, the bundles are not fully embedded in the nylon (air bubbles) resulting into a low interfacial strength between the matrix and the carbon fiber and impact resistance.



Figure 2.10-2: Mark 2 printed samples

2.11.Filaments

There is a wide range of thermoplastics used in Additive manufacturing like: PLA, ABS, PET, PC, PEEK or Nylon. Beside PEEK these thermoplastics once extruded are not suitable for aerospace nor automotive application unless they are used for internal components or for an environment where high mechanical properties are required. Injected moulding is a costly manufacturing and time consuming method. The moulds are expensive and the injection system needs a constant maintenance in order to avoid clogging of the hotend. In additive manufacturing mechanical properties of thermoplastics can be combined with additives like: Carbon fiber, Glass fiber, or Kevlar, which have better mechanical properties than thermoplastics under their raw form. The additives for the existing CFRTP samples are added to the thermoplastic during its manufacturing process with fiber under the form of powder or short pieces. CFRTP manufactured using 3D printing has been attempted by several companies with different approaches. Proto Paste, Rigidink, ColorFabb, Markforged. Only Marforged and Rigidink manufacture a Carbon Reinforced Nylon Onyx (Markforged) and NylonX (Rigidink) where the Carbon fiber is under the form of short fibers with a fiber content of 15%. Nylon is more suitable than any thermoplastic on the market. It has the highest tensile strength and a considerable impact resistance, moreover it is a lot cheaper than modified Thermoplastics like ULTEM thermoplastics or PEEK used for aerospace applications. Most companies on the market blend their Carbon fiber powder with PLA (Polylactic Acid) or ABS (Acrylonitrile butadiene). PLA is extracted from the biomass like: crops, sugar or beets. It is a biodegradable short molecular material and its structure is very brittle after being extruded. The problem with short molecules in additive manufacturing is their weak bonds but PLA and ABS price per kilogram are more attractive than other thermoplastics. After being recycled short molecules degrade very quickly. Their molecular degradation has a direct effect on their mechanical properties and makes them weaker. Also 3D printed parts are very sensitive to heat. For instance if a 3D printed UAV made of PLA would fly on a sunny day, the structure would start warping and deforming ending in a failure of the structure. PLA doesn't require any specific heat for the print bed and it doesn't produce any toxic fumes when processed. Whereas ABS is extracted from oil and has a much higher tensile strength than PLA but during its printing process toxic fumes are

produced. ABS has a higher flexural strength than PLA, it is used for car bumpers, dashboard and Legos. It doesn't make it suitable for rigid structures or parts which are under high mechanical stress. ABS needs to be heated at 250 degrees in order to be extruded correctly. At this temperature the Carbon fiber bundle is affected by the heat and degrades. Therefore, a Carbon fiber surface coating can be applied to the bundle, which is derived from a similar chemical composition than ABS. To save time Markforged Carbon Fiber bundle has a surface coating matching the chemical composition of Nylon. Due to this surface coating, the carbon fiber is easily embedded with the Nylon in the heat chamber of the hotend and extruded. The critical settings for this process to succeed is the material flowrate, which has to be determined in order to give the carbon fiber enough time to absorb the nylon and be fully embedded in the thermoplastic. For this research we used the Taulman Nylon Alloy 910, which is the only Nylon on the market with the highest mechanical properties for automotive, naval, medical and aerospace applications.

2.12. Design requirements for aerospace structures

Aerospace manufacturers like Boeing, Airbus, Lockheed Martin, Northrop Grumman) substantially try to reduce the total life cycle costs of their products. By reducing the life cycle costs to acceptable levels including all acquisition costs, design, personnel and manufacturing costs many nations will be interested to replace their manned aircrafts by UAVs. They don't need life systems, handle longer flight times, be very small and stealthy and can fly at higher speeds than a human piloted aircraft. The answer is UAVs can be small enough to be transported in a soldier's backpack or in the cargo compartment of a vehicle and be operated easily piloted by a single operator.

In order to reduce the overall costs of a UAV, a few steps can be followed:

- Reduce the overall weight
- Low cost materials
- Recyclable materials
- Environmentally friendly materials
- Reduce part count (assembly parts)
- Efficiently use the cargo capacity (more compact)
- Simplified tooling
- Reduce energy consumption
- Minimise waste (cost effective manufacturing)

By reducing the size and the weight, the manufacturing and total life cycle costs will decrease. The time attributed to assemble a fighting jet like the F-16 is 60'000 hours, which represents for one employee working 40h per week 28 years to reach the 60'000h. So this represents a team of 100 people working 60h shifts for 10 weeks to assemble one aircraft. Dassault manufactures 2 Rafal fighter jets per year.

UAVs can be manufactured in a shorter time period especially by using a different manufacturing approach like rapid prototyping. Rapid prototyping technologies can influence the manufacturing time and costs considerably in fact rapid prototyping is a technology, which is highly automated and requires less technicians and engineers. Virtual prototyping, simulations, modelling and computer aided designs have a positive impact on the cycle time and costs. CAD designs and simulations can be modified in

a short period of time and at very low cost. Simulations can be used to predict or evaluate problems before resources have been committed to manufacture a physical prototype. Manufacturing an aircraft requires the consideration of a range of failure modes (buckling, yielding, fracture, fatigue, corrosion, creep, impact, deformation, etc.). In order to move from the idea to an actual prototype, some variables have to be considered:

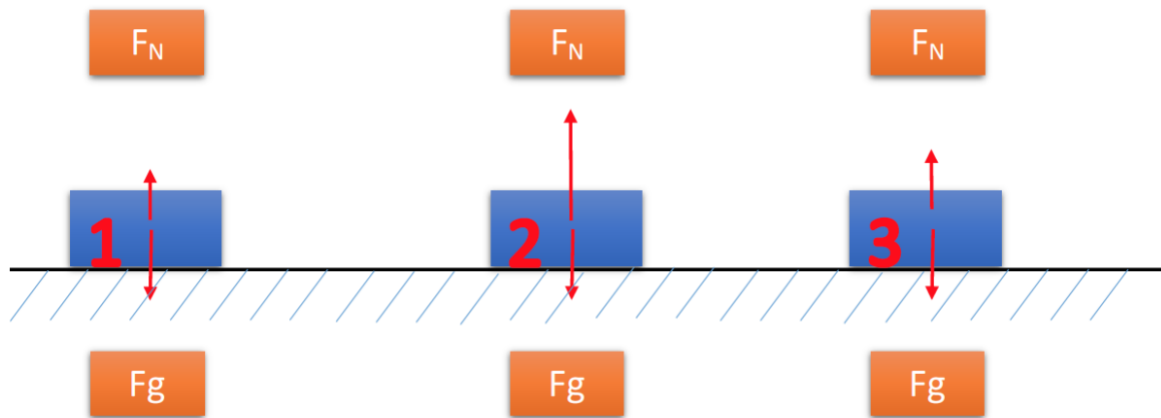
- Define the environment in which the UAV will operate (range, loads, aero elasticity, manoeuvre ability).
- Manufacturing costs reduction by designing a cost effective airframe structure (composites, multifunctional material)
- Enhance the design to reduce the cycle time using rapid prototyping
- Novel control, smart materials, health monitoring (sensors, actuators)

The structure is affected by primary material parameters like stiffness and strength, which are characterized by design property values. These values are based on experimental data and statistic models. In aerospace more specifically in aircraft manufacturing a safety factor of 1.5 is a safety parameter, which has to be encountered in the design conditions. It is based on the ratio of ultimate strength to yield strength of common materials used for aircraft designs. So a design is made to meet a safety goal, simulations are a less expensive and more accurate method to archive structural performances without undertaking expensive tests and experimentations [31].

2.13. Energy absorption

Low velocity impact tests give us the energy transmitted to a structure or component of a structure and its ability to absorb this energy ideally without structural disintegration. This scenario can be represented when for example a UAV is performing an emergency crash landing. When a UAV loses contact with the ground or the tank/batteries run out of fuel/power, an emergency crash landing will be executed. Common UAVs fly at low altitude, for this study we will consider the example of a UAV performing a crash landing just after an engine shut off after take. When the

UAV hits the ground there is a change in kinetic energy equal to the net work done from the ground to the UAV figure (2.1-1).



- 1** First impact touch on the ground
- 2** F_N will reach a pic
- 3** End of impact phase

Figure 2.13-1: Impact behaviour of an object air to ground

Furthermore, let's assume the object, which is in this case a small UAV its mass is equal to 5kg and the time laps the object absorbs the shock is 0.1 second.

2.14. Low velocity impact setup

There are three different categories of impact testing, low-, high velocity/ballistic impact and hypervelocity impact. Hypervelocity impact is referred to space vehicles and hypersonic structures [32]. For this research we will initially focus on the low velocity impact testing using a drop weight impact machine. The drop weight impact machine is a testing method commonly used for low velocity impact to analyse the impact behaviour of the of a composite. The plastic and elastic deformation done to the part are called energy absorption in form of a deformation, friction from the frame holding the part and the part itself and the kinetic energy reached by the part. The amount of stress applied to the part depends on the amount of energy absorbed by the deformation [33]. In figure (2.14-1) is the drop tower used of this experiment.



Figure 2.14-1: Drop tower

A mass is driven in its free fall and accelerate up to a desired impact energy when it reaches the test sample. The parameters for this experiment are the mass of the impactor W and the impact velocity v_0 . In addition to the weight of the impactor a calibrated disc weight was added to the gantry to reach a total mass of 5kg. A pneumatic break is engaged in order to avoid multiple strikes when the impactor hits the surface of the sample. At amount of energy at the moment of the impact is 10J. A 4 point clamping system with rubber tips is used to hold the sample in place figure (2.14-2).

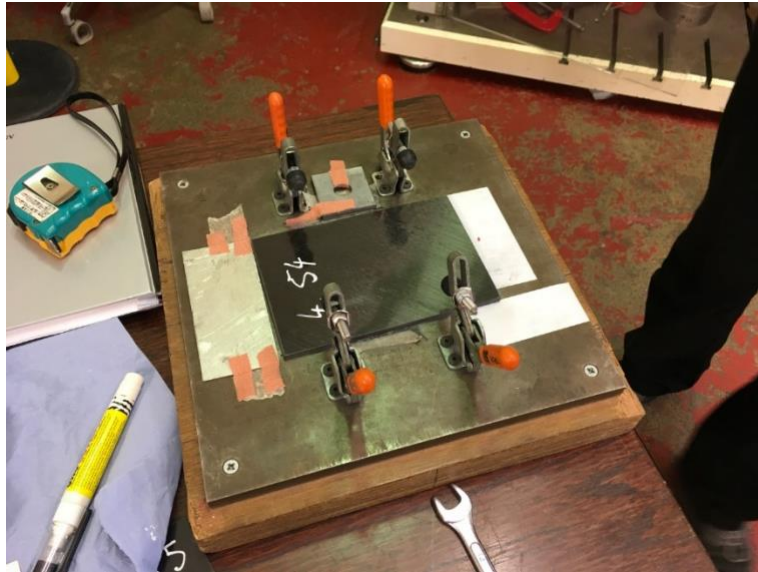


Figure 2.14-2: Low velocity impact test sample clamping system

2.14.1. Impactor

The shape of the impactor has an effect on the low velocity behaviour of the test sample. Therefore a study has been conducted to investigate the difference between a conical, hemispherical and flat impactor on the test sample. Each impactor had a different peak load on the test samples. The larger the contact area the higher is the load force applied to the test sample [34]. Another study prove that the more blunt the shape of the impactor gets the more penetration is observed on the test sample. [35] Therefore less energy is absorbed during impact. A larger contact area increases the contact force and decreases the duration of contact. In conclusion with a sharp impactor a higher amount of damage occurs to the sample with the same energy. In this study we are looking for the highest amount of energy that the test sample can absorb without undergoing a penetration of both sides of the sample. Therefore, a hemispherical impactor has been chosen for our low velocity impact tests.

2.15. Mechanical properties and process parameters

The mechanical properties of the thermoplastic Nylon 910, carbon reinforced thermoplastic need to be determined. By testing the mechanical properties of our test samples, we will be able to conclude if the carbon reinforced thermoplastic Nylon 910 can compete with existing CFRTPs on the market. Due to these mechanical

properties, we will be able to understand the fracture during flexural and tensile tests of the CFRP thermoplastic. The samples will be tested through American Society for testing and materials (ASTM) standards [36][37]. For tensile testing the ASTM D638-10 standard will be followed [37] and for the flexural testing the ASTM D790-10 standard (Test methods for flexural properties of unreinforced and reinforced plastics and electrical insulating materials).

2.16. Test samples

The tensile samples have been designed according to the BSI BS EN ISO 527-2-2012 standards for plastic determination of properties. A series of tensile samples have been manufactured. We initially started our test with pure Nylon samples, SCFRN and finally CCFRN samples. 3 samples of each Nylon and SCFRN were manufactured using an 0.6mm nozzle and 3 samples of each Nylon, SCFRN and CCFRN were manufactured using an 0.8mm nozzle. The dimensions can be seen in figure (2.16-1).

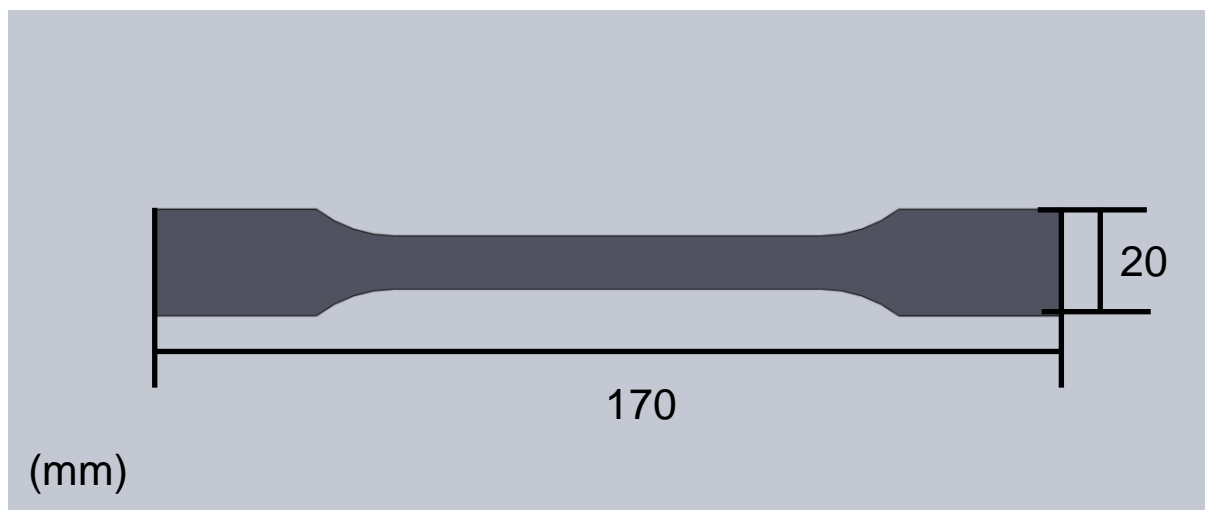


Figure 2.16-1: Tensile sample geometry

The low velocity impact samples have been designed according to the ASTM D7136/D7136M -15 standards for measuring damage resistance of a fiber reinforced polymer matrix composite to drop weight event. Regarding the fiber orientation for each sample the following code has been followed: [-45/45/0/90/0/90]^os. This lamination code has been chosen according to the literature.

A series of impact samples have been manufactured. We initially started our test with pure Nylon samples, SCFRN and finally CCFRN samples. 3 samples of each Nylon and SCFRN were manufactured using an 0.6mm nozzle and 3 samples of each Nylon, SCFRN and CCFRN were manufactured using an 0.8mm nozzle. The dimensions can be seen in figure (2.16-2).

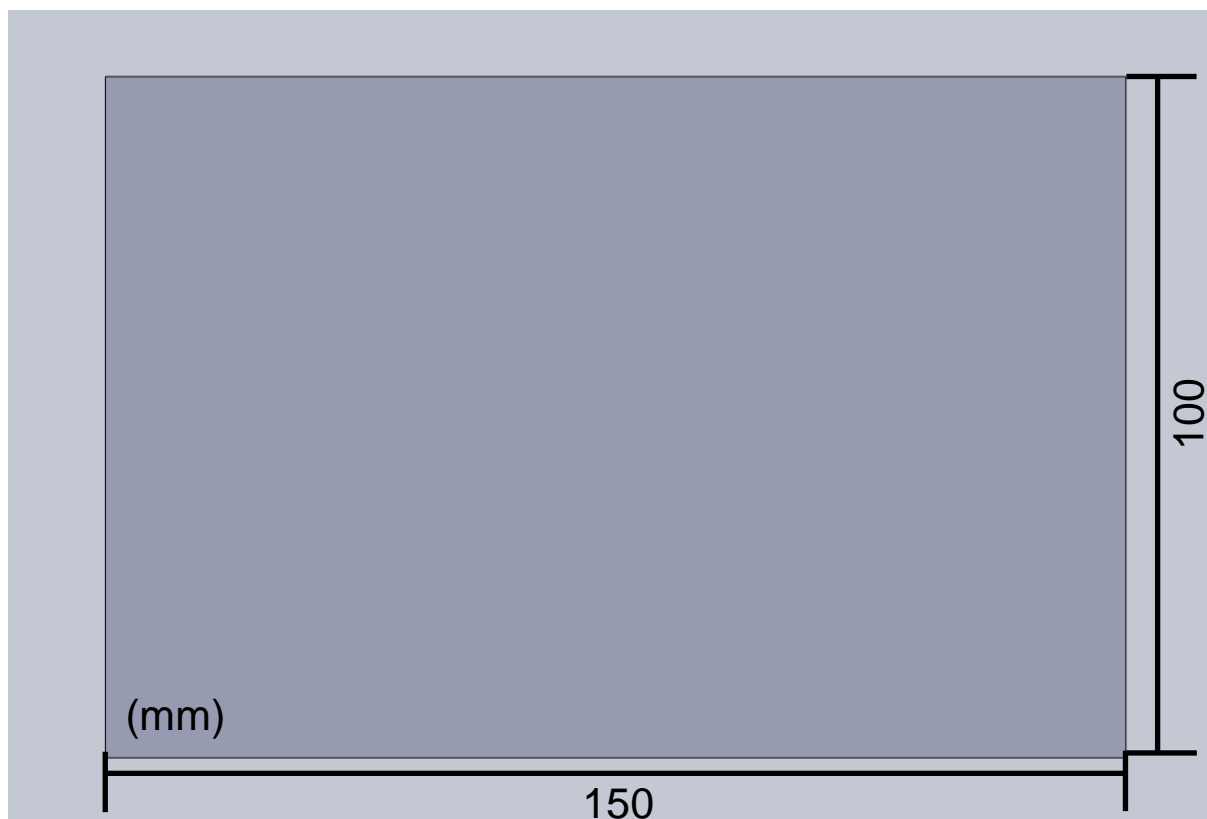


Figure 2.16-2: Low velocity impact sample dimensions

2.17. G code

G code is a numerical control programming language for automated machines. Designed by the MIT in 1950. Later in the late 60s G codes became more standard through Binary Cutter Language, which primary purpose was to be used on CNC tooling machines [38]. Unfortunately, G coding is a very poor programming language as it executes code line one at a time. It is far from any C coding language where loops and functions can be applied. Although its weaknesses G coding is ideal for additive manufacturing methods such as 3D printing as the material is deposited on a planar sequence and stack on top of each other.

2.18. Problem definition and objectives

Pure Thermoplastics are not reliable and suffer from critical lack of improvements in strength. Thermoplastic reinforced composites represent an effective solution for the future applications with several parameters which have to be investigated in order to improve the strength. Once every single parameter is taken into consideration and the 3D printer is perfectly calibrated, the manufacturing process can be launched without any supervision. The key to achieve a quality product is to design and build an FDM machine capable of printing a continuous carbon fiber integrated into a thermoplastic matrix. Therefore not only the structural part of the machine need to well thought off but also the programming part more specifically the PID tuning of the machine and servo actuation of the cutting tool. Moreover a specific G code sequence needs to be developed in order to precisely tell the servo when to actuate to cut the fiber at the right time. The mechanical properties and weight of coupon samples from nylon-carbon fiber composite will be compared with other samples made of pure nylon 910 and Carbon fiber reinforced composite. In order to avoid voids/gaps in the composite structure a solution has to be found to treat the carbon fiber filament [39]. This will reinforce the interfacial bonding between the fiber and the matrix improving the flexural strength, stiffness and impact resistance of the composite [17].

Chapter 3

Design

3.1. Introduction

The most common manufacturing methods in additive manufacturing are Injected Moulding and FDM or also called FFF. None of these existing methods can provide a fully integrated continuous carbon fiber bundle into a thermoplastic resin matrix. The only company that provides a similar product capable of combining continuous Carbon Fiber and a Thermoplastic is Markforged [40]. The CFRTP Carbon Fiber Reinforced Thermoplastics are a future solution for producing less waste using recyclable material compared to composites. CFRP Carbon Fiber Reinforced Polymers are difficult to recycle. Only a small percentage of the composite can be recycled and reused. The concerns with recycling CFRPs is the recycled carbon fiber, which is transformed into powder. Carbon fiber powder has low mechanical properties and can only be used for limited applications, where less mechanical properties are required.

3.2. Actual design

For this research a base 3D printing model has been chosen for the high quality aluminium T frame and low price. The 3D printer is a Cartesian printer an assembly kit from Tevo Tarantula [30]. After a few test many problems immerged while printing caused by the poor quality of the components. After a few tests the regularity of the layers was inconsistent, which had a direct effect on the part geometry and mechanical properties.

3.2.1. Frame

The main factors affecting the print quality were the vibrations caused by the poor structure quality of the moving axis of the printer. Each axis was mounted on acrylic plates fitted with wheels figure (3.2-1). Each axis plate moved along the T aluminium frame of the printer. The vibrations caused by this method had a direct effect on the z axis shifting of the layers. This led to a poor interfacial bonding between the layers of the printed parts reducing significantly its mechanical properties.



Figure 3.2-1: Original rail guides for x axis gantry

The solution for this matter was to replace the axis mounting system with linear guided ball bearing steel rails figure (3.2-2). Steel rails prevent vibrations and axial shifting. These rails are used in high precision machines like CNCs.

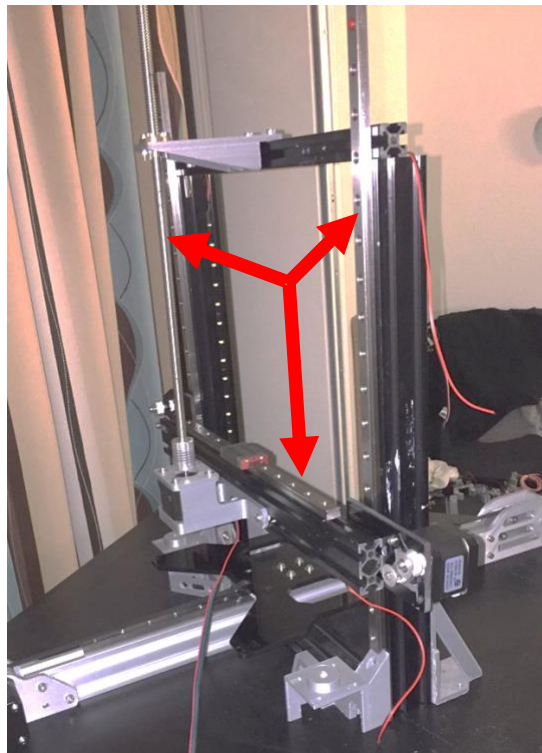


Figure 3.2-2: Linear bearing rails for x, y and z axis

This had a direct effect on the print quality but there were still some issues in the z axis where the hotend is mounted. The problems came from the single z axis lead screw, which was mounted in the centre of the x axis but the latency (left and right motion of the frame) caused by the moving hotend generated oscillations of the x axis affecting the layer deposition on the build platform. The layers were inconsistent and off course of their initial print path leading to layer skipping problems

3.2.2. Vibrations

To cancel the latency (left and right motion of the frame) dual z axis lead screws had to be added to the 3D printer, resulting to a more stable motion of the z axis. The corrections made to the machine had a direct effect on the print quality. Although, there were still irregularities in the layers. On each lead screw vibration dampeners had to be mounted with backlash spring-loaded brass nuts and specific mount had to be model and manufactured figure (3.2-3/b). This system is commonly used for high torque stepping motors, which rotate a lead screw or a shaft. After each layer a retraction of the z axis stepping motor is conducted by the system in order to avoid any pulling of the fresh deposited material.

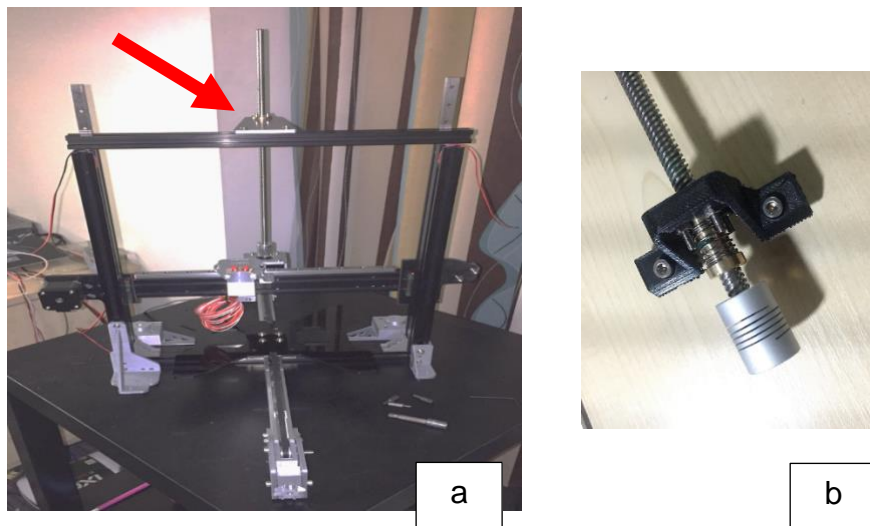


Figure 3.2-3: Single Z axis lead screw a, Z axis spring loaded backlash system b.

In order to cancel the latency dual z axis lead screws had to be built into the 3d printer, leading to a more stable motion of the z axis. The corrections made to the machine had a direct effect on the print quality. Although, there were still irregularities in the layers. On each lead screw vibration dampeners had to be mounted with backlash

spring-loaded brass nuts. This system is commonly used for high torque stepping motors, which rotate a lead screw or a shaft. After each layer a retraction of the z axis stepping motor is conducted by the system in order to avoid any pulling of the fresh deposited material. Another upgrade has been added to the z axis by adding another stepping motor to the left hand side of the printer figure (3.2-4/a). This had a direct effect on the load distribution of the moving z axis offering a higher retraction of the axis when changing layer. The result was a perfect layer adhesion and layer deposition. The vibrations and latency of the hotend caused by the unstable z axis has been solved figure (3.2-4/b).

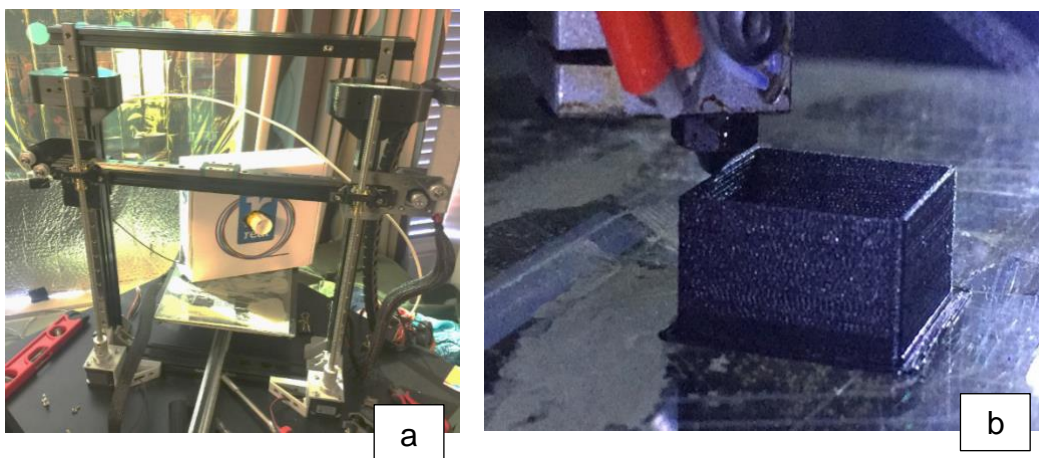


Figure 3.2-4: Final FDM design and test print

3.2.3. Electrical components

The initial 3D printer control board was a MKS 1.4 (12V) 8 byte. MKS motherboards are cheap and widely used on the 3D printing market. They are similar to an Arduino mega with an ATmega1280 microcontroller. Unfortunately, one stepper drive after another started failing causing the printing processes of the machine to fail. The motherboard has been replaced by the duet 2 WIFI board, which has a 32 byte with inbuild stepper drivers and a much higher processing power figure (3.2-5).

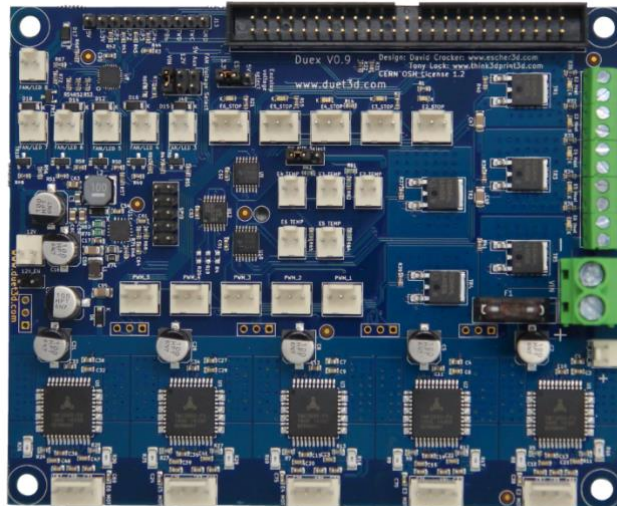


Figure 3.2-5: Duet WiFi 2 32 bit board [42]

Cooling fans have been added on top of the motherboard to preventing the stepper motor drivers to overheat. An additional fan has been added to the power converter to prevent it to overheat. The power converter (500W) converts the input voltage of 230V to 12V, which supplies power to the motherboard and additional electrical components of the printer. The Critical electrical components have been mounted under the machine in order to have more clearance to access the components and to prevent them from overheating in the containment chamber (40°C). The cables run along the printed straight through the table directly to the components.

3.2.4. Extrusion system

Experimental extrusion systems like the Cyclops hot end form e3d ltd. or the dual path system are able to extrude two materials at the same time unfortunately these extrusion systems are built to extrude simultaneously materials, which have the same mechanical and thermal properties figure (3.2-6/a). In order to integrate Continuous Carbon Fiber a homogeneous integration system has to use in order to avoid any clogging while extruding the material. Moreover, a homogeneous heat distribution is required along the passage of the Fiber through the throat of the hotend in order to embed the Fiber into the Thermoplastic matrix. To prevent any curling of the fiber the hotend needs to be cleared of any disruptions in the internal structure of the hotend figure (3.2-6/b). A constant and undisturbed flow of the Fiber through the throat of the

hotend is crucial to achieve a successful deposition of the material. Two hotend design have been compared and tested figure (3.2-14).

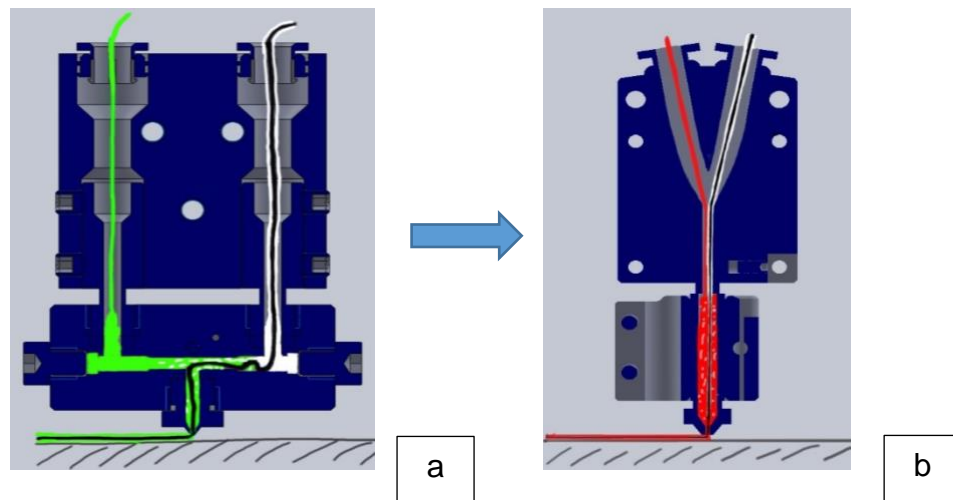


Figure 3.2-6: a) Extrusion systems Cyclops vs b) Dual extrusion hot end

The long heater cartridge represents a significant advantage over any other hotend on the market. It offers a more constant and stable heat propagation throughout the throat of the hotend. This system is ideal to combine two similar materials and extrude them simultaneously. Unfortunately, due to its right angle transition area between the throat and the heat block the Fiber will curl pushed by the feed of the incoming material from the first input throat. The dual extrusion hotend has shown more promising results than the cyclops hotend.

A dual cyclops hotend originally used for dual colour prints has been modified in a way to print simultaneously two different materials. Unfortunately, the high heat generated by the hotend had to be controlled. A novel method to cool the hotend has been developed using high speed radial fans integrated to the hotend structure and a cooling structure design has been introduced to the hotend for a more efficient airflow around the heatsinks of the hotend. Moreover, a probing sensor had to be programmed into the motherboard of the printer to use an advanced probing system to determine the optimal high of the hotend before the printing process started figure (3.2-7).



Figure 3.2-7: Final design dual extrusion system with radial fans

3.2.5. Heated bed

Some of the filaments required a steady high temperature of the heated bed in order to keep the adhesion as steady as possible. The high power 500 W heated bed from e3d is one of the fewest heated beds on the market able to keep a steady temperature, which can go up to 200°C in a very short period of time. Compared to the previous heated bed, which was an unbranded aluminium plate using a 40W heater cartridge using 12V DC the e3d bed is on the other hand a 240V AC independently powered through the power socket figure (3.2-8). With such power hardware extra safety precautions have to be taken in order to prevent any accidents.

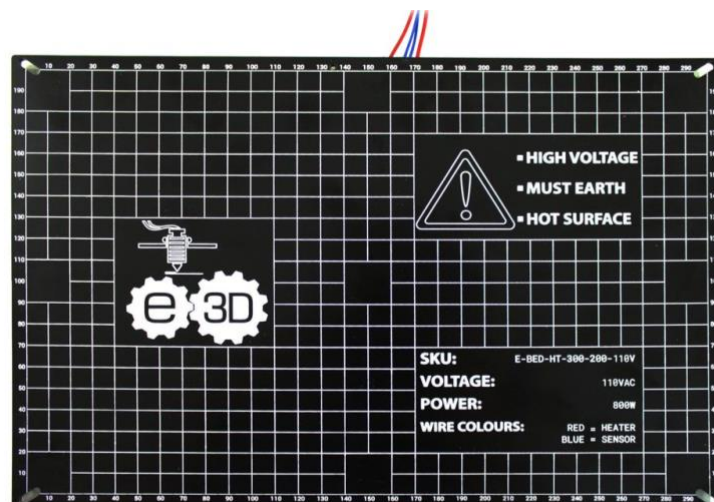


Figure 3.2-8: e3D 240V AC heated bed [29]

The heater cartridge is a silicon based patch covering the entire surface of the bed spreading simultaneously the heat evenly across the surface of the bed. For safety a Solid State Relay had to be installed in order to have reliable power control for the heated bed. In figure (3.2-9) a high heat silicon thermistor can be seen, which uses to achieve high temperature with a more even distribution of the heat on the surface of the heated bed



Figure 3.2-9: e3D silicon thermistor pad [29]

3.3. Fiber cutter

After designing and testing different fiber cutter designs one design has shown more potential than the other. Even if the first design showed positive results the second design was more reliable but needed more coding for the motherboard and the g code used by the slicer needed to be adjusted in order to cut the fiber at the right moment. In order to have a sufficient amount of force to cut the Carbon Fiber a 20 kg/cm digital servo had to be added to the design and a 200 micron thick titanium blade, which is actuated by the servo in a shear motion.

3.3.1. Design 1

The initial idea was to use a direct drive stepper motor mounted on the hotend feeding the filament through a PTFE tube. The clamping system was similar to a robot arm used by NASA for the Mars rover, which would cut the fiber at the end of each deposited layer. In order to actuate the closing and opening motion of the arm both the servo as well as the arm had to be mounted to the hotend. With a significant weight increase and compromising the travel distance of the hotend along the X axis the travel speed of the X axis stepper motor had to be significantly reduced. With a reduced

travel speed the printing time was doubled. Moreover, the arm had to be open at its widest in order to avoid any collision with the printed parts. Furthermore, to prevent the collision of the arm with the printed parts a specific sequence in the g code of the slicer had to be added in order to end each layer on the right hand side if the printed object as the support structure and joints of the arm were lower than the nozzle height of the hotend. Design 1 is represented in figure (3.3-1).

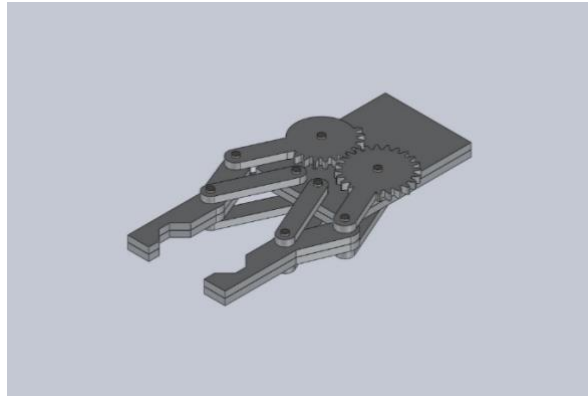


Figure 3.3-1: Cutter 1 clamping design

3.3.2. Design 2

With a Bowden system the exact length of material deposited for each layer needs to be known as the distance between the Bowden stepper motor and the hotend is significantly longer than a direct drive system. Before the filament enters the PTFE tube at the end of the Bowden system the cutting servo is actuated cutting the Carbon Fiber filament. The distance between the beginning and the end of the PTFE tube needs to be considered in the printing sequence of the slicer in order to extrude the exact amount of pre-cut Carbon Fiber from the beginning of the layer to the end. For the next layer the stepper motor of the Bowden extruder accelerated the feed rate of the Carbon Fiber until it reaches the hotend and is ready for another layer. When the feed rate is accelerated the length of the tube has to be considered in the g code of the slicer and in the programming of the cutter on the motherboard firmware. Design 2 is represented in figure (3.3-2).

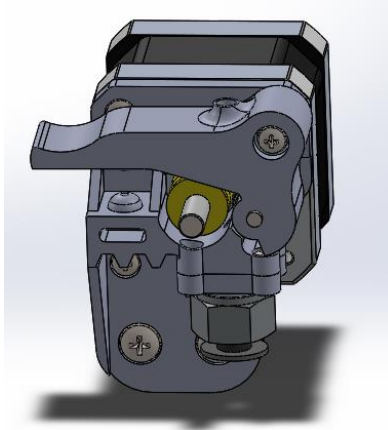


Figure 3.3-2: Cutter 2 Bowden design

3.4. G code for slicer and programming

The transition sequence between the layers of the deposited material on the heated bed. G coding has very specific coding commands predefined in the main firmware of the motherboard controlling the machine. The key is to develop a specific G code sequence in order to push forward the fiber through the PTFE tube attached to the cutting system of the printer. Once the fiber is pushed forward a new layer of material can be extruded. It is important to have a G code sequence pushing the fiber forward otherwise for the new layer of material that needs to be extruded the continuous carbon fiber will be missing. On the other hand the C code needs to actuate the cutting system at the right moment in relation to the G code sequence. A specific library has been developed for the communication between the motherboard and the servo motor of the cutting system in relation to the G code sequence of the slicing software. In Appendix A parts of the C coding sequence can be found, most importantly the PID tuning of the machine allowing a smooth motion of the stepper motors.

G28 X0 Y0	X and Y axis are homed
G91	Relative position for XYZ set
G1 Z5	Z axis raised by 5mm
G90	Absolute position set for XYZ
G1 E70.00 F5400	Extrusion motor CF push forward to heat treat
G91	Relative position for XYZ set
G1 Z-5	Z axis lowered by 5mm
G90	Absolute position set for XYZ
G92 E0	Extruder origin reset

3.5. Containment chamber

Printing Nylon requires high temperatures not just from the hotend but also for the environments in which it is printed. If the environmental temperature is too cold the Nylon will come off or warp from the build platform. Integrating Carbon fiber to an unstable thermoplastic matrix won't be feasible if a stable environmental temperature is not achieved. Therefore, a containment chamber with fumes evacuation system, has been developed. The walls are made of blue foam (high density) coated with 2mm of concrete (high thermal mass) providing an optimal thermal isolation figure (3.5-1).



Figure 3.5-1: Containment chamber with extraction fans and temperature regulator

To prevent any excess heat in the chamber a relay fitted with a thermostat triggers five fans, three that push fresh air in and two that suck air out through the active coal. The thermostat is mounted in the back of the chamber at the same height than the hotend while it prints the first layers of a part. The reason for this configuration is for its simplicity and because heat rises upwards in a closed room at the bottom the temperature needs to be stable to have the best possible environmental conditions for the printing process. To avoid any environmental contamination, a particle filter had to

be implemented to filter any burned Nylon from the hotend filling the containment chamber with toxic gases. A novel design has been introduced using charcoals as a particle filter and two high-speed fans to suck air out of the containment chamber figure (3.5-2). The fans are automatically triggered by a relay and a temperature sensor as soon as the temperature reaches 40°C. This temperature is the optimal environmental temperature to print nylon 910.



Figure 3.5-2: Filtration system

Chapter 4

Manufacturing

4.1. Introduction

Carbon fiber reinforced thermoplastic polymers are a future solution for producing less waste using recyclable material compared to composites. Carbon fiber reinforced Polymers are difficult to recycle and only a small percentage of the composite can be recycled and reused. Thermoplastics are easy to reuse with deteriorating the fiber during the recycling process. On the other long molecular Thermoplastics like Nylon can be recycled a few time without losing any mechanical properties on the matrix. A few parameters need to be investigated before manufacturing our CFRTP composite. In this chapter we investigated the process parameters required to manufacture CFRTP composite. Test samples have been manufactured and tested to determine their mechanical properties such as tensile and low velocity impact according to British Standard Testing Methods.

4.2. Material consideration

Material consideration is crucial when printing a composite especially the combination two different material with different material properties. In this research we chose to use a nylon as our thermoplastic material for the matrix of our composite. There are many thermoplastic materials available on the market, which have different material potteries from each other. In this chapter we focus on the quality control of the filament and several process parameters affecting the quality of our CFRTP samples.

4.2.1. Filament quality control

3D printing initially used filament that had been intended for welding plastic tanks. The filament did not need to be very precise for that application. In the early days of filament based 3d printing the quality control on filament diameter was often inadequate. As the 3d printer filament market has grown, quality control is improving but there are still occasional inconsistencies. Common filament diameter are 3 and 1.75 mm. However, there are nominal diameters and the actual diameter may vary. To test the continuity of the filament diameter some methods are possible. The first one with a pair of callipers the diameter of the filaments thickness can be measure. Depending on the

material's density a 750 g filament spool can go from 169 m for PLA to 193.5 m for Nylon. In our case we are using a 450 g filament spools for Nylon, which represents 77.76 m. In order to save time there is another method. By printing an object (a) with one material from a manufacturer and the same object (b) with some material but from another manufacturer. For both (a) and (b) the same printing parameters were chosen as well as the same material. The only difference is the quality and price of the material. (a) is for instants a PLA from a cheap material manufacturer and (b) from an expensive manufacturer. In figure (4.2-1/a) we can clearly see the under extrusion due to the lack of continuity in the filament compared to figure (4.2-1/b).

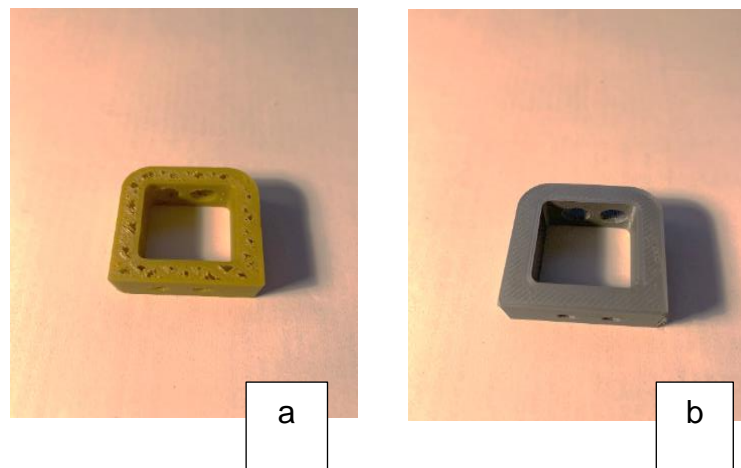


Figure 4.2-1: Uneven filament diameter (a) vs even filament diameter (b)

In some cases filament quality can clog the nozzle of the hot end because of particles contained in the material. This can also happen when the filament is recycled, therefore it is very important to have objects cleaned and cleared of debris to get recycled and extruded on a spool.

4.3. Filament storage

The storage of Nylon is crucial as the material is extremely hydroscopic. Right after purchase the material needs to be processed in an oven at 100°C for a period of 60 min. Nylon can absorb humidity up to 4% from its total mass and once printed the material will have poor mechanical properties. Further test to prove the effect of humidity on the matrix are conducted in chapter 05 testing. In order to keep our matrix

filament as well as our CF coated dry an efficient storage box had to be manufactured. A 370 x 310 x 280 mm storage box has been chosen for this experiment. 1 kg of silica gel has been added to the bottom of the box to absorb any infiltrating moisture. A 370 mm long PVC rod has been added along the length of the box in order to carry the filament spools. To prevent any humidity to build up inside the box a heater had to be incorporated. The heater used for this purpose is a reptile/ vivarium heater as it produces a gradual heat increase along the surface of the heater, which can reach 35°C. This heater has been chosen as it doesn't produce a high heat on a certain area of the heating surface when it is in contact with the silica gel and melt it down. A temperature and humidity monitoring unit has been incorporated to the box to monitor and control a trigger switch, which triggers the heater until the humidity levels drop down to 20% and turns it off once the target humidity level is reached figure (4.3-1).



Figure 4.3-1: Filament storage container with dehumidifying system

Unfortunately, within the first few day Nylon loses its mechanical properties exponentially because of its tendency to absorb water in the ambient air. therefore samples need to be manufactured within this short timeframe, which makes it rather challenging.

4.4. Process parameters

Process parameters can affect the mechanical and structural integrity of the manufactured samples dramatically if not set correctly. Such parameters are the flow rate at which the material is pushed through the nozzle, temperature of the hotend, temperature of the heated platform, layer height, extrusion speed, extrusion width and environmental process temperature.

4.4.1. Surface treatment

Only specific material can stick to a heated bed without surface treatment. Unfortunately, nylon is not one of those. Nylon has the tendency to warp and shrink after being deposited on the heated bed. There are many different methods to solve this problem. In the past hobbyists used blue masking tape, which unfortunately took time to apply on the heated bed and for some materials didn't work. Nylon is a synthetic crystalline polymer made of long repeated molecule units linked by amide links to the peptide bonds in the protein. A chemical solvent, which has the ability to debond the molecule chains of the nylon had to be investigated and tested. According to some petrochemical research on nylon a few chemicals are capable to dissolve nylon but only a few are accessible on the market. Table (4.4-2) shows the dissolution percentage of nylon over a period of 24hrs cold and with added heat. The amount of heat is according to the glass transition temperature of the Nylon at which the material starts to liquefy. The heat is provided by placing a glass jar with the chemical material and the imbedded nylon on the heated bed of the FDM printer. With a heated bed perimeter of 1000mm 10g of nylon per chemical has been tested and dissolved. After 24 hrs the remaining material percentage has been measured according to its original mass before exposure to the chemical material. In table (4.4-2) we can see the difference between the chemicals used to dissolve the nylon in cold and heated process.

Table 4.4-1: Heated bed surface treatment

Chemical	Low temp. dissolution [%]	High temp. dissolution [%]
Resorcinol	60	70
Formic acid	72	78
Calcium chloride	78	83
Phenol	90	92

Once the adequate chemical material has been found and the Nylon dissolved, the mixture is applied to the glass surface of the heated bed via a brush. After a period of 15min the material dries on the glass surface of the heated bed and will act as a primary layer providing an excellent adhesion for the first layer of the print.

4.4.2. Material flow

The flow is the amount of material pushed through the hotend over a certain period. The flow is a crucial parameter. If two adjacent deposited material paths are too close, they will overlap and if they are too distant, the gaps will be visible leading to a delamination and debonding of the layers figure (4.4-1). Thicker paths will have better bonding with the lower layer, which is ideal for mechanical parts. However the paths are not able to approximate the object shape and fill small gaps or narrow curves. On the other hand, thinner paths compromise the bonding but provide better shape accuracy. Also, the extrusion width can be controller only when extruding over an existing surface. If we extrude in free air, the resulting shape will be always round and inequal to the nozzle diameter.

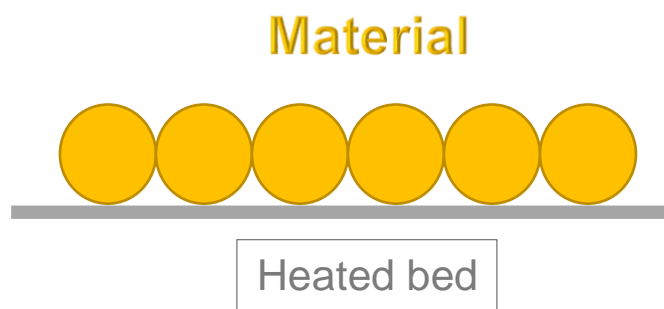


Figure 4.4-1: Material deposition on heated bed

If the material flow is reduced smaller circles will be extruded, until the plastic viscosity breaks the linkage because of too much tension. If, on the contrary, too much material is extruded, the shape of the extruded filament won't change but you'll get a loose bonding. As said above, there's only one correct flow rate for bridging: the one that doesn't make the bonding break. Extrusions are round and their diameter is equal to the nozzle diameter. Parallel paths will be positioned so that they are tangent, thus the spacing between one path and its adjacent path is equal to the nozzle diameter as well figure (4.4-3). When target extrusion width is thinner than layer height the shape is unpredictable so we just use the same rectangular formula but discourage usage of such thin extrusion values. In figure (4.4-2) we can see the effect of nozzle height on material deposition on the build platform of the FDM machine.

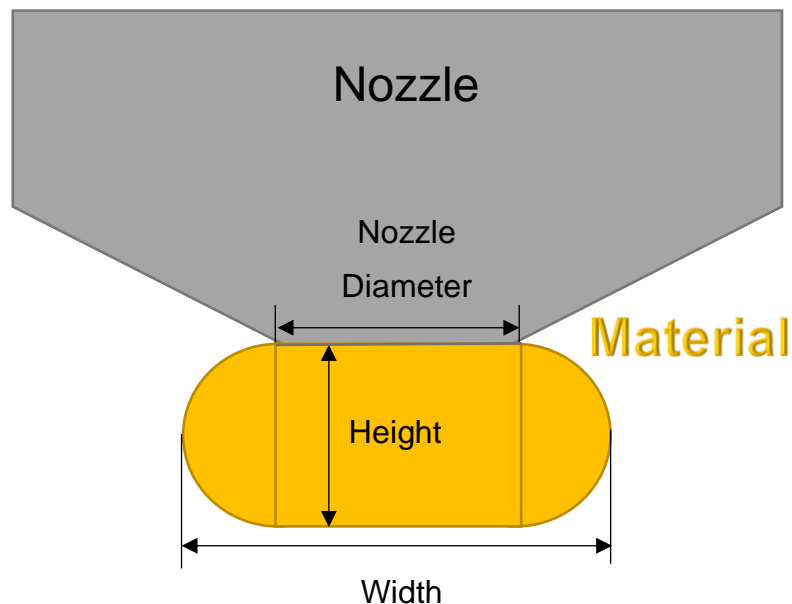


Figure 4.4-2: Effect of nozzle height on material deposition

The correlation that targets the extrusion width with the amount of material to extrude per distance unit is measured as follow:

$$A = \text{rectangle} + \text{circle} = (W - H) \times H + \pi \times \left(\frac{H}{2}\right)^2 \quad \text{Equation (4.4-1)}$$

In equation (4.4-1) A is the sum of rectangle and a circle. It represents the extruded material coming out of the nozzle and pressed on the build platform.

In our slicing software we can add the new value of the desired extrusion flow for a single path, which is represented as our E value.

$$E = f(\text{extrusion_width}, \text{layer_height}) \quad \text{Equation (4.4-2)}$$

Equation (4.4-2) basically represent the amount of material extruded though the nozzle in respect of the width of the material extruded and the layer height.

4.4.3. Spacing paths

To achieve a perfect bonding between the adjacent extruded material paths the amount of overlap needs to be determined.

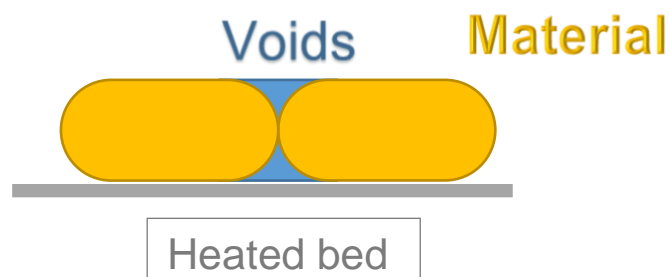


Figure 4.4-3: Voids between material paths along the plane

Voids can be determined by the following formula:

$$\text{void_area} = (\text{layer_height})^2 - \left(\frac{\text{layer_height}}{2}\right)^2 \times \pi \quad \text{Equation (4.4-3)}$$

In the equation (4.4-3) we can determine the area in blue of the void between one tool path and the other, which is represented by two rectangles and two full circles. The unit for the layer height is in millimetre. If we could fill all of that blue area by placing the extrusions closed to each other this would eliminate the voids between each adjacent material deposition. However, it's very unlikely that the second extrusion will fill the space below the previous one because the first deposition has already solidified therefore pushes the hot material extruded on the second path. Ideally:

$$0 < (\text{overlap_factor} \times \text{void_area}) < \text{void_area} \quad \text{Equation (4.4-4)}$$

Ideally the void area should be between the size of the extruded material and 0 equation (4.4-4).

The overlap factor represents how much void remains between the extrusions. It's difficult to estimate this amount, since it also depends on viscosity of the plastic, extrusion speed and temperature. In the past, several values were tried for the overlap factor but there are still voids to be seen inside the object after impact. A value of 1 is currently being used to guarantee that the error is on an overflow of material extruded rather than a lacking of material. The formula equation (4.4-5) for the path of material deposition on the heated bed is as follow:

$$\text{spacing} = (\text{extrusion_width} - \text{layer_height}) \times \left(1 - \frac{\pi}{4}\right) \quad \text{Equation (4.4-5)}$$

With the equation (4.4-5) we can determine how much space is between each material deposition in respect of the dimension of the material extruded for each path.

4.5. Extrusion

The extruder calibration is one of the most important factors for manufacturing parts that need the required mechanical properties for their application. It is often overlooked especially with plug and play FDM machines, which have to be fine-tuned. There are some key factors to concentrate on when finding the optimal steps/mm settings for the extruder. Once the correct value for the extruder is found among the corresponding nozzle diameter and layer height, the next step is to dial in an extrusion multiple. To obtain the correct value for the steps/mm a formula must be applied:

$$E_steps_per_mm = \frac{(\text{gear_ratio} \times (\text{steps_per_motor_rotation} \times \mu_stepping))}{2 \times \pi \times \text{effective_extruder_gear_radius}} \quad \text{Equation (4.5-1)}$$

It is crucial to adapt this formula accordingly to the change of material and nozzle diameter. The slicing software will recognize the equation (4.5-1) as an E10 command that 10 mm of material needs to be pushed by the extruder stepper motor through the nozzle. Unfortunately, the 10 mm recognized from the slicing software do not automatically report the amount of material extruded from the nozzle.

In order to measure the right amount of material, which need to get extruded a calibration is required. In the case of Nylon the material is flexible and less stiff then other materials the effective diameter of the hobbed gear is smaller than the actual diameter of the hobbed gear itself. This means the teeth of the gear penetrate the material more than any other material, which means that more steps/mm are required to extrude a desired amount of material from the extruder. In figure (4.5-1) the effect of the diameter of the hobbed gear teeth on the filament can be seen.

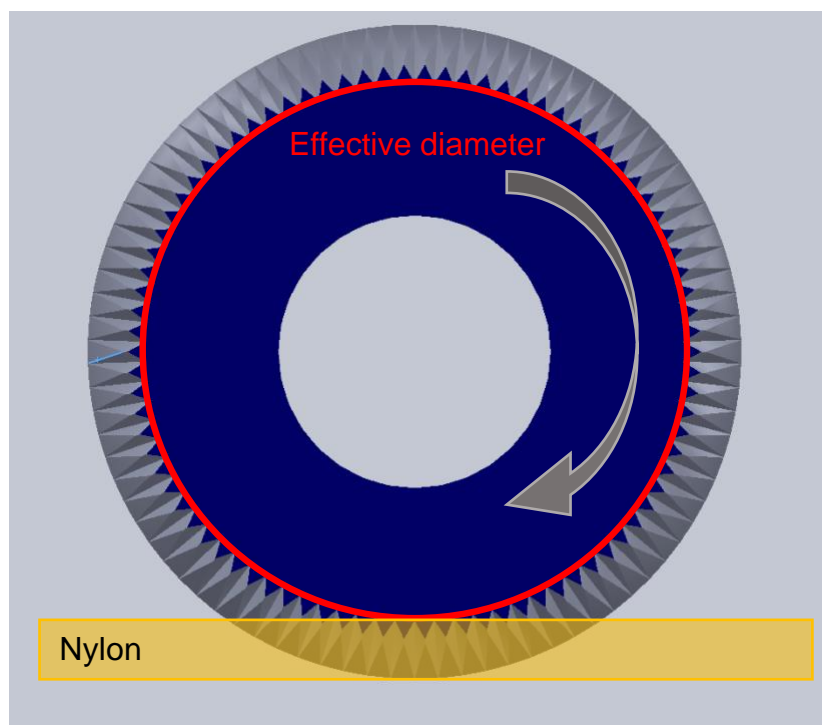


Figure 4.5-1: Hobbed gear cross-section and nylon filament

To calibrate our extrusion motor a theoretical amount needs to be taken into consideration divided by the actual amount of material extruded. This correlation can be measured with:

$$\text{Extrusion_multiplier} = \frac{\text{theoretical_extrusion}}{\text{actual_extrusion}} = \frac{10 \text{ mm}}{6.4 \text{ mm}} = 1.56 \quad \text{Equation (4.5-2)}$$

After analysing our data we came to a number of conclusions. To extrude the carbon fiber without clogging the nozzle a layer height of at least 110 % of the optimal layer height reached with the 0.4 mm need to be considered. Also it is not recommended to

print more than half of the diameter of the nozzle in layer height in order to avoid gaps/voids between the paths. This means for a 0.4 mm nozzle the layer height shouldn't exceed 0.2 mm, which has been demonstrated in chapter 05. A 0.8 mm nozzle has then been tested and the optimal layer height of 0.35 mm has been gathered from our conclusion. This layer height allows the carbon fiber to be extruded without damaging the surface of the fiber allowing and avoiding the nylon coating to degenerate due to the heat inside the melting zone of the nozzle.

4.6. Nozzle diameter

The nozzle size can affect in many ways the printed object. Not only from a mechanical point of view but also for the surface finish and printing time. The bigger the nozzle the more material will be extruded resulting in fast print time. Also the embedded carbon fiber is less exposed to the high heat in the melting zone of the nozzle, which allows the fiber to get extruded uniformly. In order to determine the adequate nozzle diameter, a range of tensile tests have been conducted on each material used in this thesis at different layer height and with different nozzle diameters. In respect of the Fiber bundle diameter of 0.33 mm, we started our test with 0.4 mm nozzle. Test results can be found in the chapter testing. The dimensions and manufacturing procedures for the tensile, flexural and impact samples are described in their respective paragraphs in this chapter. After analysing our data we came to a number of conclusions. With an 0.4 mm diameter nozzle the highest failure load was reached with the layer height of 0.15 mm. Unfortunately, in order to extrude the CF without clogging the nozzle a layer height of at least 110% of the optimal layer height reached with the 0.4mm need to be considered. Also it is not recommended to print more than half of the diameter of the nozzle in layer height in order to avoid gaps/voids between the paths. This means for a 0.4 mm nozzle the layer height shouldn't exceed 0.2 mm, which has been demonstrated in the tensile testing chapter. A 0.8 mm nozzle has then been tested and the optimal layer height of 0.35 mm has been gathered from our conclusion. This layer height allows the CF to be extruded without damaging the surface of the fiber allowing and avoiding the nylon coating to degenerate due to the heat inside the melting zone of the nozzle.

4.7. Skirt

The skirt is a base layer of material printing around the perimeter of the printed object. When the skirt is deposited around the object that will be printed, it allows us to quickly see whether there are any problems. This can be useful during a filament change of colour or material from the previous print. It is recommended to print a skirt when a different material was used for an early print because there are still residues of the previous material in the nozzle, which can end up in the new printed object and contaminate it. This nozzle cleaning procedure is also called nozzle priming. For this research printing a skirt is crucial for a successful print. Nylon has the tendency to warp. The skirt will force the printed object to stick to the heated bed especially in the corners figure (4.7-1).

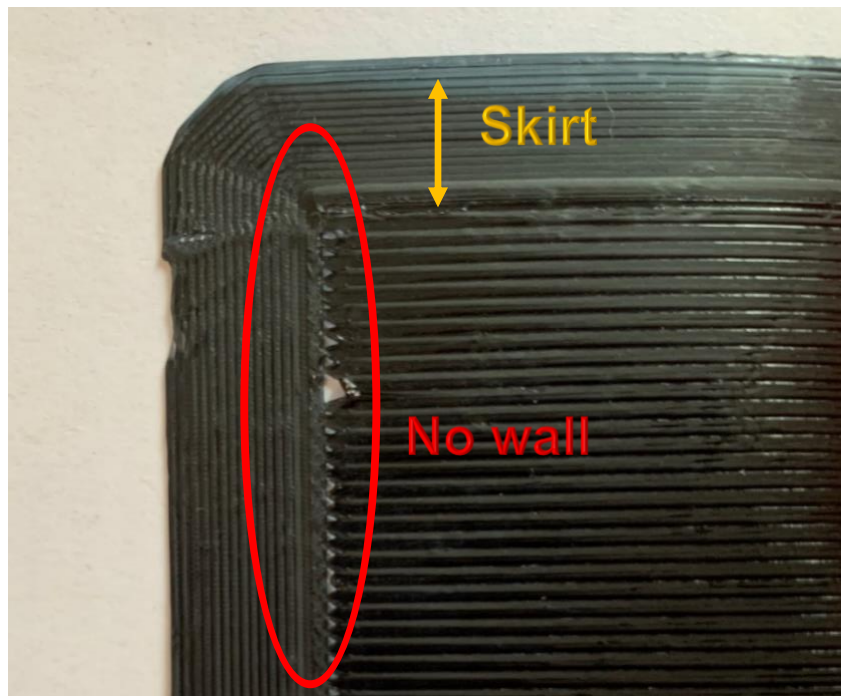


Figure 4.7-1: Skirt deposition around the printed sample

4.8. Influence of temperature and speed

Three crucial settings have to be determined before attempting a CFRTP print. The hot end temperature, heated bed temperature and print speed. Surprisingly the values given by the filament manufacturer aren't always that accurate. There are many

reasons why the filament isn't showing the exact mechanical properties as advertised by the manufacturer. The most common reason is the humidity absorption between the moment the material is rolled on the spool and delivered to the customer. There is also the fact that once acquired the material needs to be dried and stored in a dry environment. According to the manufacturer Nylon 910 need to be printed a temperature of 250-260°C. When printed at the recommended temperatures the material doesn't show the same mechanical properties as advertised by the manufacturer. Therefore the effect of the nozzle temperature has been tested in the chapter testing using tensile test bone samples with temperatures ranging from 250-300°C. After gather the result the best tensile strength of the sample has been reached for the sample printed at 300°C. Although the 300°C is the optimal temperature for the matrix material the CF on the other hand can starts degrading at 280°C, therefore the CFRTP samples have been printed at a temperature of 275°C. Also in order to reach the maximum strength capacity of the fiber the tensile bone samples have been printed in the longitudinal direction of the fiber.

4.9. Toolpath control

The start point, end point and printing direction of a single layer printing path are have been optimised in the slicing software in order to avoid any fiber crossing. By simplifying the toolpath pattern the CF cutter actuation is reduced allowing the printer to layup the layer one by one in the simplest way. This reduces the numerical processing power of the motherboard. Moreover each new layer start and end point has been optimised to start and end from the same star and end points as the previous layers. For the first 2 layers the layup direction -45° for the first layer and +45° for the second as well as the 2 last layers. The angle change for the Z axe with the hot end moves upwards to the next layer the stepper motors are slowed down in order to ease the integration of the fiber for the next layer. Also the retraction speed is augmented at the moment of the layer change, this prevents the fiber to ooze out of the nozzle and stick to the bottom layer before the stepper motors set the hotend in motion to its starting point. When the path nears to the starting point of the first printing path, the nozzle changes direction to the second path and the printing process circulates until reaching the end point of the single layer. The material stacking along the thickness

direction of each composite part follows the printing path of single layer. By taking these printing path control methods, the 3D printer efficiently achieved the aim of rapid prototyping of continuous carbon fiber reinforced Nylon composites part. Every single fiber path are uniformly compacted by employing an appropriate space between the nozzle and heating panel.

4.10. Tensile test samples

In order to determine the process parameters of each material of our composite it is necessary to run a tensile test. Not only have the mechanical properties been determined but also the process parameters necessary to manufacture our CFTRP composite. dog bone samples have been manufactured according to BSI standards ISO 527-2.1A.50 with a thickness of 7.2 mm figure (4.10-1).

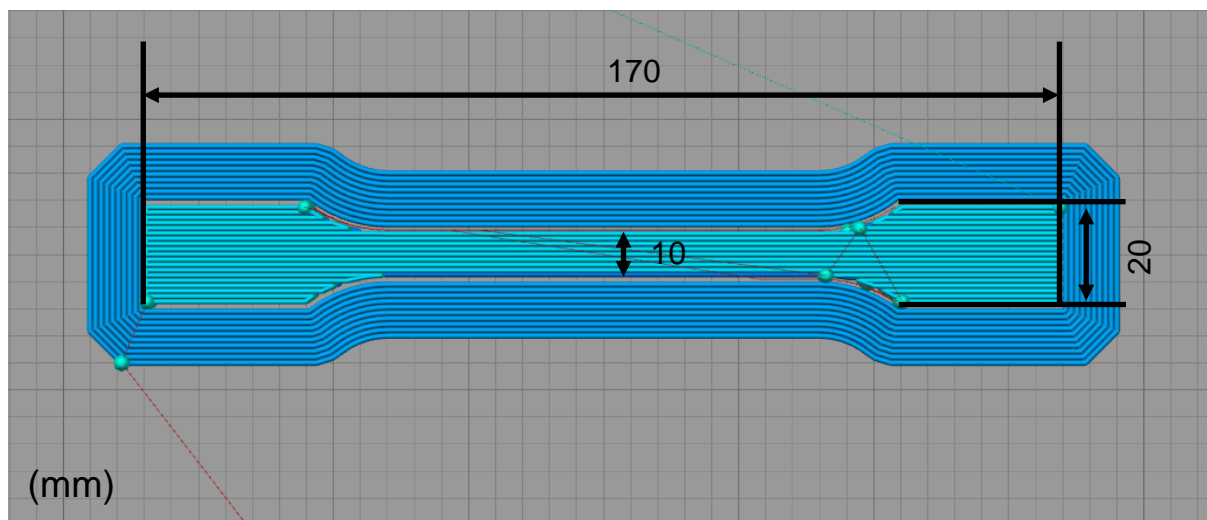


Figure 4.10-1: Tensile test sample

Two different types of samples have been tested. Continuous fiber, short fiber and pure Nylon 910. For the Nylon 910 the tensile strength reached was 0.056 GPa Surprisingly the short fiber samples performed really well with a tensile strength of 110 GPa.

4.11.Low velocity impact sample

Composites are lightweight structures due to their excellent strength/ weight and stiffness to weight ratio. The application of composite materials with continuous fibers was limited to those with thermosetting matrix. Recently the interest in thermoplastic matrix grew due to their considerable advantages not only in mechanical but also environmental applications. Thermoplastics applications for non-structural parts and potential impact sensitive areas on a structure can be used offering an alternative to thermosets, which time consuming and expensive to manufacture. In order to determine the amount of energy absorbed by our composite low velocity impact test samples test are manufactured. The layer orientation is described in the literature. In the case of a low velocity impact test for CFRP composite the ideal layer orientation is $[45/-45/0/90/0/90/0/90]_s$. The samples have been manufactured according to ASTM standard for low velocity impact testing of thermoplastics figure (4.11-1).

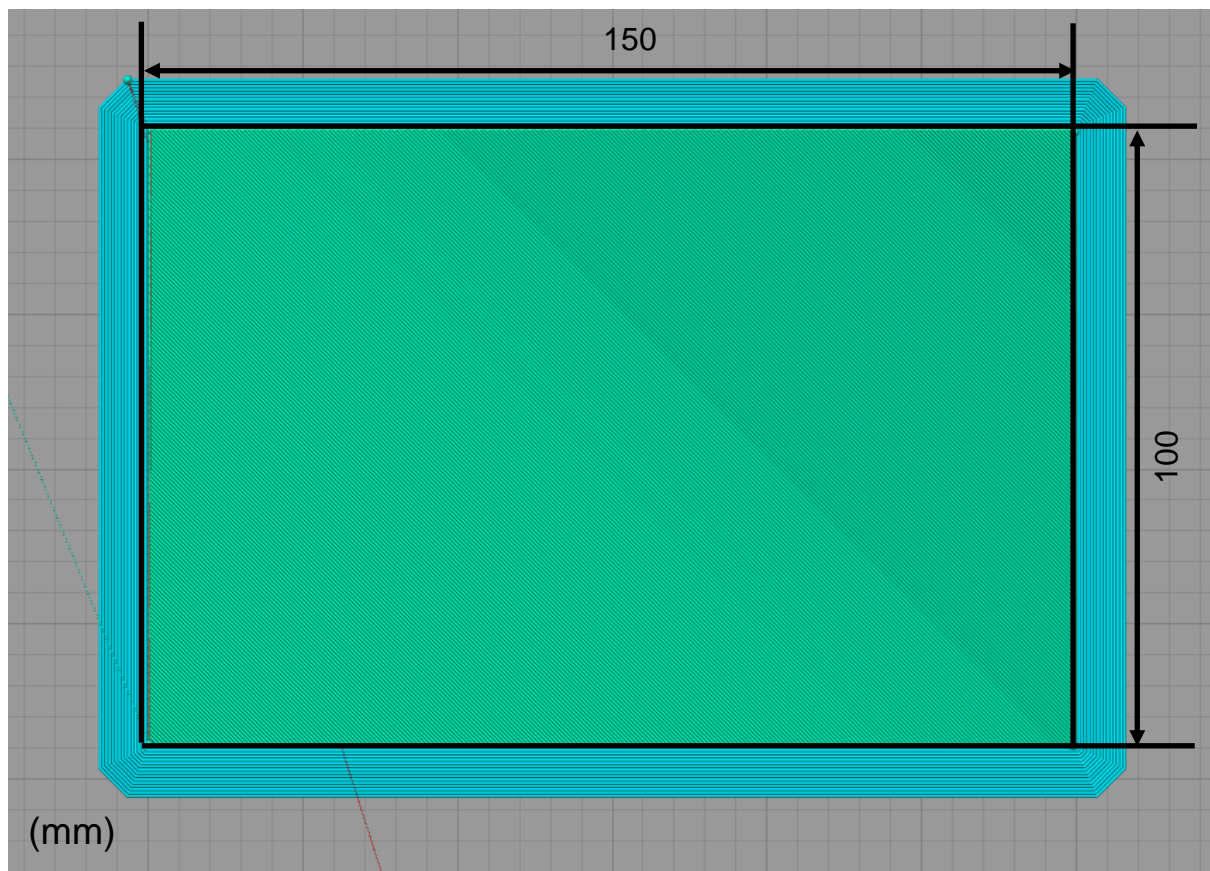


Figure 4.11-1: Low velocity impact sample

Three different types of samples have been tested. Pure nylon 910, short fiber and continuous carbon fiber. Three samples have been tested with an impact energy of 10 J and an impactor mass of 4.1 kg. The test results are as follow table (4.11-1).

Table 4.11-1: Impact test results

	Nylon 910	Chopped CF	Continuous CF
Max load [kN]	1.8	1.9	3.2
Absorbed Energy [J]	4.4	10.3	10.5
Impact velocity [m/s]	2.2	2.2	2.2

The continuous CF samples have a significant increase in energy absorption compared to pure nylon or chopped fibres. It can be deduced that the continuous fiber prevent the fiber pulling during a loading condition whereas the short fiber are dependent on the matrix, which holds them on place. Moreover, the fiber content of the short fiber filament is at 20 % and the continuous carbon fiber sample is at 30 % of the total mass of the sample.

Chapter 5

Experimental testing

5.1. Introduction

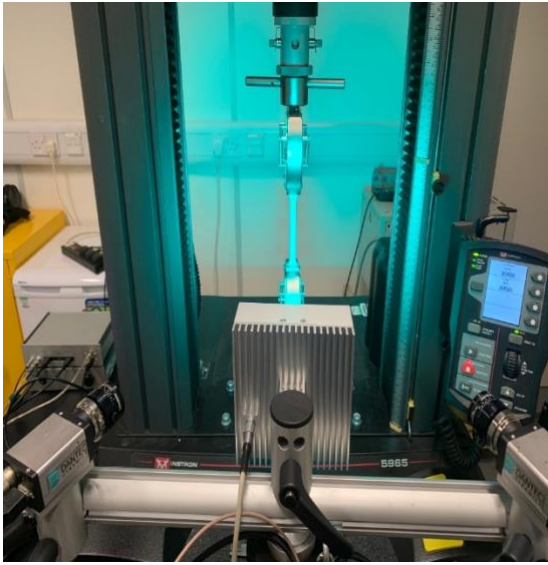
Once the FDM machine has been developed, tuned and tested. The mechanical properties of our composite can be determined through testing. It is important to investigate these properties in order to begin our impact test. To determine the mechanical properties of our materials several test specimen have to be manufactured with under different process parameters as these can fundamentally influence the mechanical properties and impact behaviour. This chapter aims to focus on investigation of mechanical properties and impact behaviour of newly developed thermoplastic composite materials.

5.2. Material characterisation

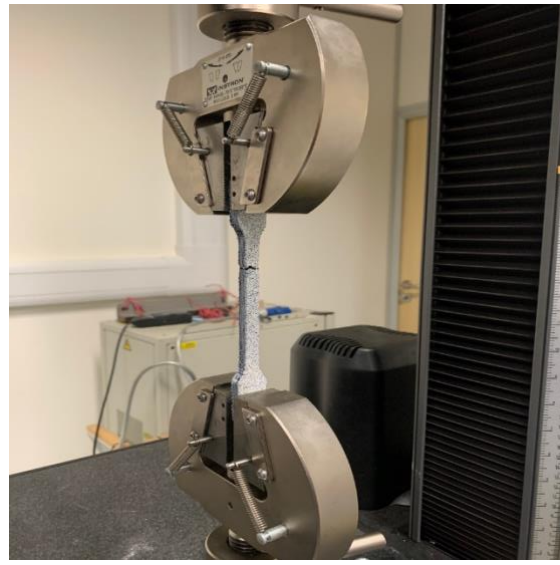
To ensure quality results for our low velocity impact testing a range of mechanical properties have to be determined. To understand the behaviour of engineering materials a range of material characterisations need to be investigated through testing coupon samples and manufacturing parameters that can influence the mechanical properties of our carbon fiber reinforced thermoplastic polymer composite. The following characterisations will be investigated in this chapter: Tensile strength, Flexural modulus, Layer height, Extrusion, Nozzle diameter and Layer adhesion [43].

5.2.1. Tensile testing

Tensile tests were performed at Cranfield University in order to analyse the tensile behaviour of the material. To measure the mechanical performances of our material a method called Digital Imaging Correlation (DIC) has been applied to the Nylon, chopped carbon fiber and continuous carbon fiber dog bone samples. The Instron machine was set for each sample to acquire measurement over a period of 300 seconds at a speed of 5mm/min. The maximum tensile force was set at 5 kN. To avoid the negative impact on the clamping of the machine both contact areas of the sample have been taped.



a



b

Figure 5.2-1: DIC tensile test

Once the machine is setup and the cameras of the DIC calibrated the sample can be clamped in position in the machine clamps and the test can start figure (5.2-1/a). Within the 300 seconds of test period the sample will break and the machine can be stopped after the test period figure (5.2-1/b). Thereafter a new sample can be placed in and the test can be repeated for the following samples. Tensile dog bone samples have been manufactured according to BSI standards ISO 527-2.1A.50 (170 x 20 x 7.2) mm figure (5.2-2).

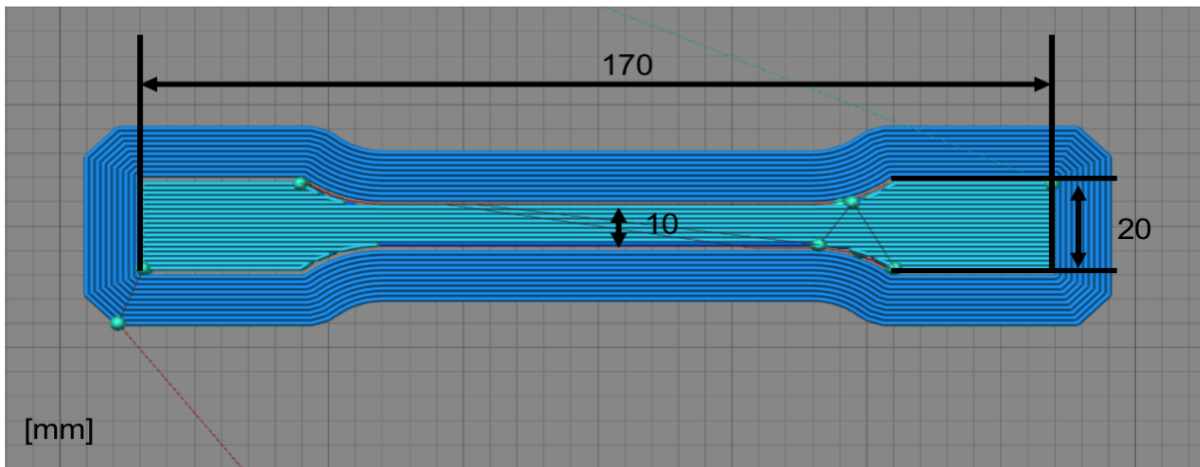


Figure 5.2-2: Tensile test samples

5.2.2. Nozzle diameter and layer height correlation

The nozzle size can affect in many ways the printed object. Not only from a mechanical point of view but also for the surface finish and printing time. The bigger the nozzle the more material will be extruded resulting in fast print time. Also the embedded carbon fiber is less exposed to the high heat in the melting zone of the nozzle, which allows the fiber to get extruded uniformly. In order to determine the adequate nozzle diameter, a range of tensile tests have been conducted on each material used in this thesis at different layer height and with different nozzle diameters. In respect of the fiber bundle diameter of 0.33 mm, we started our test with 0.6 mm nozzle. First the Nylon samples were tested with a layer height ranging from 0.35 mm – 0.6 mm on a 0.6 mm nozzle.

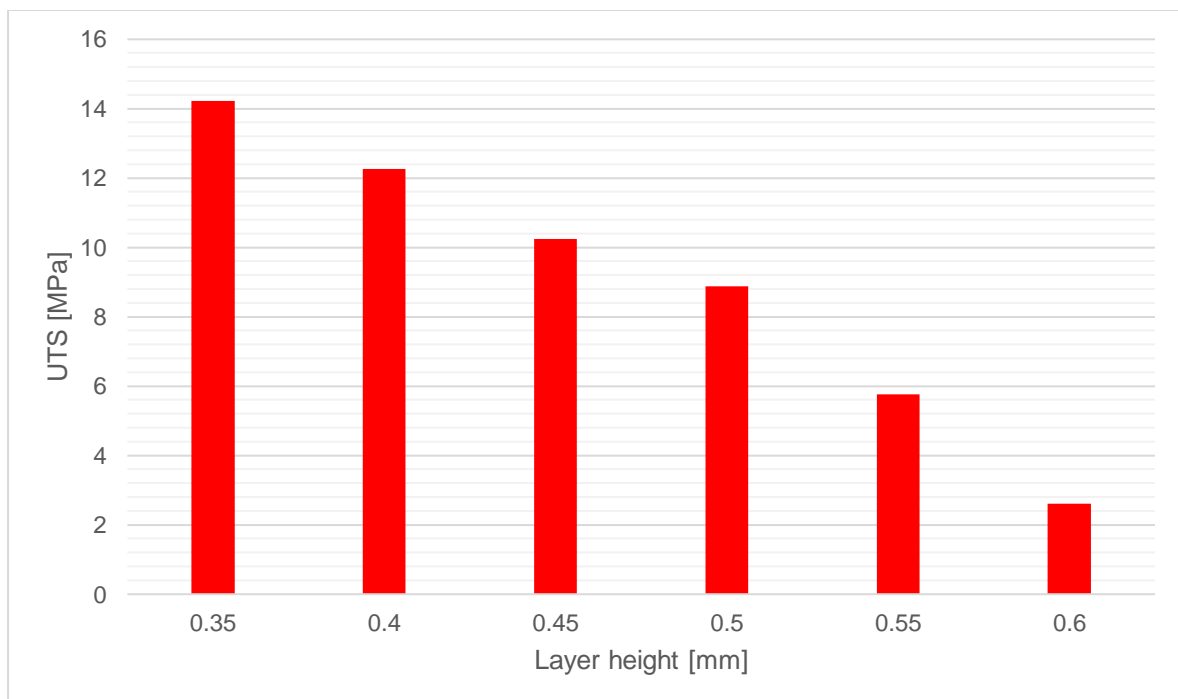


Figure 5.2-3: Effect of layer height on UTS Nylon samples with 0.6mm nozzle

As shown in figure (5.2-3) the highest UTS has been reached at a layer height of 0.35 mm. The reason why a lower height was not considered is related to the carbon fiber used for the composite which has a diameter of 0.33 mm. By using a lower layer height the carbon fiber wouldn't be able to be extruded and cause a clogging of the nozzle. For chopped fiber the same test has been conducted and the results have been analysed.

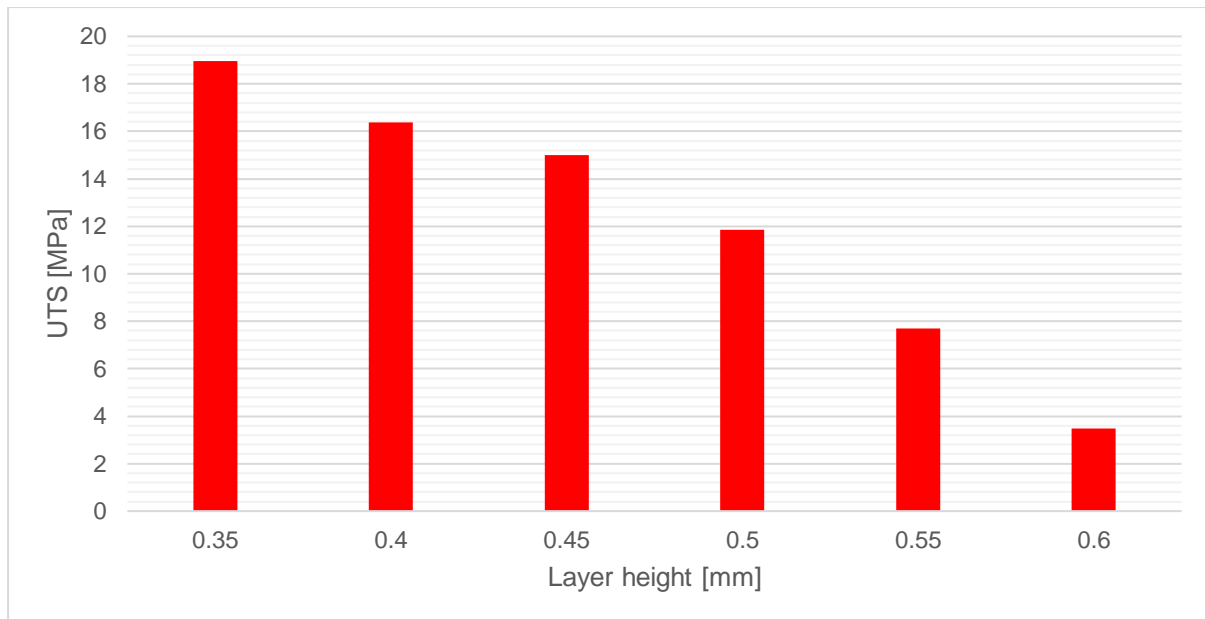


Figure 5.2-4: Effect of layer height on UTS SCFRN samples with 0.6 mm nozzle

From the figure (5.2-4) a significant increase in UTS has been achieved due to the chopped fibers contributions. The reason for the decay of UTS along the increase of the layer height is due the ratio:

$$\frac{\text{Nozzle diameter}}{\text{layer height}}$$

Equation (5.2-1)

Due to the ration in equation (5.2-1) we can determine an accurate correlation between the nozzle diameter and the layer height of the extruded material.

The ratio for a 0.35 mm layer height with a 0.6 mm nozzle gives us the value of 1.7. For a layer height of 0.6 mm, which represent the exact diameter of the nozzle the ratio is 2. We can conclude that the decay of the UTS can be related to the relation between the nozzle diameter and the layer height. Moreover the closer we come to a ratio of 2 the more UTS decreases. This can be explained by the material flow and spacing paths explained in chapter 04 weakening the layer adhesion of the stacks of material. In order to investigate if the UTS can be increased by changing the nozzle diameter further tests have been conducted using a 0.8 mm nozzle.

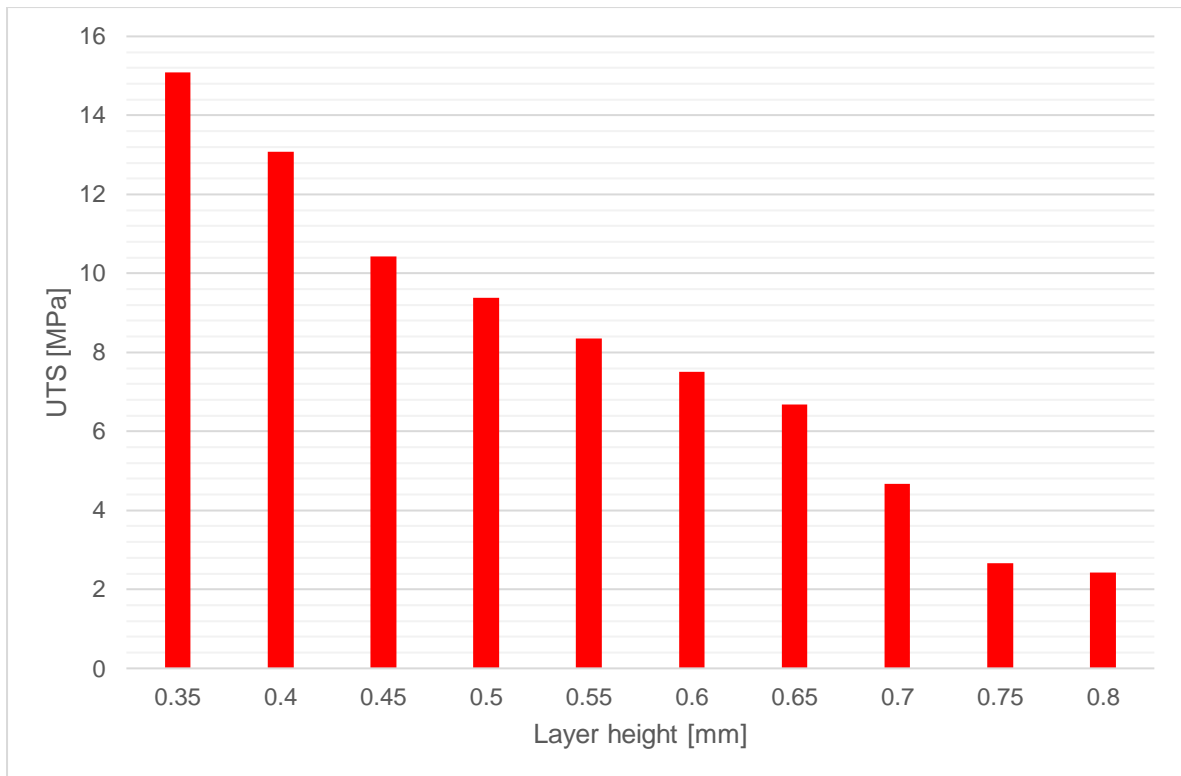


Figure 5.2-5: Effect of layer height on UTS Nylon samples with 0.8 mm nozzle

A significant increase in UTS has been achieved for nylon printed with a 0.8 mm nozzle. This brings us back to the relation between the nozzle diameter and the layer height. For a 0.35 mm layer height on a 0.8 mm nozzle a ratio of 0.4 has been acquired. We can conclude that the smaller the ratio the higher the UTS gets. In the following graph the comparison between the test results on nylon with a 0.6 (yellow) and a 0.8 (red) mm nozzle is clearly visible.

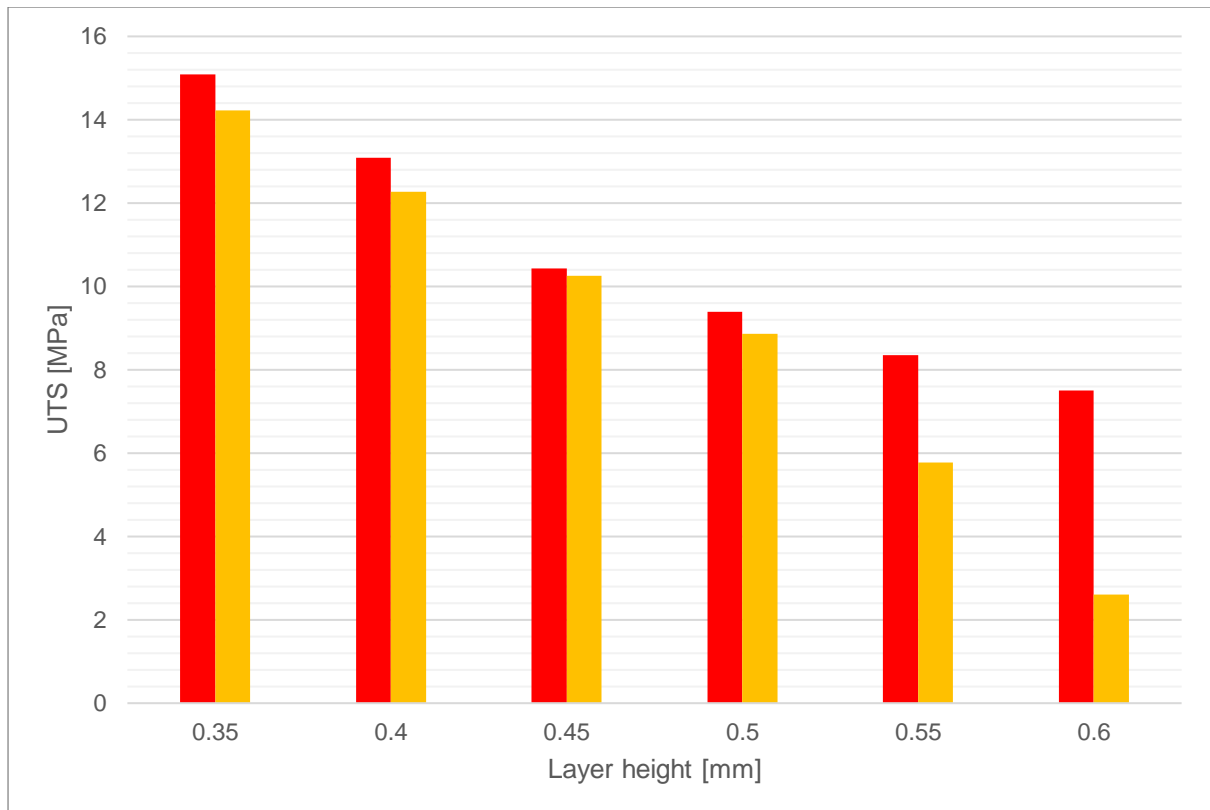


Figure 5.2-6: Effect of layer height on UTS SCFRN samples with 0.6 mm (yellow) vs 0.8 mm (red) nozzle

As the 0.6 mm nozzle comes close to its original diameter the UTS drops dramatically. This effect can be countered by changing the material flow and steps/mm explained in the next paragraph. In order to avoid any material waste the 0.8 mm nozzle has been used to manufacture our Continuous Carbon Fiber Nylon (CCFRN) composite bone samples. With a layer height of 0.35 mm the UTS for CCFRN composite is 36.3 MPa.

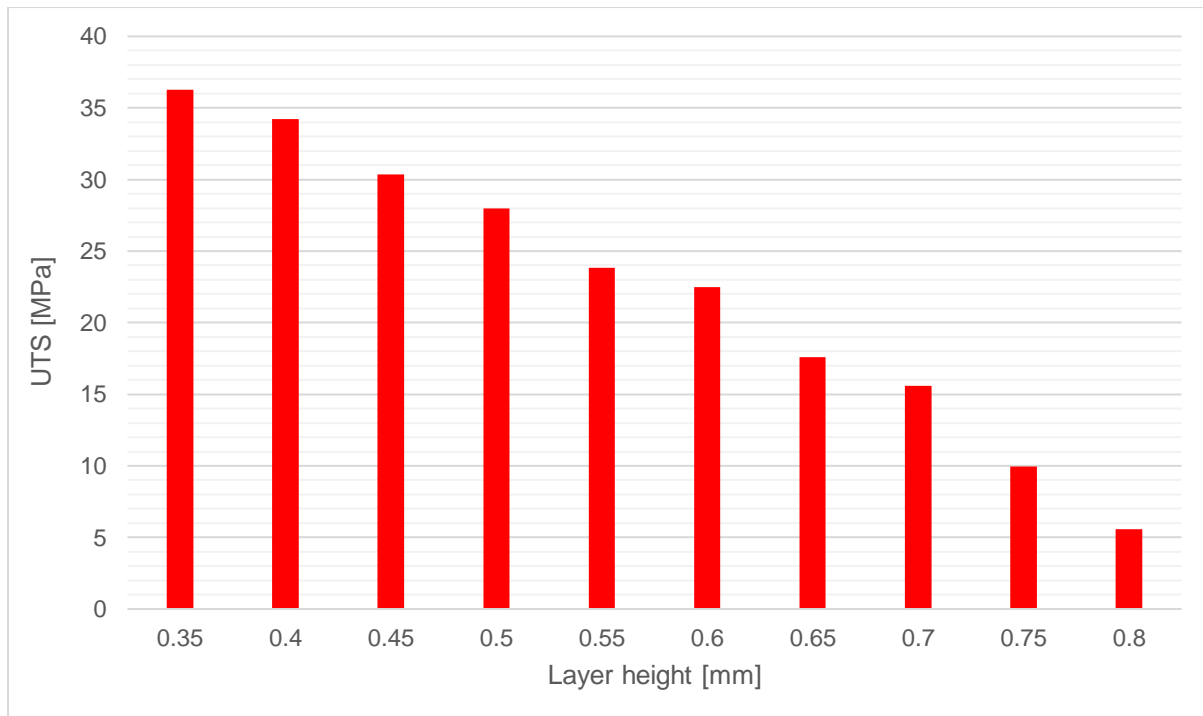


Figure 5.2-7: Effect of layer height on UTS CCFRN samples with 0.8 mm nozzle

In figure (5.2-7) at a layer height of 0.35mm UTS reaches 36.3 MPa with an 0.8mm nozzle. The reason for the decay in UTS in correlation to the increase of layer height can be justified by the amount of void increasing in the internal structure of the composite. Resulting in a weaker structure of the composite and a lower energy absorption.

5.2.3. Effect of temperature on layer adhesion

The effect of an increase in temperature on the tensile test samples and their effect on the layer adhesion were investigated. The nylon 910 manufacturer recommended to print the material in a temperature range between 250 - 275 °C. Surprisingly, samples printed at higher temperatures performed better when printed along the heated bed. The highest performance has been achieved at 285 °C. Unfortunately, the temperature test was not worth carrying on because the upmost maximal temperature that our carbon fiber could be printed is 280 °C. If the temperature goes higher than the limit for the carbon fiber the polyamide coating will dissolve before it reaches the heat chamber of the hotend and the fibers will curl inside the nozzle causing a clog. In figure (5.2-10) the yellow graph represents the samples printed in Z

direction, which means perpendicular to the heated bed. In red area the samples printed along the heated bed platform.

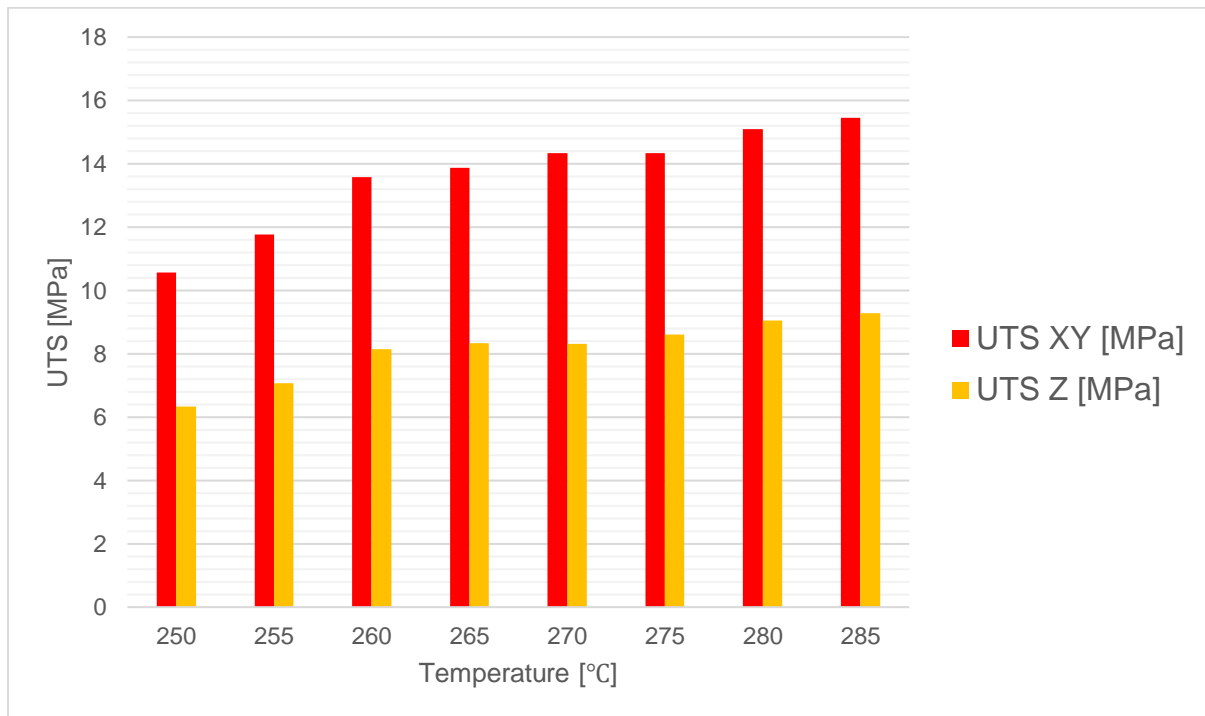


Figure 5.2-8: Effect of temperature on UTS with samples printed on XY plane (red) and Z plane (yellow)

Both categories (SCFRN and CCFRN) of samples have been tested and the following conclusion has been made. The higher we increase the temperature in the hotend the more the molecules inside the nozzle have time to bond. The result is similar to an injection moulding part. The downside of an increase in temperature is the crystallisation of the material, which results in a brittle final part. In our case if Nylon becomes brittle the impact properties of the material will disappear. Moreover, the polyamide coating of the fiber will decay before the fiber reaches the heat chamber of the hotend.

5.3. Experiment Setup

To investigate the impact behaviour of our CFRTP samples we followed the ASTM D7136/D7136M-12 standard, which is a standard test method for measuring the damage resistance of a fiber reinforced polymer matrix composite to a drop weight event. A drop-weight impact test is performed using a balanced, symmetric laminated plate. Damage is imparted throughout-of-plane, concentrated impact perpendicular to the plane of the laminated plate using a drop weight with a hemispherical striker tip. The damage resistance is quantified in terms of the resulting size and type of damage in the specimen. The damage response is a function of the test configuration. The impact samples used have the following dimensions 150 x 100 mm² with a thickness of 7.2 mm.

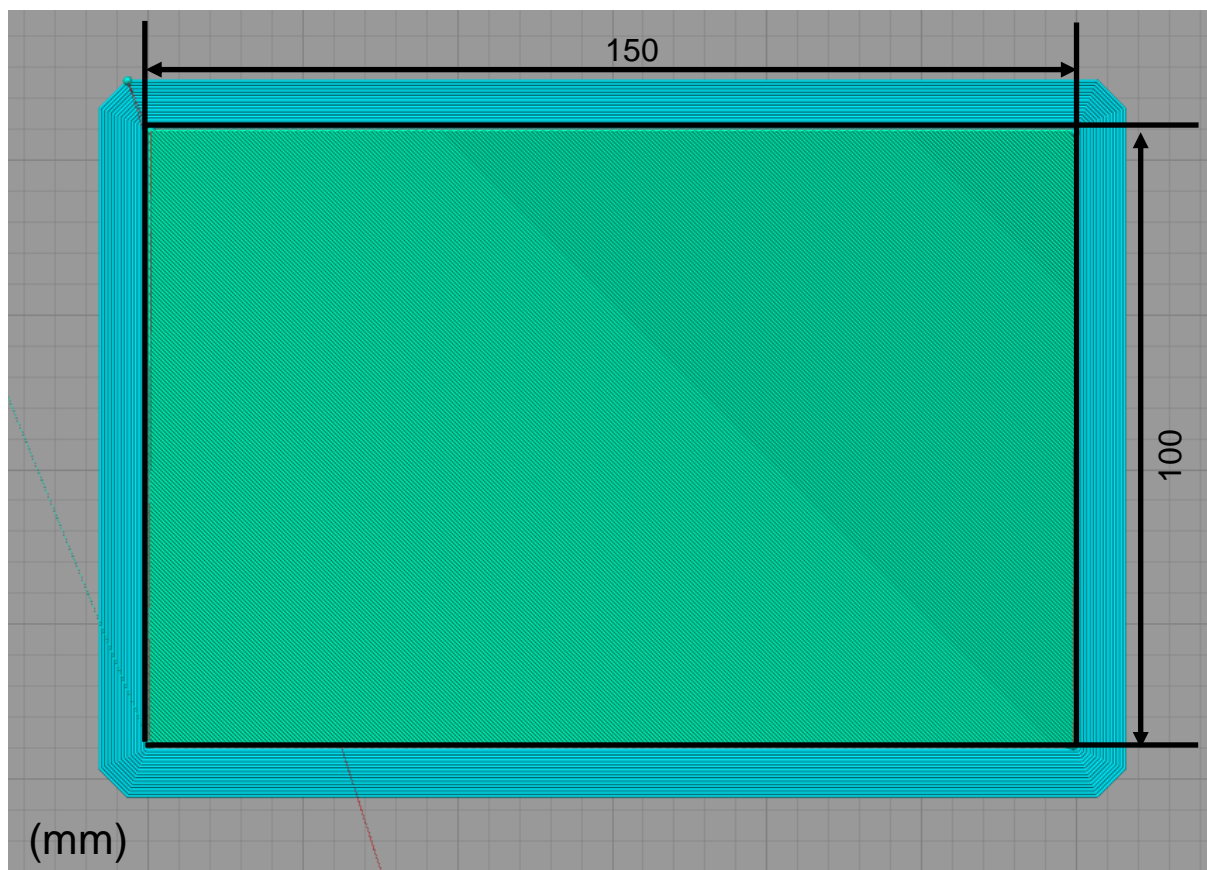


Figure 5.3-1: CCFRN low velocity impact sample

The impactor shape can affect the impact response of the composite and damage mechanism of the CFRTP composite. A few comparisons and investigations have been made in the literature to guide us towards the right impactor for our test. With a diameter of 12 mm and a length of 6 mm for the impactor tip.

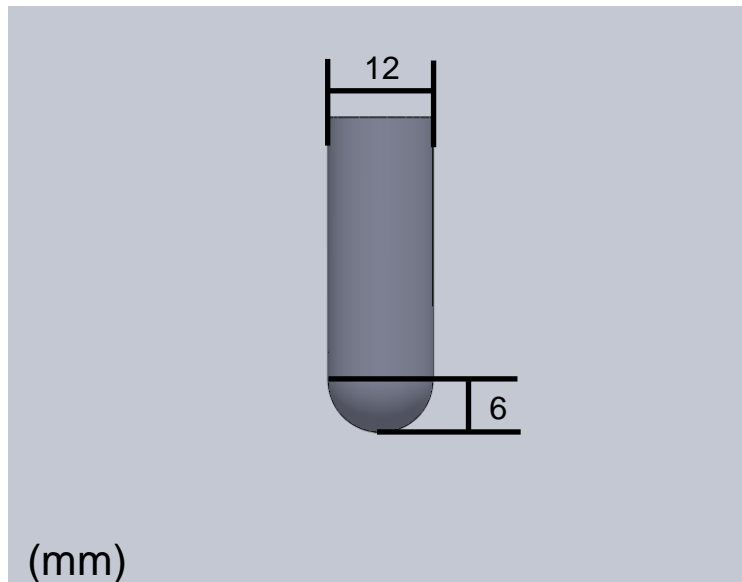


Figure 5.3-2: Impactor dimensions

The total weight of the impactor + gantry at the moment of impact is 4.185 kg. To hold the specimens in place base plate with rectangular cut out has been used. The clamping system is 4 point rubber clamping mounts and the sample is aligned on top of the out cut of the base plate.

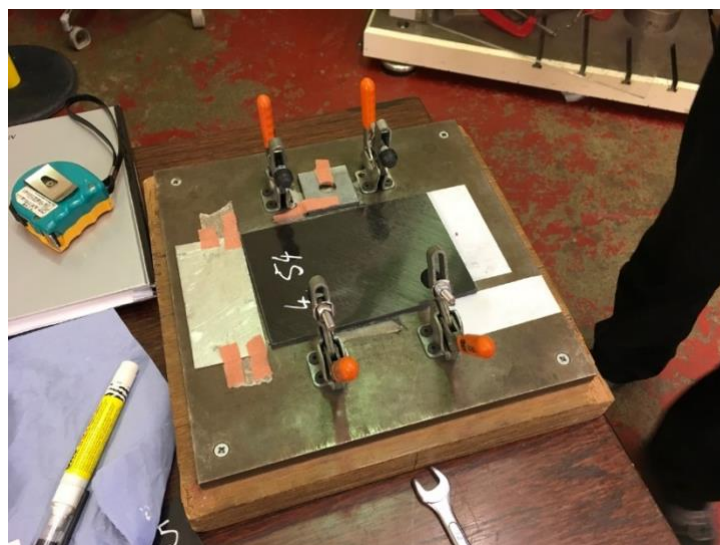


Figure 5.3-3: Drop tower sample gantry

Once setup of the base plate is placed in the drop weight machine and the machine is calibrated. The speed at which the impactor will hit the surface of the test sample is set at 2.21 m/s.

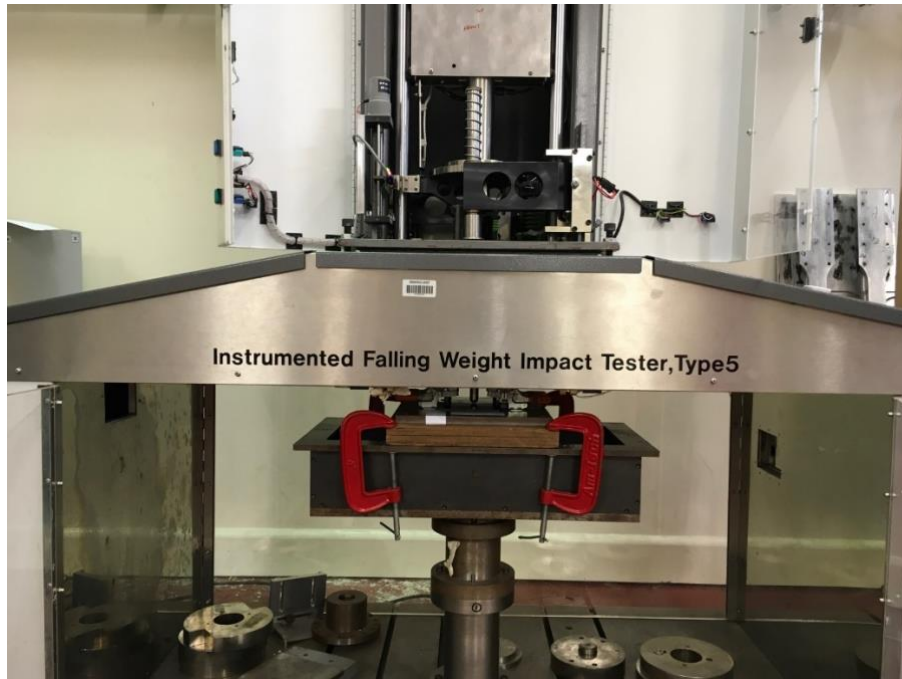


Figure 5.3-4: Drop tower setup

By following the safety requirements and calibration procedures the low velocity impact testes was carried out.

5.4. Low velocity impact test results

In order to have viable samples a curing process has been applied to the spool of pure material by heating the spool in an oven at 100 °C for a period of 6 hours. The reason behind is the hydrophilic behaviour of the Nylon, which can take up to 4% of its original weight. The sample test conditions and parameters have been applied to the nylon 910, SCFRN and CCFRN samples. The continuous CF hasn't been cured to avoid any delamination of the CF bundle coated with the polyamide coating.

5.4.1. Nylon 910

The low velocity impact test was carried out with the nylon 910 samples. The denomination letter N has been chosen for the nylon 910 samples.

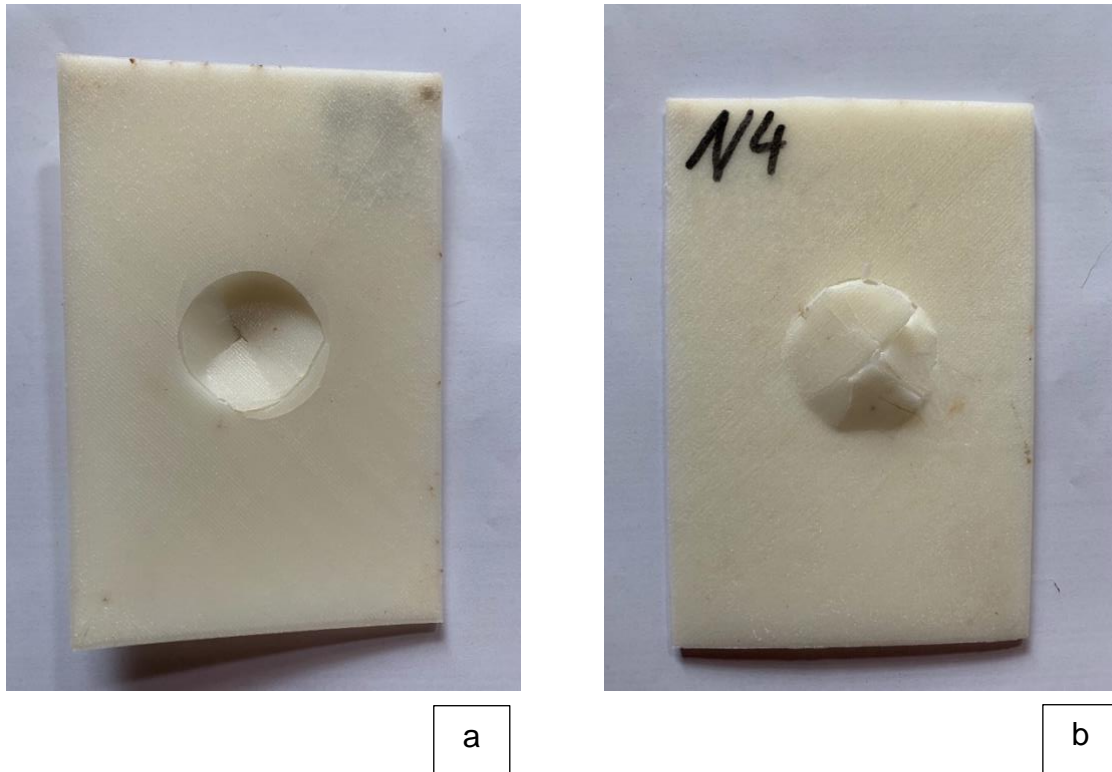


Figure 5.4-1: Nylon 910 samples after impact

As shown in figure (5.3-1) the impact when through the composite chowing almost no sign of resistance of the sample to stop the impactor. The energy displacement graph can be seen in figure (5.3-1/a). In conclusion the impact resistance and energy absorption of the nylon 910 is poor. N1.2.3 samples were not able to absorb a sufficient amount of energy to stop the striker and have been perforated through the samples.

5.4.2. Short Carbon Fiber Nylon (SCFRN)

The same test procedure as for the nylon 910 samples has been applied to the SCFRN samples. SCFRN samples have higher performance compare to the nylon 910 samples. The SCFRN samples were all able to stop the striker and absorbed the expected amount of energy. The energy displacement graph can be seen in figure (5.4-2/b).



Figure 5.4-2: SCFRN low velocity impact samples

5.4.3. Continuous Carbon Fiber Nylon (CCFRN)

The same test procedure as for the Nylon 910 samples has been applied to the CCFRN samples figure (5.5-1). CCFRN samples have a minor surface dent compare to the nylon 910 and SCFRN samples. The amount of energy absorbed by the samples is equal to the SCFRN samples, which is positive as it shows that the 10 J energy from the striker has been absorbed by the SCFRN and CCFRN samples. The improvement lies in the amount of force that the CCFRN sample was able to take in comparison to SCFRN. The energy displacement graph can be seen in figure (5.5-1/b).

5.5. Test values

The amount of energy set for the low velocity impact test was 10 J besides the Nylon 910 samples both SCFRN and CCFRN were able to absorb the full amount of energy delivered during the impact of the strike to the surface of the test samples. In (Fig.5.5-1/a) are resented the impact top plane where the impactor dented the surface and figure (5.5-1/b) is rear surface of the sample.

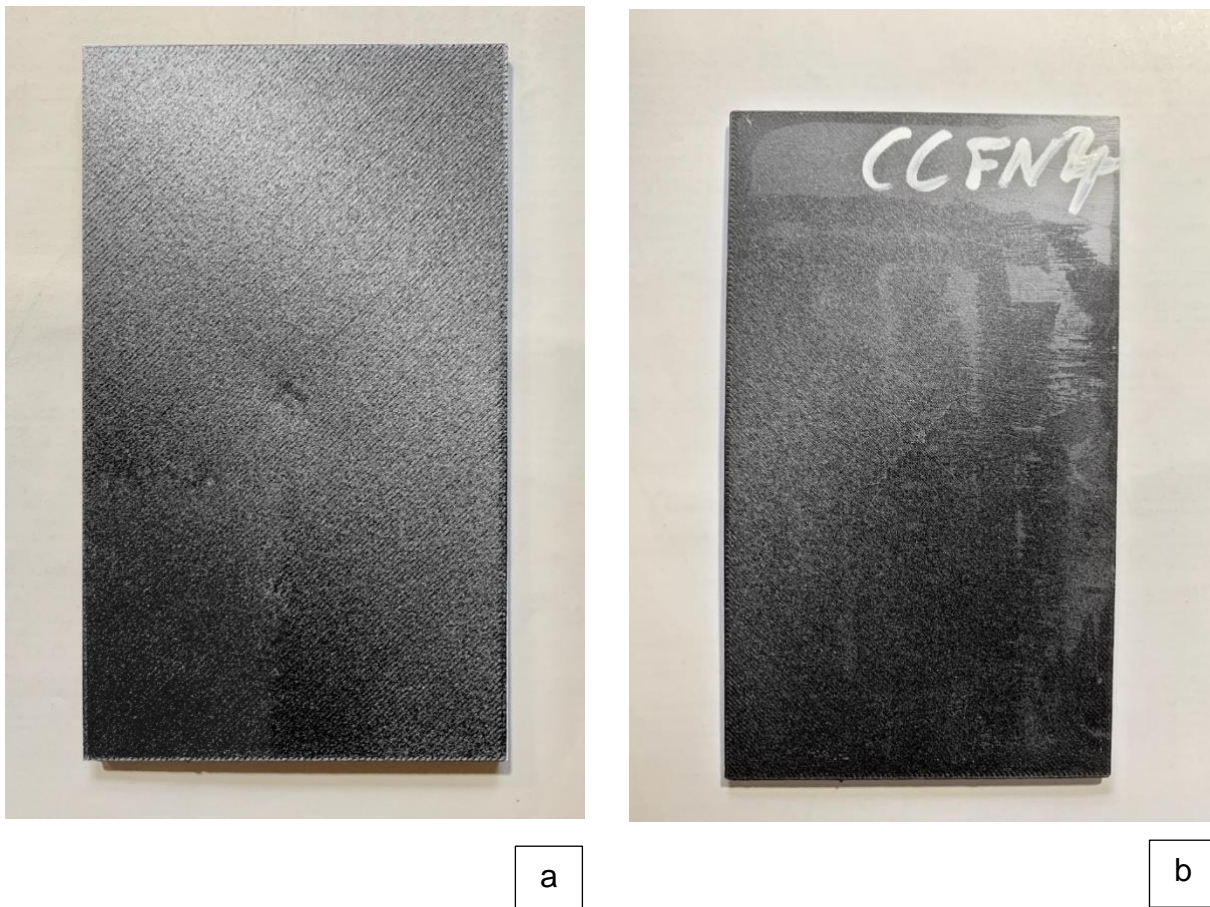


Figure 5.5-1: CCFRN low velocity impact samples

From the test result we can compare the amount of Energy absorbed by the test samples. In figure (5.5-1) it is clearly visible that the impactor has clearly induced several failure mods including penetration. As we can see on the backside of the composite an X shaped damage has been induced by the impactor during impact.

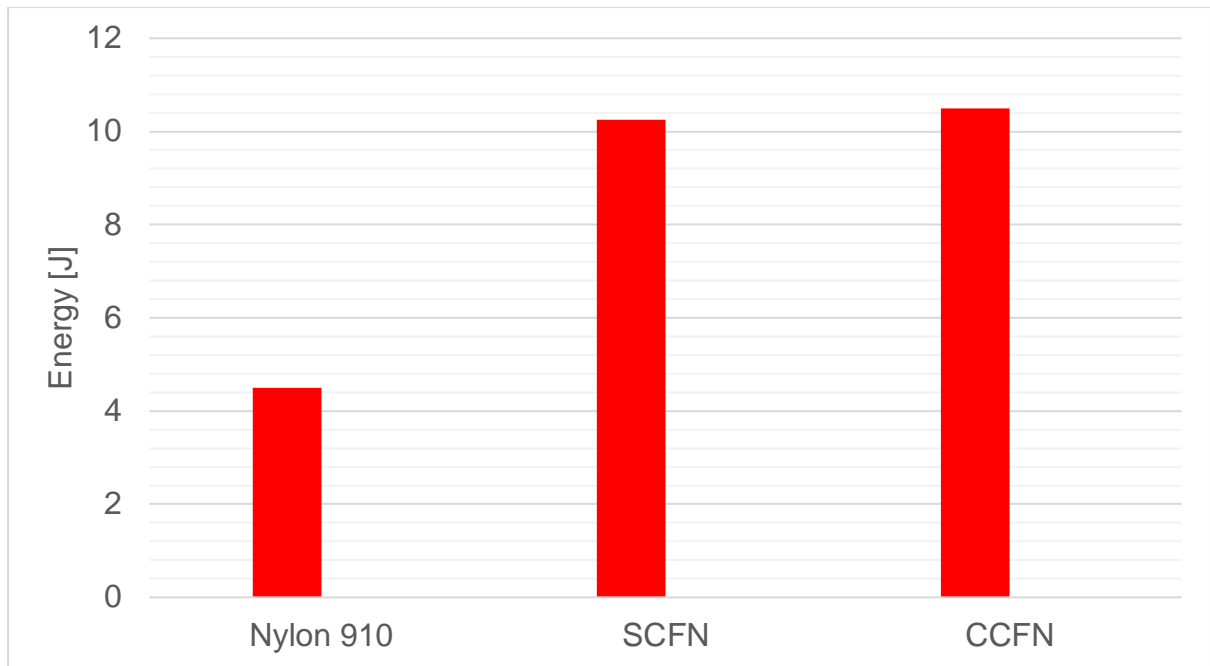


Figure 5.5-2: Energy absorption of the samples

The test results are gathered through impact testing conducted on three individual samples of each material: nylon 910, RN. The test results and force displacement graphs can be found in Appendix B. For nylon 910 samples, the reason why only 4.5 J have been absorbed is because the striker perforated the samples. On the other hand, the amount of force that each sample was able to take has been represented in figure (5.5-2).

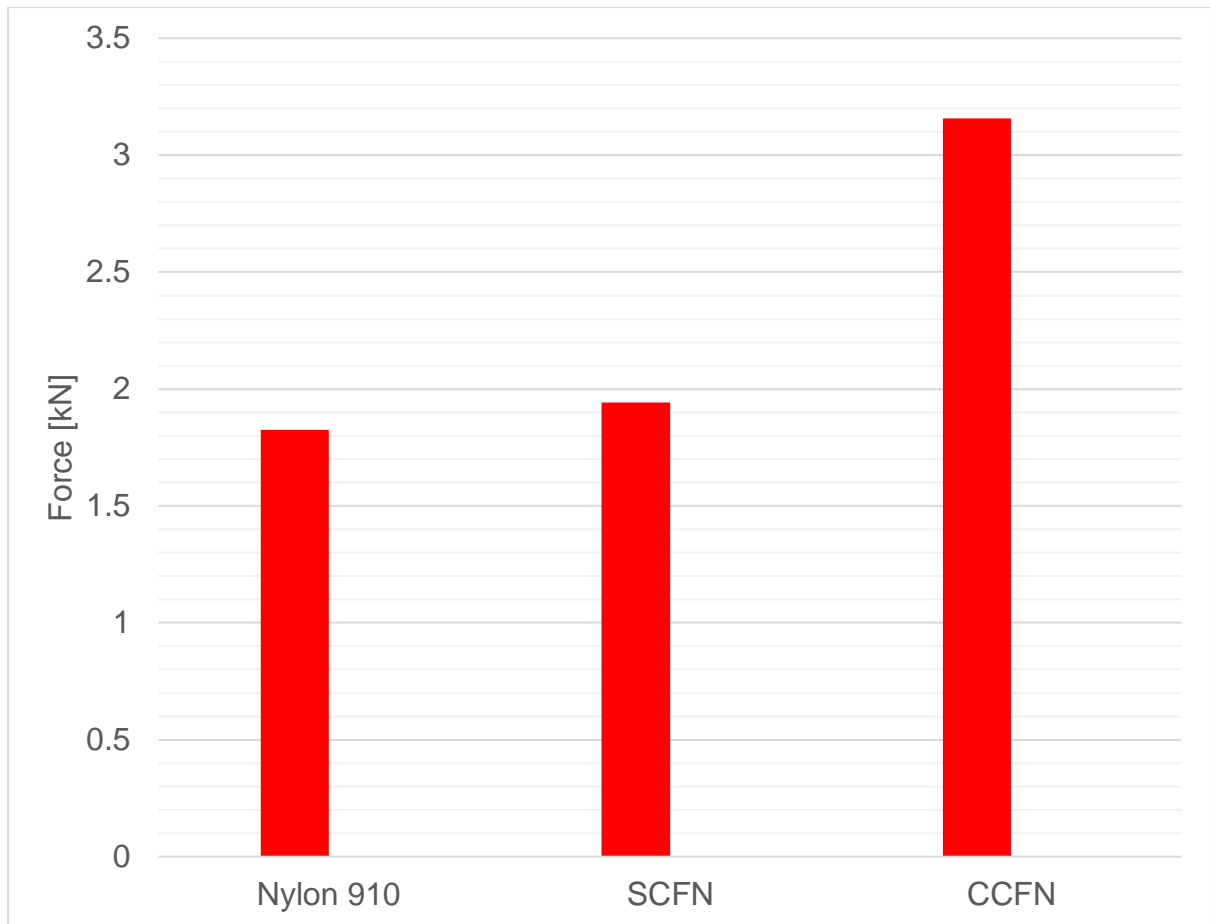


Figure 5.5-3: Force generation of the samples

We can clearly see that the CCFRN samples have around 60% more impact resistance than the SCFRN samples, which concludes the following observation. Because of the random orientation of the short carbon fibers in the SCFRN samples, the fibers do not redistribute the same amount of energy to the matrix. Although it is clearly visible that the short fibers are able to improve the energy absorption compared to the nylon 910 samples. Finally, the CCFRN samples show the difference between the efficiency of having continuous fiber in the matrix, which redistributes the energy from the impact to the matrix. In figure (5.5-3) we can see the comparison of the test results between the nylon 910, SCFRN and CCFRN samples.

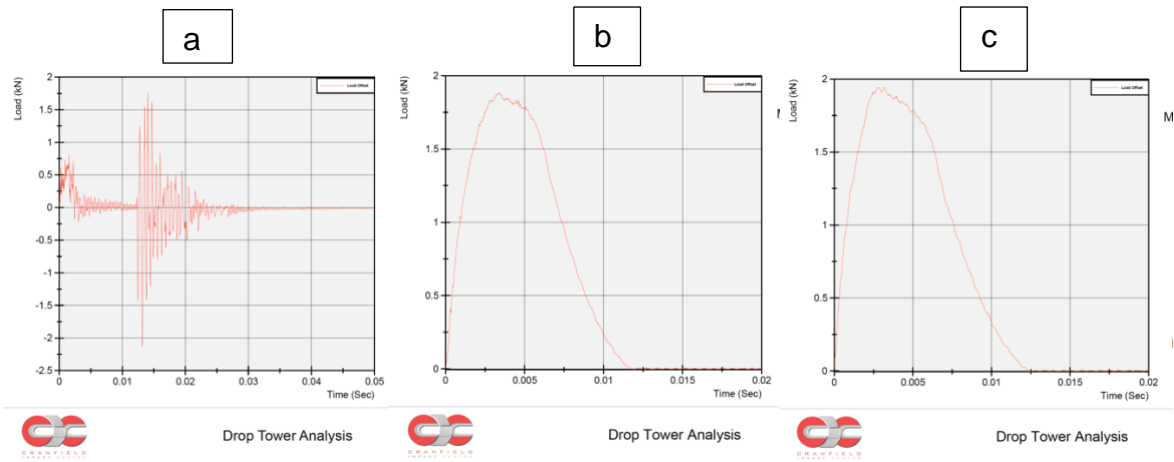


Figure 5.5-5: Force- time diagram

An impact can cause damage to the facing, core facing and core material. In our case we have a typical low velocity impact behaviour of the composite where the damage is on the top face, core-top and core face. The nylon 910 has suffered from the five typical failure mods (core buckling, impacted face delamination, core cracking, matrix cracking and fiber cracking) with a full penetration of the impact through the lower core. In conclusion the samples have performed as expected besides the nylon 910 samples, which were not able to stop the striker and have suffered the five failure mods as seen in figure (5.5-5/a). It can also be observed that the computer recorded the effect of the second striker, which stops the impactor from going further through the sample after the moment of penetration. In the force-time diagram in figure (5.5-5/b) the SCFRN samples have absorbed the impact energy from the impactor the five failure mods are also present as the fiber in the composite are under powder form, which means that if the matrix has cracked by default the fiber have cracked too. For the CCFRN sample an impressive amount of energy has been absorbed by the composite and in order to proof all five failure mods a scanning electron microscope should be used.

5.6. Experimental errors

A few experimental errors have to be considered for this experiment. First of all the slight variance in air temperature, humidity present in the air or inconsistency in the hotend can lead to voids formation in the composite, internal delamination, warping or poor fiber embedding in the thermoplastic material. It is very difficult to reproduce samples which are 100% identical to each other even if all process parameters and material handle are done correctly. There is a variance of approximately 8% for each low velocity impact test on samples from the same type. Therefore five of each composite including the pure nylon 910 samples have been tested and an average of these values have been taken to generate our force generation graph in figure (5.5-9). Another observation has been made when setting up the clamping base for the samples for our low velocity impact. Initially a circular base has been used with a pneumatic fork clamping system to run some pre-tests rather than a rectangular base figure (5.3-3). The composite samples suffered greater damage leading to a full perforation on almost all samples besides two out of three CCFRN samples. This phenomena can be explained through the fact that the circular mount was smaller than the actual sample therefore it limited the energy distribution of the impactor to a much smaller surface than on a rectangular clamping base. Also the clamps used on the rectangular base had rubber feet preventing the clamps to apply force on the corners of the samples.

Chapter 6

Conclusions & Future

Work

6.1. Conclusions

In this research I have been able to manufacture carbon fiber reinforced thermoplastic polymer with continuous carbon fiber regardless of the orientation of the toolpath due to the carbon fiber cutter tool. In Chapter 2 design improvements were necessary as standard nor industrial machines were able to achieve our final product. The improvements regarding the structure of the FDM machine were necessary in order to achieve high quality samples. The cancellation of any vibration causing layer shifts or uneven surfaces was an utmost priority. The addition of a second lead screw for the Z-axis has dramatically improved the print quality and vibrations cancellation. In addition to achieve the vibration cancellation, a spring loaded backlash system was added to each lead screw in order to eliminate the negative motion of the gantry when moving along the Z axis. Regarding the cutting system, a few methods have been tested. The direct drive system mounted to the print head showed a few advantages but more disadvantages compared to the Bowden setup. The actuation of the cutter needed to be programmed and tuned in order to consider the time and steps/mm of material pushed through the extruder. The containment chamber is not necessary but allows to use and move the machine in different environments. For instance if the room temperature can be raised and kept between 30-35 °C at a moisture level between 10-20% and if the machine is attached to a professional fumes evacuations system then a containment chamber is not necessary. In addition to the structure of the printer a suitable surface treatment for the heated bed had to be used in order to avoid warping of our material during deposition. Nylon has 5% shrinkage after being processed through the extrusion therefore a surface treatment to force the material to stick to the print surface was necessary.

For the tensile tests many process parameters were determined and investigated. We considered the effect of nozzle diameter on the layer strength through different layer height as well as the effect of temperature on the mechanical properties of the material. From the impact we discovered that even if nylon 910 was advertised to have a UTS of 54 MPa only 34 MPa have been gathered from our test. Also from the impact test, only half the energy used during our test has been absorbed by the sample leading to the conclusion that our pure Nylon samples were perforated by the impactor.

On the contrary, the short carbon fiber reinforced nylon and continuous carbon fiber reinforced nylon samples performed well as the impact test for the energy absorption of the impactor on the surface of the samples. The continuous carbon fiber nylon samples absorbed 60 % more force than the short carbon fiber nylon samples giving the following conclusion. When integrated to a thermoplastic the continuous carbon fiber improve the energy absorption of the material drastically compared to a similar matrix material but with chopped fibers.

6.2. Contribution to the science

Vibration cancellation method for even and continuous integration of continuous carbon fiber cutting method for precise carbon fiber cutting and integration to thermoplastic via Bowden extrusion system. Coding for the motherboard firmware as well as G code for the slicer have been optimised in order to produce quality samples. The effect of hardware on process parameters have been investigated through tensile tests. Low velocity impact performance of continuous carbon fiber polyamide has been also investigated and tested. Continuous carbon fiber reinforced thermoplastic polymer manufacturing and manufacturing method.

6.3. Future Work

From the hardware point of view many improvement can be done using high-end components, which can withstand more load. Due to higher quality components a lot of time can be saved not only for the daily replacement of broken components but also for manufacturing components faster. The program can be improved as well as the communication from the board with the G code of the slicing software. Various mechanical testing such as high velocity impact, buckling and fatigue are required to be performed on these new developed samples to find out their performance in comparison with existing thermoplastic composites used in aerospace and automotive industry. Finally, a numerical analysis could be conducted in order to optimise the 3D printed composite through a finite element analysis using Ansys Is-dyna. In order to prove the failure modes of our composite an SEM analysis should be conducted as well as a numerical FEA analysis to validate the failures in the structure.

Chapter 7

References

- [1] X. Tian, T. Liu, C. Yang, Q. Wang, and D. Li, "Interface and performance of 3D printed continuous carbon fiber reinforced PLA composites," *Compos. Part A Appl. Sci. Manuf.*, vol. 88, pp. 198–205, 2016.
- [2] A. Nanni, *Fiber-Reinforced-Plastic (FRP) Reinforcement for Concrete Structures*. 1993.
- [3] S.-J. Park, *Carbon fibers*. Springer, 2015.
- [4] Y. Yang, R. Boom, B. Irion, D. J. van Heerden, P. Kuiper, and H. Wit, "Recycling of composite materials," *Chem. Eng. Process. Process Intensif.*, vol. 51, pp. 53–68, 2012.
- [5] R. Stewart, "Thermoplastic composites — recyclable and fast to process," *Reinf. Plast.*, vol. 55, no. 3, pp. 22–28, May 2011.
- [6] A. K. Van der Vegt and L. E. Govaert, *Polymeren : van keten tot kunststof*. DUP Blue Print, 2003.
- [7] "Everything about today's PEEK 3D printing market - 3D Printing Media Network." [Online]. Available: <https://www.3dprintingmedia.network/everything-about-peek-3d-printing/>. [Accessed: 17-Dec-2019].
- [8] S. Abrate, *Impact on Composite Structures*. Cambridge University Press, 1998.
- [9] P. W. R. Beaumont and C. Soutis, "Structural integrity of engineering composite materials: a cracking good yarn," *Philos. Trans. R. Soc. A Math. Phys. Eng. Sci.*, vol. 374, no. 2071, p. 20160057, Jul. 2016.
- [10] M. Biron, *Material Selection for Thermoplastic Parts*. 2016.
- [11] M. W. Akhtar, Y. S. Lee, C. M. Yang, and J. S. Kim, "Functionalization of mild oxidized graphene with O-phenylenediamine for highly thermally conductive and thermally stable epoxy composites," *RSC Adv.*, vol. 6, no. 102, pp. 100448–100458, Oct. 2016.
- [12] F.-L. Jin, S.-Y. Lee, and S.-J. Park, "Polymer matrices for carbon fiber-reinforced polymer composites," *Carbon Lett.*, vol. 14, no. 2, pp. 76–88, Apr. 2013.
- [13] TECAMID Ensinger, "PA Polyamide Nylon." [Online]. Available: <https://www.ensingerplastics.com/en/shapes/engineering-plastics/pa-polyamide>. [Accessed: 17-Dec-2019].
- [14] M. . Montes-Morán, A. Martínez-Alonso, J. M. . Tascón, M. . Paiva, and C. . Bernardo, "Effects of plasma oxidation on the surface and interfacial properties

- of carbon fibres/polycarbonate composites,” *Carbon N. Y.*, vol. 39, no. 7, pp. 1057–1068, Jun. 2001.
- [15] S. Kuciel, P. Kuznia, and P. Jakubowska, “Properties of composites based on polyamide 10.10 reinforced with carbon fibers,” *Polimery*, vol. 61, no. 02, pp. 106–112, Feb. 2016.
- [16] “Nylon 910,” vol. 910, no. Alloy 910, p. 910.
- [17] H. Tekinalp, V. Kunc, G. M. Velez-Garcia, and C. E. Duty, “Highly oriented carbon fiber-polymer composites via additive manufacturing,” *Compos. Sci. Technol.*, vol. 105, 2014.
- [18] R. W. Gray IV, D. G. Baird, and J. H. Bohn, “Thermoplastic composites reinforced with long fiber thermotropic liquid crystalline polymers for used deposition modeling,” *Polym. Compos.*, vol. 19, no. 4, pp. 383–394, 1998.
- [19] P. Kulkarni, A. S. Dhoble, and P. Padole, “A Review of Research and Recent Trends in Analysis of Composite Plates,” *Sadhana - Acad. Proc. Eng. Sci.*, vol. 43, no. 6, 2018.
- [20] P. Thornton and P. Edwards, “Energy absorption in composite tubes,” *J. Compos. Mater.*, vol. 16, no. 521, 1982.
- [21] D. Schmueser and L. Wickliffe, “Impact energy absorption of continuous fiber composite tubes,” *J. Eng. Mat. Trans. ASME*, vol. 72, no. 77, 1987.
- [22] P. K. Mallick, *Fiber Reinforced Composites - Materials, Manufacturing and Design*. 2007.
- [23] A. Equbal, A. K. Sood, V. Toppo, R. K. Ohdar, and S. S. Mahapatra, “Prediction and analysis of sliding wear performance of fused deposition modelling-processed ABS plastic parts,” *Proc. Inst. Mech. Eng. Part J J. Eng. Tribol.*, vol. 224, no. 12, pp. 1261–1271, Dec. 2010.
- [24] A. Anon, “The solid future of of rapid prototyping,” *Econ. Quaterly - USA Econ.*, pp. 47–49, 2001.
- [25] S. Ford and M. Despeisse, “Additive manufacturing and sustainability: an exploratory study of the advantages and challenges,” *J. Clean. Prod.*, vol. 137, pp. 1573–1587, May 2016.
- [26] J. Park, M. Tari, and H. Hahn, “Characterization of the laminated object manufacturing (LOM) process,” *Rapid Prototyp. J.*, vol. 6, no. 1, pp. 36–50, 2000.

- [27] F. Ning, W. Cong, J. Wei, and S. Wang, "Additive Manufacturing of CFRP Composites Using Fused Deposition Modeling: Effects of Carbon Fiber Content and Length," *MSEC 2015 Conf. Proceeding*, 2015.
- [28] J. Horvath, *3D Printing*. .
- [29] "E3D Online: The Home of 3D Printing. Buy 3D Printer Parts Online. | E3D Online." [Online]. Available: https://e3d-online.com/?gclid=EAIaIQobChMI6j3aS_5glVibHtCh3FgAx4EAAYASAAEgKP9PD_BwE. [Accessed: 18-Dec-2019].
- [30] "TEVO Tarantula Pro – TEVO 3D Onlinestore." [Online]. Available: <https://tevo3dprinterstore.com/products/2016-newest-tevo-tarantula-i3-aluminium-extrusion-3d-printer-kit-printer-3d-printing-2-rolls-filament-8gb-sd-card-lcd-as-gift>. [Accessed: 17-Dec-2019].
- [31] C. Ferro, R. Grassi, C. Secli, and P. Maggiore, "Additive Manufacturing Offers New Opportunities in UAV Research," *Procedia CIRP*, vol. 41, pp. 1004–1010, Jan. 2016.
- [32] M. Grujicic, B. Pandurangan, C. L. Zhao, S. B. Biggers, and D. R. Morgan, "Hypervelocity impact resistance of reinforced carbon–carbon/carbon–foam thermal protection systems," *Appl. Surf. Sci.*, vol. 252, no. 14, pp. 5035–5050, May 2006.
- [33] C. G. Kim and E. J. Jun, "Impact Resistance of Composite Laminated Sandwich Plates," *Compos. Mater.*, vol. 26, pp. 2247–2261, 1992.
- [34] J. Liu, W. He, D. Xie, and B. Tao, "The effect of impactor shape on the low-velocity impact behavior of hybrid corrugated core sandwich structures," *Compos. Part B Eng.*, vol. 111, pp. 315–331, 2017.
- [35] J. Liu, W. He, D. Xie, and B. Tao, "The effect of impactor shape on the low-velocity impact behavior of hybrid corrugated core sandwich structures," *Compos. Part B Eng.*, vol. 111, pp. 315–331, Feb. 2017.
- [36] M. Pinnell, R. Fields, and R. Zabora, "Results of an Interlaboratory Study of the ASTM Standard Test Method for Tensile Properties of Polymer Matrix Composites D 3039," *J. Test. Eval.*, vol. 3, no. 1, pp. 27–31, 2005.
- [37] G. Rueda, F. L. Matthews, and E. W. Godwin, "An Experimental Comparison of Standard Test Methods for the Determination of Tensile, Compressive and Flexural Properties of Kevlar Fibre/Epoxy Laminates," *J. Reinf. Plast. Compos.*,

- vol. 9, no. 2, pp. 182–193, Mar. 1990.
- [38] “A Little CNC History - TORMACH LABS.” [Online]. Available: <https://www.tormach.com/blog/cnc-history/>. [Accessed: 18-Dec-2019].
- [39] Y. Li, Q. Li, and H. Ma, “The voids formation mechanisms and their effects on the mechanical properties of flax fiber reinforced epoxy composites,” *Compos. Part A Appl. Sci. Manuf.*, vol. 72, pp. 40–48, May 2015.
- [40] Markforged, “Metal & Carbon Fiber 3D Printers.” .
- [41] “Anycubic 3D Printing: Best & Affordable 3D Printers | Materials | Part – ANYCUBIC 3D Printing.” [Online]. Available: https://www.anycubic.com/?gclid=EAlaIQobChMIsePi0KO_5glVxrTtCh35GQ_rEAAYAAEgJU6PD_BwE. [Accessed: 18-Dec-2019].
- [42] “Duet 2 Wifi.” [Online]. Available: <https://www.duet3d.com/DuetWifi>. [Accessed: 18-Dec-2019].
- [43] BSI Group, “BS ISO Carbon Fiber-reinforced composites.”

Chapter 8

Appendices

Appendix A

```
//=====
//===== PID Settings =====
//=====

// Comment the following line to disable PID and enable bang-bang.
#define PIDTEMP
#define BANG_MAX 255 // limits current to nozzle while in bang-bang mode; 255=full current
#define PID_MAX BANG_MAX // limits current to nozzle while PID is active (see PID_FUNCTIONAL_RANGE below); 255=full current
#if ENABLED(PIDTEMP)
  // #define PID_AUTOTUNE_MENU // Add PID Autotune to the LCD "Temperature" menu to run M303 and apply the result.
  // #define PID_DEBUG // Sends debug data to the serial port.
  // #define PID_OPENLOOP 1 // Puts PID in open loop. M104/M140 sets the output power from 0 to PID_MAX
  // #define SLOW_PWM_HEATERS // PWM with very low frequency (roughly 0.125Hz=8s) and minimum state time of approximately 1s useful for heaters driven by a relay
  // #define PID_PARAMS_PER_HOTEND // Uses separate PID parameters for each extruder (useful for mismatched extruders)
  //                               // Set/get with gcode: M301 E[extruder number, 0-2]
  #define PID_FUNCTIONAL_RANGE 30 // If the temperature difference between the target temperature and the actual temperature
  //                               // is more than PID_FUNCTIONAL_RANGE then the PID will be shut off and the heater will be set to min/max.
  #define K1 0.95 //smoothing factor within the PID

  // If you are using a pre-configured hotend then you can use one of the value sets by uncommenting it
  // Ultimaker
  // #define DEFAULT_Kp 22.2
  // #define DEFAULT_Ki 1.08
  // #define DEFAULT_Kd 114

  // MakerGear
  // #define DEFAULT_Kp 7.0
  // #define DEFAULT_Ki 0.1
  // #define DEFAULT_Kd 12

  // Mendel Parts V9 on 12V
  // #define DEFAULT_Kp 63.0
  // #define DEFAULT_Ki 2.25
  // #define DEFAULT_Kd 440

  // E3D V6 Clone
  #define DEFAULT_Kp 3.16 //Kp 13.53
  #define DEFAULT_Ki 0.42 //Ki 1.69
  #define DEFAULT_Kd 140.85 //Kd 27.15
#endif // PIDTEMP

#define PIDTEMPBED

// #define BED_LIMIT_SWITCHING

// This sets the max power delivered to the bed, and replaces the HEATER_BED_DUTY_CYCLE_DIVIDER option.
// all forms of bed control obey this (PID, bang-bang, bang-bang with hysteresis)
// setting this to anything other than 255 enables a form of PWM to the bed just like HEATER_BED_DUTY_CYCLE_DIVIDER did,
// shouldn't use it unless you are OK with PWM on your bed. (see the comment on enabling PIDTEMPBED)
#define MAX_BED_POWER 255 // limits duty cycle to bed; 255=full current

#if ENABLED(PIDTEMPBED)

  // #define PID_BED_DEBUG // Sends debug data to the serial port.

  //120V 250W silicone heater into 4mm borosilicate (MendelMax 1.5+)
  //from FOPDT model - kp=.39 Tp=405 Tdead=66, Tc set to 79.2, aggressive factor of .15 (vs .1, 1, 10)
  // #define DEFAULT_bedKp 10.00
  // #define DEFAULT_bedKi .023
  // #define DEFAULT_bedKd 305.4

  //120V 250W silicone heater into 4mm borosilicate (MendelMax 1.5+)
  //from pidautotune
  // #define DEFAULT_bedKp 97.1
  // #define DEFAULT_bedKi 1.41
  // #define DEFAULT_bedKd 1675.16

  #define DEFAULT_bedKp 44.06
  #define DEFAULT_bedKi 7.37
  #define DEFAULT_bedKd 65.87

  // "M303 E-1 C8 S90" to run autotune on the bed at 90 degreesC for 8 cycles. ////////////////
#endif // PIDTEMPBED

// @section extruder

// This option prevents extrusion if the temperature is below EXTRUDE_MINTEMP.
// It also enables the M302 command to set the minimum extrusion temperature
// or to allow moving the extruder regardless of the hotend temperature.
#define PREVENT_COLD_EXTRUSION
#define EXTRUDE_MINTEMP 170
```

```

// Probe Type
// Probes are sensors/switches that are activated / deactivated before/after use.
//
// Servo Probes, Z-Sled Probes, FIX_MOUNTED_PROBE, etc.
// You must activate one of these to use Auto Bed Leveling below.
//
// M851 to set the Z probe vertical offset from the nozzle. Store with M500.
//

// A Fix-Mounted Probe either doesn't deploy or needs manual deployment.
// For example an inductive probe, or a setup that uses the nozzle to probe.
// An inductive probe must be deactivated to go below
// its trigger-point if hardware endstops are active.
// #define FIX_MOUNTED_PROBE

// The BLTouch probe emulates a servo probe.
// The default connector is SERVO 0. Set Z_ENDSTOP_SERVO_NR below to override.
#define BLTOUCH

// Z Servo Probe, such as an endstop switch on a rotating arm.
#define Z_ENDSTOP_SERVO_NR 0
#define Z_SERVO_ANGLES {10,90} // Z Servo Deploy and Stow angles

// Enable if you have a Z probe mounted on a sled like those designed by Charles Bell.
// #define Z_PROBE_SLED
// #define SLED_DOCKING_OFFSET 5 // The extra distance the X axis must travel to pickup the sled. 0 should be fine but you can push it further if you'd like.

// Z Probe to nozzle (X,Y) offset, relative to (0, 0).
// X and Y offsets must be integers.
//
// In the following example the X and Y offsets are both positive:
// #define X_PROBE_OFFSET_FROM_EXTRUDER 10
// #define Y_PROBE_OFFSET_FROM_EXTRUDER 10
//
//      +-- BACK ---+
//      |             |
//      L | (+) P | R <-- probe (20,20)
//      E |             | I
//      F | (-) N (+) | G <-- nozzle (10,10)
//      T |             | H
//      | (-)         | T
//      |             |
//      O-- FRONT ---+
//      (0,0)
#define X_PROBE_OFFSET_FROM_EXTRUDER 30 // X offset: -left +right [of the nozzle]

#ifdef CONDITIONALS_POST_H
#define CONDITIONALS_POST_H

/**
 * Axis lengths and center
 */
#define X_MAX_LENGTH (X_MAX_POS - X_MIN_POS)
#define Y_MAX_LENGTH (Y_MAX_POS - Y_MIN_POS)
#define Z_MAX_LENGTH (Z_MAX_POS - Z_MIN_POS)
#define X_CENTER float((X_MIN_POS + X_MAX_POS) * 0.5)
#define Y_CENTER float((Y_MIN_POS + Y_MAX_POS) * 0.5)
#define Z_CENTER float((Z_MIN_POS + Z_MAX_POS) * 0.5)

/**
 * CoreXY, CoreXZ, and CoreYZ - and their reverse
 */
#define CORE_IS_XY (ENABLED(COREXY) || ENABLED(COREYX))
#define CORE_IS_XZ (ENABLED(COREXZ) || ENABLED(COREZX))
#define CORE_IS_YZ (ENABLED(COREYZ) || ENABLED(COREZY))
#define IS_CORE (CORE_IS_XY || CORE_IS_XZ || CORE_IS_YZ)
#if IS_CORE
  #if CORE_IS_XY
    #define CORE_AXIS_1 A_AXIS
    #define CORE_AXIS_2 B_AXIS
    #define NORMAL_AXIS Z_AXIS
  #elif CORE_IS_XZ
    #define CORE_AXIS_1 A_AXIS
    #define NORMAL_AXIS Y_AXIS
    #define CORE_AXIS_2 C_AXIS
  #elif CORE_IS_YZ
    #define NORMAL_AXIS X_AXIS
    #define CORE_AXIS_1 B_AXIS
    #define CORE_AXIS_2 C_AXIS
  #endif
  #if (ENABLED(COREYX) || ENABLED(COREZX) || ENABLED(COREZY))
    #define CORESIGN(n) (-n)
  #else
    #define CORESIGN(n) (n)
  #endif
#endif
#endif

```

```

#define IS_SCARA (ENABLED(MORGAN_SCARA) || ENABLED(MAKERARM_SCARA))
#define IS_KINEMATIC (ENABLED(DELTA) || IS_SCARA)
#define IS_CARTESIAN !IS_KINEMATIC

/**
 * SCARA cannot use SLOWDOWN and requires QUICKHOME
 */
#if IS_SCARA
#undef SLOWDOWN
#define QUICK_HOME
#endif

/**
 * Set the home position based on settings or manual overrides
 */
#ifdef MANUAL_X_HOME_POS
#define X_HOME_POS MANUAL_X_HOME_POS
#elif ENABLED(BED_CENTER_AT_0_0)
#define X_HOME_POS 0
#else
#define X_HOME_POS ((X_MAX_LENGTH) * (X_HOME_DIR) * 0.5)
#endif
#else
#if ENABLED(DELTA)
#define X_HOME_POS (X_MIN_POS + (X_MAX_LENGTH) * 0.5)
#else
#define X_HOME_POS (X_HOME_DIR < 0 ? X_MIN_POS : X_MAX_POS)
#endif
#endif

#ifdef MANUAL_Y_HOME_POS
#define Y_HOME_POS MANUAL_Y_HOME_POS
#elif ENABLED(BED_CENTER_AT_0_0)
#define Y_HOME_POS 0
#else
#define Y_HOME_POS ((Y_MAX_LENGTH) * (Y_HOME_DIR) * 0.5)
#endif
#else
#if ENABLED(DELTA)
#define Y_HOME_POS (Y_MIN_POS + (Y_MAX_LENGTH) * 0.5)
#else
#define Y_HOME_POS (Y_HOME_DIR < 0 ? Y_MIN_POS : Y_MAX_POS)
#endif
#endif

#ifdef MANUAL_Z_HOME_POS
#define Z_HOME_POS MANUAL_Z_HOME_POS
#else
#define Z_HOME_POS (Z_HOME_DIR < 0 ? Z_MIN_POS : Z_MAX_POS)
#endif

/**
 * Auto Bed Leveling and Z Probe Repeatability Test
 */
#define HOMING_Z_WITH_PROBE (HAS_BED_PROBE && Z_HOME_DIR < 0 && ENABLED(Z_MIN_PROBE_USES_Z_MIN_ENDSTOP_PIN))

/**
 * Z Sled Probe requires Z_SAFE_HOMING
 */
#if ENABLED(Z_PROBE_SLED)
#define Z_SAFE_HOMING
#endif

/**
 * DELTA should ignore Z_SAFE_HOMING and SLOWDOWN
 */
#if ENABLED(DELTA)
#undef Z_SAFE_HOMING
#undef SLOWDOWN
#endif

/**
 * Safe Homing Options
 */
#if ENABLED(Z_SAFE_HOMING)
#ifdef Z_SAFE_HOMING_X_POINT
#define Z_SAFE_HOMING_X_POINT ((X_MIN_POS + X_MAX_POS) / 2)
#endif
#ifdef Z_SAFE_HOMING_Y_POINT
#define Z_SAFE_HOMING_Y_POINT ((Y_MIN_POS + Y_MAX_POS) / 2)
#endif
#define X_TILT_FULCRUM Z_SAFE_HOMING_X_POINT
#define Y_TILT_FULCRUM Z_SAFE_HOMING_Y_POINT
#else
#define X_TILT_FULCRUM X_HOME_POS
#define Y_TILT_FULCRUM Y_HOME_POS
#endif
#endif

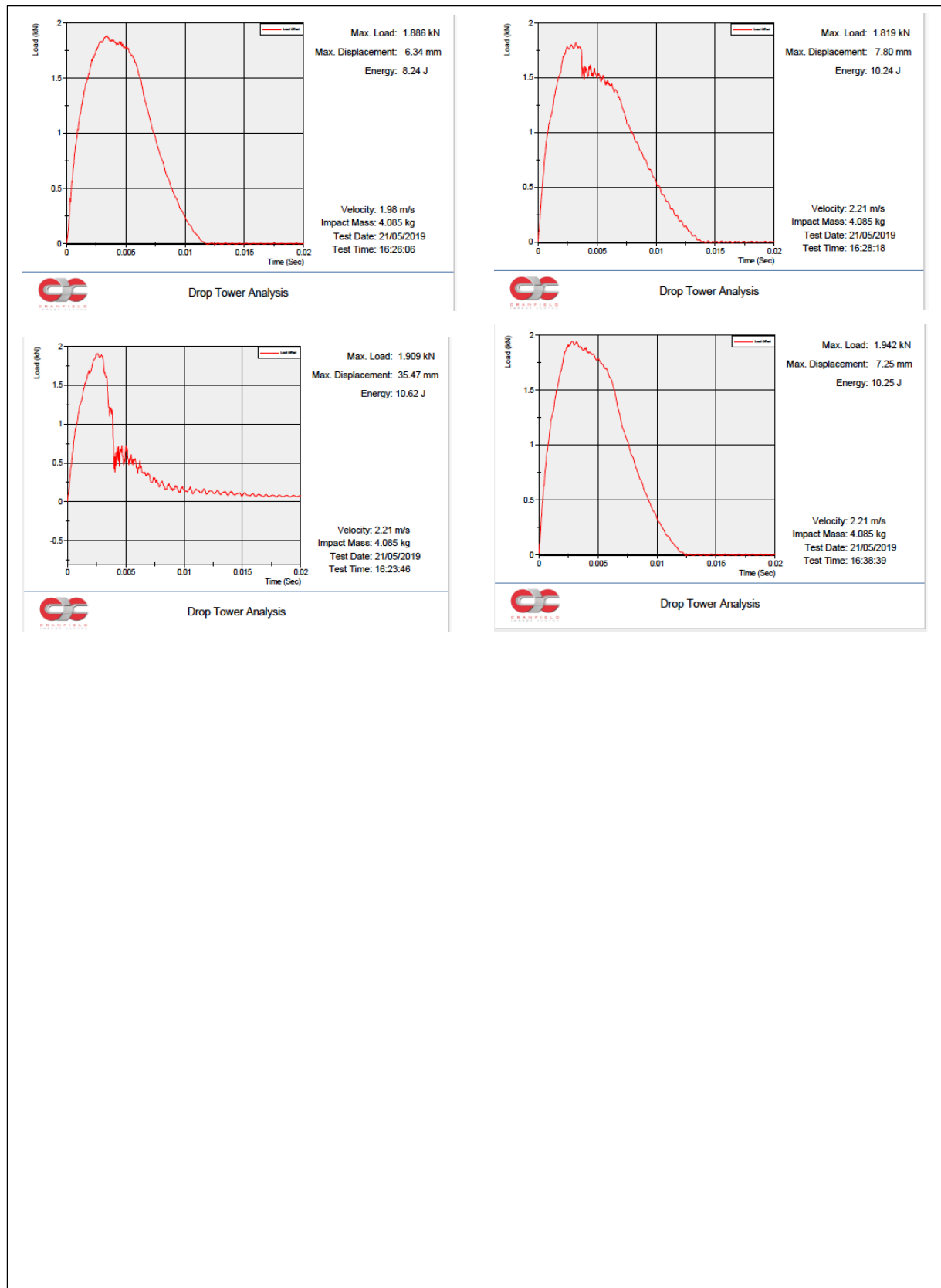
```

```

#define HAS_TEMP_0 (PIN_EXISTS(TEMP_0) && TEMP_SENSOR_0 != 0 && TEMP_SENSOR_0 > -2)
#define HAS_TEMP_1 (PIN_EXISTS(TEMP_1) && TEMP_SENSOR_1 != 0 && TEMP_SENSOR_1 > -2)
#define HAS_TEMP_2 (PIN_EXISTS(TEMP_2) && TEMP_SENSOR_2 != 0 && TEMP_SENSOR_2 > -2)
#define HAS_TEMP_3 (PIN_EXISTS(TEMP_3) && TEMP_SENSOR_3 != 0 && TEMP_SENSOR_3 > -2)
#define HAS_TEMP_BED (PIN_EXISTS(TEMP_BED) && TEMP_SENSOR_BED != 0 && TEMP_SENSOR_BED > -2)
#define HAS_HEATER_0 (PIN_EXISTS(HEATER_0))
#define HAS_HEATER_1 (PIN_EXISTS(HEATER_1))
#define HAS_HEATER_2 (PIN_EXISTS(HEATER_2))
#define HAS_HEATER_3 (PIN_EXISTS(HEATER_3))
#define HAS_HEATER_BED (PIN_EXISTS(HEATER_BED))
#define HAS_AUTO_FAN_0 (PIN_EXISTS(E0_AUTO_FAN))
#define HAS_AUTO_FAN_1 (HOTENDS > 1 && PIN_EXISTS(E1_AUTO_FAN))
#define HAS_AUTO_FAN_2 (HOTENDS > 2 && PIN_EXISTS(E2_AUTO_FAN))
#define HAS_AUTO_FAN_3 (HOTENDS > 3 && PIN_EXISTS(E3_AUTO_FAN))
#define HAS_AUTO_FAN (HAS_AUTO_FAN_0 || HAS_AUTO_FAN_1 || HAS_AUTO_FAN_2 || HAS_AUTO_FAN_3)
#define AUTO_1_IS_0 (E1_AUTO_FAN_PIN == E0_AUTO_FAN_PIN)
#define AUTO_2_IS_0 (E2_AUTO_FAN_PIN == E0_AUTO_FAN_PIN)
#define AUTO_2_IS_1 (E2_AUTO_FAN_PIN == E1_AUTO_FAN_PIN)
#define AUTO_3_IS_0 (E3_AUTO_FAN_PIN == E0_AUTO_FAN_PIN)
#define AUTO_3_IS_1 (E3_AUTO_FAN_PIN == E1_AUTO_FAN_PIN)
#define AUTO_3_IS_2 (E3_AUTO_FAN_PIN == E2_AUTO_FAN_PIN)
#define HAS_FAN0 (PIN_EXISTS(FAN0))
#define HAS_FAN1 (PIN_EXISTS(FAN1) && CONTROLLERFAN_PIN != FAN1_PIN && E0_AUTO_FAN_PIN != FAN1_PIN && E1_AUTO_FAN_PIN != FAN1_PIN && E2_AUTO_FAN_PIN != FAN1_PIN && E3_AUTO_FAN_PIN != FAN1_PIN)
#define HAS_FAN2 (PIN_EXISTS(FAN2) && CONTROLLERFAN_PIN != FAN2_PIN && E0_AUTO_FAN_PIN != FAN2_PIN && E1_AUTO_FAN_PIN != FAN2_PIN && E2_AUTO_FAN_PIN != FAN2_PIN && E3_AUTO_FAN_PIN != FAN2_PIN)
#define HAS_CONTROLLERFAN (PIN_EXISTS(CONTROLLERFAN))
#define HAS_SERVOS (defined(NUM_SERVOS) && NUM_SERVOS > 0)
#define HAS_SERVO_0 (PIN_EXISTS(SERVO0))
#define HAS_SERVO_1 (PIN_EXISTS(SERVO1))
#define HAS_SERVO_2 (PIN_EXISTS(SERVO2))
#define HAS_SERVO_3 (PIN_EXISTS(SERVO3))
#define HAS_FILAMENT_WIDTH_SENSOR (PIN_EXISTS(FILWIDTH))
#define HAS_FIL_RUNOUT (PIN_EXISTS(FIL_RUNOUT))
#define HAS_HOME (PIN_EXISTS(HOME))
#define HAS_KILL (PIN_EXISTS(KILL))
#define HAS_SUICIDE (PIN_EXISTS(SUICIDE))
#define HAS_PHOTOGRAPH (PIN_EXISTS(PHOTOGRAPH))
#define HAS_X_MIN (PIN_EXISTS(X_MIN) && !IS_ZZ_OR_PROBE(X_MIN_PIN))
#define HAS_X_MAX (PIN_EXISTS(X_MAX) && !IS_ZZ_OR_PROBE(X_MAX_PIN))
#define HAS_Y_MIN (PIN_EXISTS(Y_MIN) && !IS_ZZ_OR_PROBE(Y_MIN_PIN))
#define HAS_Y_MAX (PIN_EXISTS(Y_MAX) && !IS_ZZ_OR_PROBE(Y_MAX_PIN))
#define HAS_Z_MIN (PIN_EXISTS(Z_MIN) && !IS_ZZ_OR_PROBE(Z_MIN_PIN))
#define HAS_Z_MAX (PIN_EXISTS(Z_MAX) && !IS_ZZ_OR_PROBE(Z_MAX_PIN))
#define HAS_ZZ_MIN (PIN_EXISTS(ZZ_MIN))
#define HAS_ZZ_MAX (PIN_EXISTS(ZZ_MAX))
#define HAS_Z_MIN_PROBE_PIN (PIN_EXISTS(Z_MIN_PROBE))
#define HAS_SOLENOID_1 (PIN_EXISTS(SOL1))
#define HAS_SOLENOID_2 (PIN_EXISTS(SOL2))
#define HAS_SOLENOID_3 (PIN_EXISTS(SOL3))

```


Appendix B



Appendix C

Publications in progress upon permission agreement with Luxembourg MOD and defence commission.

- 1- Delporte, Y. and Ghasemnejad, H., 2020. Effect of process parameters on mechanical properties of CFRTP nylon 910. *Composite Structures*,
- 2- Delporte, Y. and Ghasemnejad, H., 2021. Influence of humidity exposure on CFRTP composite material and low velocity impact performance. *Composite Interfaces*,
- 3- Delporte, Y. and Ghasemnejad, H., 2021. CFRTP recycling method and mechanical testing on recycled CFRTP composite. *Journal of thermoplastic composite materials*,